Journal of Quantitative Spectroscopy & Radiative Transfer 94 (2005) 1–50

Journal of Quantitative Spectroscopy & Radiative Transfer

www.elsevier.com/locate/jqsrt

Measurements and analysis (using empirical functions for widths) of air- and self-broadening parameters of H_2O

Robert A. Toth*

California Institute of Technology, Jet Propulsion Laboratory, MS 183/301, Pasadena, CA 91109, USA

Received 3 June 2004; received in revised form 24 August 2004; accepted 25 August 2004

Abstract

High-resolution spectra of H_2O were recorded with the McMath Fourier-transform spectrometer at the National Solar Observatory located at Kitt Peak, AZ. Seventeen laboratory spectra of water plus air mixtures were recorded at a spectral resolution of $0.01\,cm^{-1}$ covering the region between 2800 and $8000\,cm^{-1}$. Over 4000 linewidth and pressure-induced frequency shift coefficients were derived from the spectral data with sample temperatures near or at room temperature (296 K). The measurements include transitions of $H_2{}^{16}O$, $H_2{}^{17}O$, and $H_2{}^{18}O$ with the rare oxygen species observed in normal H_2O gas samples. The measurements were analyzed with consideration of collision-narrowing effects. The analysis required a knowledge of the self-broadened linewidth coefficients, and the data measured and reported in the previous study were used along with earlier results for this purpose. The self-broadened and air-broadened measured linewidth coefficients obtained here as well as those reported in earlier studies covering the 600–2400 cm^{-1}, were fitted to an empirical expression which contains up to 28 terms. Two fitting procedures were used: one considered the fit of families of transitions and the other was more global in scope. The computed linewidth coefficients derived from the fitted parameters are compared statistically to measurements in this work as well as other studies.

Keywords: H_2O; Measured widths; Analysis

*Tel.: +1 818 354 6860; fax: +1 818 354 5148.
E-mail address: toth@caesar.jpl.nasa.gov (R.A. Toth).

0022-4073/$ - see front matter
doi:10.1016/j.jqsrt.2004.08.041

1. Introduction

Previously, extensive listings of air- and nitrogen-broadening parameters of water vapor for the spectral region between 604 and 2271 cm^{-1} were presented [1] and in another study [2], the self-broadened width coefficients of H_2O was given covering transitions from 590 to 2400 cm^{-1}. Measurements of H_2O self-broadened width coefficients were presented in the previous paper [3] encompassing the region between 4356 and 7939 cm^{-1} (4533 lines). In the present work, linewidth and pressure-induced frequency shift coefficients for air-broadening of H_2O were derived from measurements covering the region between 2864 and 7759 cm^{-1}. The linewidth data from this study were combined with previous measurements [1] and analyzed using an empirical expression described in Ref. [1]. The self-broadened width data [2,3] were also analyzed in this manner.

There has been extensive research in this area and the list of publications, referenced here in chronological order of publications (3–38), include studies related to this work. Refs. [2,3,6–9,11,18–25,27,28,31–33,35] involved H_2O self-broadening measurements and Refs. [1,4,5,8,10,12–18,20,21,23–26,29–37] include measurements of air-broadening parameters of water vapor.

2. Experiment

The spectra were recorded using the Fourier transform spectrometer (FTS) located in the McMath Solar facility at the Kitt Peak National Observatory. The beamsplitter was CaF_2 and the IR radiation from a globar source was recorded on an InSb detector. Each interferogram of a run lasted about 10 min. and each run consisted of 10 or more co-added interferograms. The signal-to-noise ratios of the spectra varied from about 900 to 1 for the shortest path length runs to about 400 to 1 for runs with a path length of 433 m. The pressures were measured with a Baratron MKS gauge with an estimated uncertainty of 0.5%. Either a 10, 100 or 1000 Torr head was used in this procedure. The sample temperatures were also monitored continuously and inferred from readings of one or more thermistor probes in thermal contact with the cell walls and all data were obtained at near or room temperature, 296 K, with an estimated uncertainty of 0.5 K.

The experimental conditions of the runs are given in Table 1. A 6-m base-length multiple-transversal absorption cell was used for the 25, 73, 193, and 433 m path length runs, whereas straight cells were used for the shorter path runs. The open spaces in the optical path of all but two of the short path length runs were evacuated so that additional spectral features due to room air were removed. For two of these runs (entries 13 and 14 in Table 1), the IR source was placed in front of the entrance to the vaccum tank, which enclosed the FTS, and the radiation passed through open room air. The runs represented by the last three entries in Table 1 used the 6 m-base cell with room air in the cell and the optical space between the cell and the entrance to the vacuum tank was not enclosed and also contained room air. For this work, line strengths, S, are given in units of cm^{-2}/atm and the conversion factor to cm/molecules is 4.033×10^{-20}. The short cell data contained additional absorptions for the strongest lines ($S \geqslant 0.02\,cm^{-2}$/atm.) due to a small quantity of H_2O in the vacuum tank which enclosed the FTS; however, these narrow features were

Table 1
Experimental conditions for the air-broadened spectral runs of H_2O in which the sample temperatures were near or at 296 K

Spectral coverage (cm^{-1})	Path length (m)	H_2O partial pressure (Torr)	Air pressure (Torr)
1750–5665	25	3.0	397.0
1750–5665	73	3.0	397.0
1750–5665	193	3.0	397.0
1750–5665	433	3.0	397.0
1640–5600	0.25	2.0	306.7
1640–5600	0.25	2.0	400.1
1640–5600	0.25	2.0	504.2
1640–5600	0.25	2.0	590.0
1640–5600	1.5	2.0	300.0
1640–5600	1.5	2.0	399.0
1640–5600	1.5	2.0	499.0
1640–5600	1.5	2.0	598.8
2980–9000	0.3	9.5	589.0
2980–9000	1.5	9.5	589.0
2980–9000	29	9.5	590.0
2980–9000	101	9.3	591.0
2980–9000	197	9.0	592.0

observed on top of the broad H_2O + air absorptions and were easily accounted for in the data reduction algorithm and were used for frequency calibration with the computed $H_2{}^{16}O$ line positions derived from the energy levels given in Refs. [3,39,40]. A 2.4 m cell was placed in the optical path when the 6 m base length cell was used and the 2.4 m cell contained low-pressure CO. The CO features observed in the spectra served as additional frequency calibration using accurate CO line frequencies in the 2.4 μm region reported by Pollock et al. [41].

3. Spectral analysis

The co-added interferograms for each run were transformed into spectral data at the Kitt Peak facility. The analysis of the data was done using previously described (for example Refs. [1–3] to name a few) computer programs at JPL. The spectral analysis program uses the technique of non-linear least-squares (NLLS). Each unapodized spectrum was measured by adjusting the input values of positions, strengths and widths to reduce the differences between the observed and computed spectral absorptions. The water vapor input list consisted of $H_2{}^{16}O$, $H_2{}^{18}O$, $H_2{}^{17}O$ and HDO line positions and strengths described in earlier studies [3,39,40,42–47] with experimental values of these parameters used when accurately known, otherwise the computed values were entered. Also observed in some of the spectra were CO_2 absorptions due to its normal abundance in room air or a slight CO_2 impurity in the non room air samples. The spectral parameters for these features were taken from the HITRAN 2000 list [48] and used in the input list.

The measured linewidths, b, are related to the linewidth coefficients by

$$b = b_f^o p_f + b_s^o p_s, \tag{1}$$

where b_f^o and b_s^o are the foreign- and self-broadened width coefficients, respectively, and p_f and p_s are the foreign and self partial pressures. An accurate determination of b_f^o (which in this case is the air-broadening coefficient, b^o(air)) obtained from the measured b requires an accurate knowledge of b_s^o, p_f and p_s. The self-broadened widths measured in two other reports [2,3] were analyzed here using a fitting technique that will be described and applied in the next section.

The H_2O partial pressures given in Table 1 were derived from spectral analysis with knowledge of the line strength values. For a given spectral run, this was done by using several measured lines that were isolated and not saturated or too weak and the measured strengths of these lines, S_i(obs), determined from the NLLS program, were compared to the known line strengths, S_i(low pres.), from which the partial pressure, $p(H_2O)$, was derived

$$p(H_2O) = p_x(\{\Sigma S_i(\text{obs.})/S_i(\text{low pres.})\}/N, \tag{2}$$

where p_x is the gauge measured H_2O pressure or a first guess of that pressure and N are the number of lines used in this procedure. Although the sample temperatures of all the runs were near room temperature, the computed, low-pressure line strength values at 296 K were corrected for the sample temperature, T, when required, by the expression

$$S(T) = S(296)(296/T)^{5/2} \exp\{-1.44E''(1/T - 1/296)\}, \tag{3}$$

where E'' is the lower state rotational energy of the transition in cm^{-1} and in this case, the lower state is the ground state. The air, partial pressure, p(air) was then determined for each run from the total pressure measured by gauge minus $p(H_2O)$.

As noted earlier, a small amount residual water vapor was found in the vacuum tank which enclosed the FTS and these narrow, extra features were observed in the short path length spectra superimposed upon the pressure-broadened counterpart. They were effectively modeled for these runs in the NLLS program by inputting two components for each H_2O transition. The narrow H_2O features were present in all of the spectra but were not readily observable in the long path spectra because they were swamped by the pressure-broadened counterparts or they were too weak in absorption to appear. The minimum line strength of a H_2O narrow absorption that was observed in the empty cell runs was about $10^{-2}\,\text{cm}^{-2}/\text{atm}$ which happened to be about the same minimum strength of air-broadened H_2O lines resulting from room air in the open space, optical path between the exit of the 6-m cell and the entrance to the vacuum tank. In any case, the long-path runs (the first four entries in Table 1) were modeled in the NLLS program by inputting three components for each H_2O transition, although the narrow and the open space room air components were of little or no consequence in the analysis and in many situations, were removed after one or two iterations of the NLLS program.

The majority of the pressure broadened lines observed in all the spectra exhibited Lorentzian or Voigt profiles which were accurately simulated in the NLLS program. In a few cases, the line shape showed effects due to collision narrowing, although the pressure broadening contribution to the combined effect does not change: the Doppler contributions to the width tends toward zero when the pressure increases. The sub-Doppler behavior of these types of rotational transitions can occur over a wide pressure range. The line shape algorithm that was included in the NLLS program and used in the analysis of narrowed lines was the Galatry [49] profile based on the description given by Varaghese and Hanson [50]. The function involved the soft collision model which includes the same parameters as those applied in the Voigt function with the addition of a collision narrowing coefficient, η, given in units of cm^{-1}/atm. η was allowed to float in the fitting procedure and typical values for η ranged from 0.04 to 0.10 cm^{-1}/atm. with the smallest values corresponding to the narrowest lines. The derived values of η show no systematic form in terms of J and K_a and a further investigation of the narrowed transitions is warranted.

Figs. 1–4 are spectral scans of observed and computed H_2O spectra. The synthetic spectra overlaying the observed spectra were computed using a Voigt profile for all transitions. Fig. 1 shows, in addition, CO low-pressure absorptions which were not included in the computed spectra and the positions of these features are easily displayed in the residual plots located above each set of spectra. Figs. 2–4 contain air-broadened H_2O spectra and low pressure H_2O spectra with the low-pressure data situated below the higher-pressure spectra covering the same spectral interval. The low-pressure spectra show the importance of having an accurate input line list for application in fitting the broadened data: in several regions, a broadened absorption requires more than one line to correctly model the feature. If incorrectly modeled, the fitted linewidth could be in error by a modest amount although agreement between observed and computed spectra may be excellent.

4. Linewidth fit analysis

Gamache and Hartmann [38] stated that due to vibrational dependence, differences on the widths are rather small with slightly smaller broadening for lines of the bending band. Analysis of the measured self- and air-broadened width coefficients show this for ground state bands between 600 and 8000 cm^{-1}. Therefore the analysis applied in this study grouped data in terms of the value of the upper state v_2 vibration: those with $v_2' > 0$ formed one group and the other group included widths with $v_2' = 0$ where prime denotes upper state. The empirical function used to fit the widths has the same form as that applied in Ref. [1] and is

$$b^{\circ} = \exp\{\Sigma_i a(i)x(i)\}, \tag{4}$$

where $x(i)$ are the term elements and $a(i)$ are the parameter values. A total of 28 elements were used in various fits and these are given in Table 2. In Ref. [1], the width coefficients were least-squares-fitted with the first seven elements given in Table 2 and the data were fitted in terms of families of transitions. This was also done here and these results are called smoothed values. The definition of "families" of rotational transitions was given in Ref. [1] and, briefly, the rules follow. ΔJ, ΔK_a, K_a'', and γ'' are each the same within the family and double prime denotes lower state. γ is either 0 or 1 and γ is defined as

$$\gamma = K_a + K_c - J. \tag{5}$$

In most cases, the half-width coefficients of two related families follow the same pattern. In related families, the upper state rotational quanta in one family are the same as that of lower state of the related family and visa versa. Therefore a family of R-branch transitions has a related family of P-branch transitions. The same is true for Q-branch transitions where both related families are Q-branch transitions.

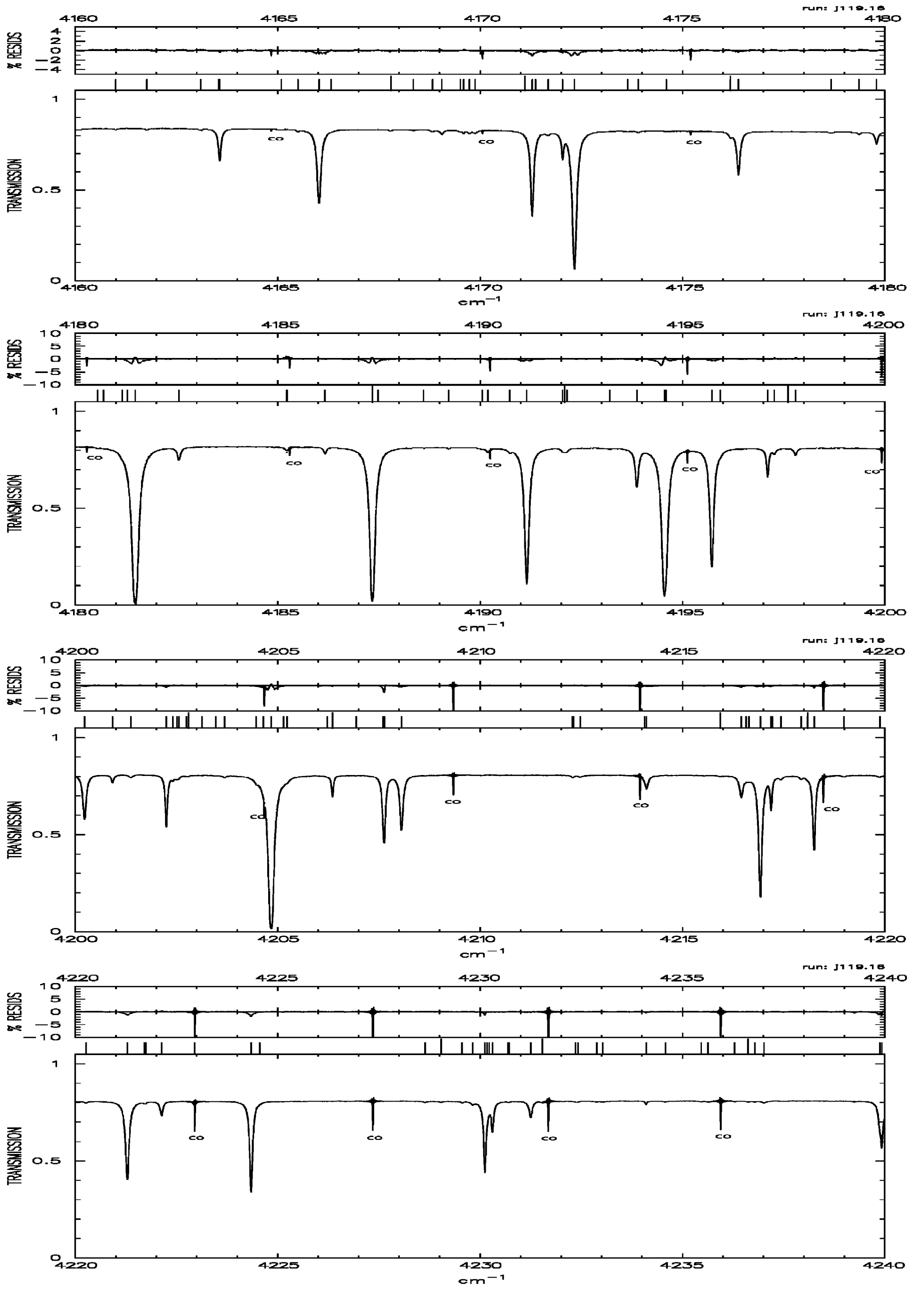

Fig. 1. Observed and computed spectra of H_2O. Observed spectra: 3 Torr H_2O, 396 Torr air, 433 m path length, and sample temperature of 296 K. Low-pressure CO absorptions also observed but not computed in synthetic spectra. CO lines were used for frequency calibration. Residual plots are located above each of the four sets of spectra and give the percent difference between the observed and computed spectra.

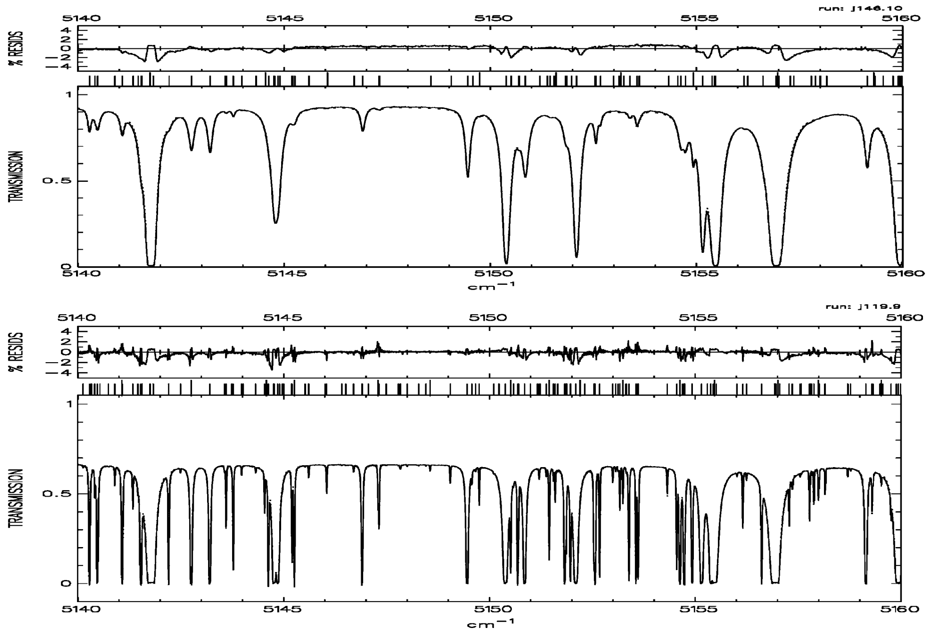

Observed upper spectrum from run J146.10 and lower one from run J119.9

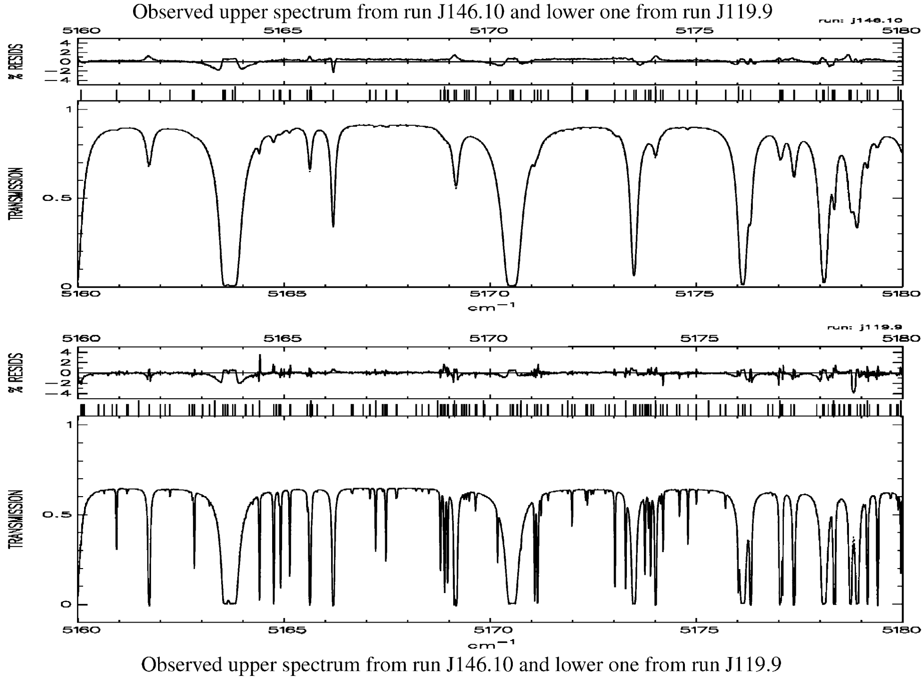

Observed upper spectrum from run J146.10 and lower one from run J119.9

Fig. 2. Observed and computed spectra of H_2O. The experimental conditions of the runs are as follows. Run J146.10: 9.5 Torr H_2O, 590 Torr air, and 29 m path length. Run J119.9: 5.47 Torr H_2O and 433 m path length. Sample temperatures for both runs were 296 K. Residual plots are located above each of the four sets of spectra and give the percent difference between the observed and computed spectra.

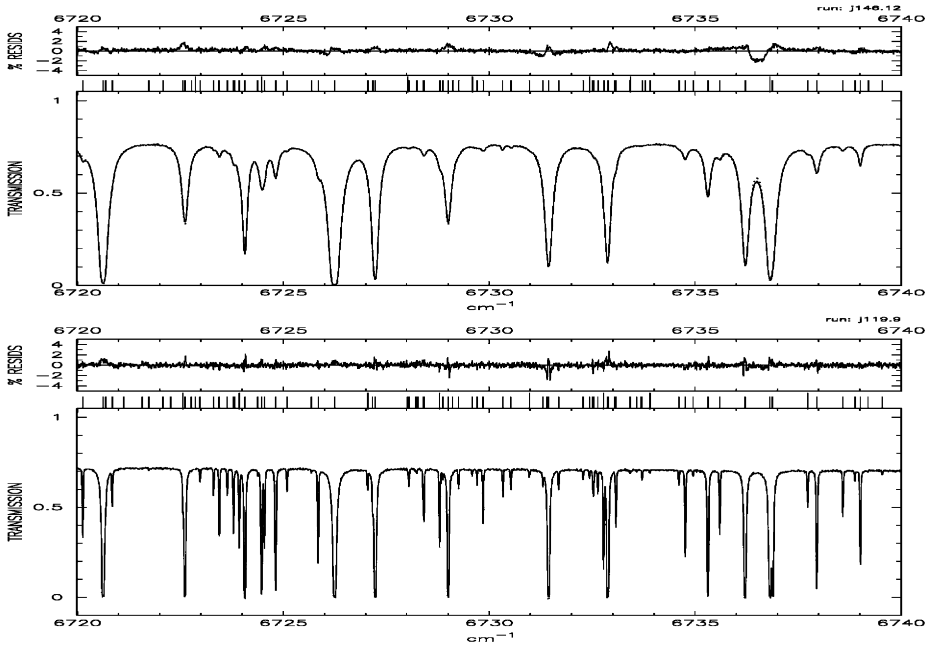

Observed upper spectrum from run J146.10 and lower one from run J119.9

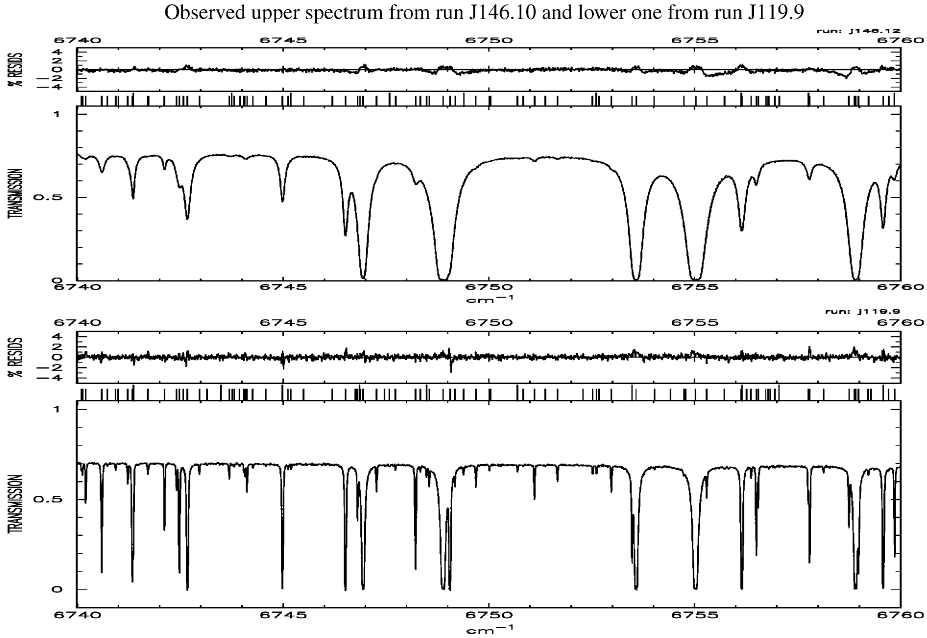

Observed upper spectrum from run J146.10 and lower one from run J119.9

Fig. 3. Observed and computed spectra of H_2O. Experimental conditions of the runs are as follows. Run J146.12: 9 Torr H_2O, 592 Torr air, and 197 m path length. Run J119.9: 5.47 Torr H_2O and a 433 m path length. Sample temperatures for both runs were 296 K. Residual plots are located above each of the four sets of spectra and give the percent difference between the observed and computed spectra.

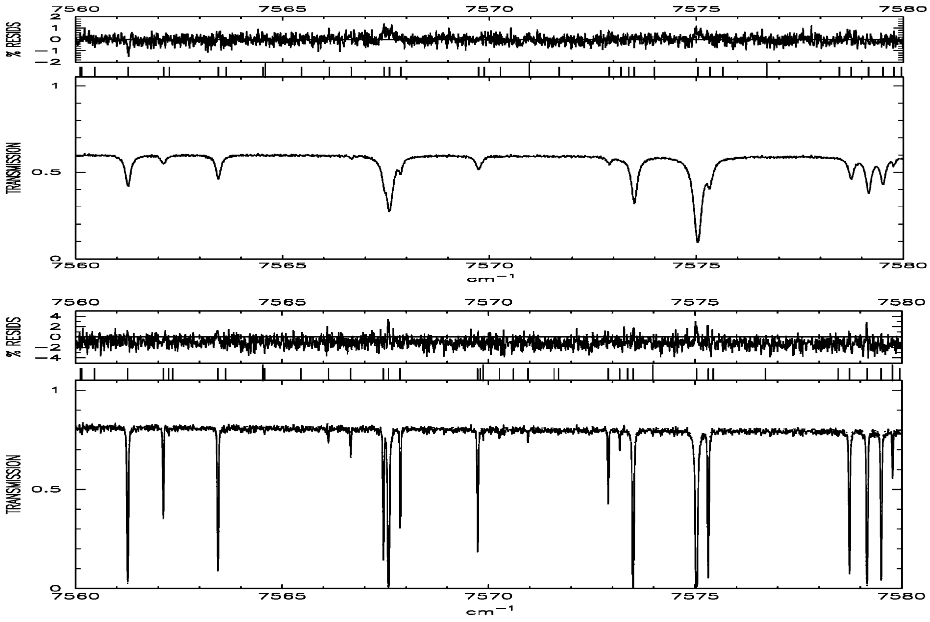

Observed upper spectrum from run J146.12 and lower one from run J119.9

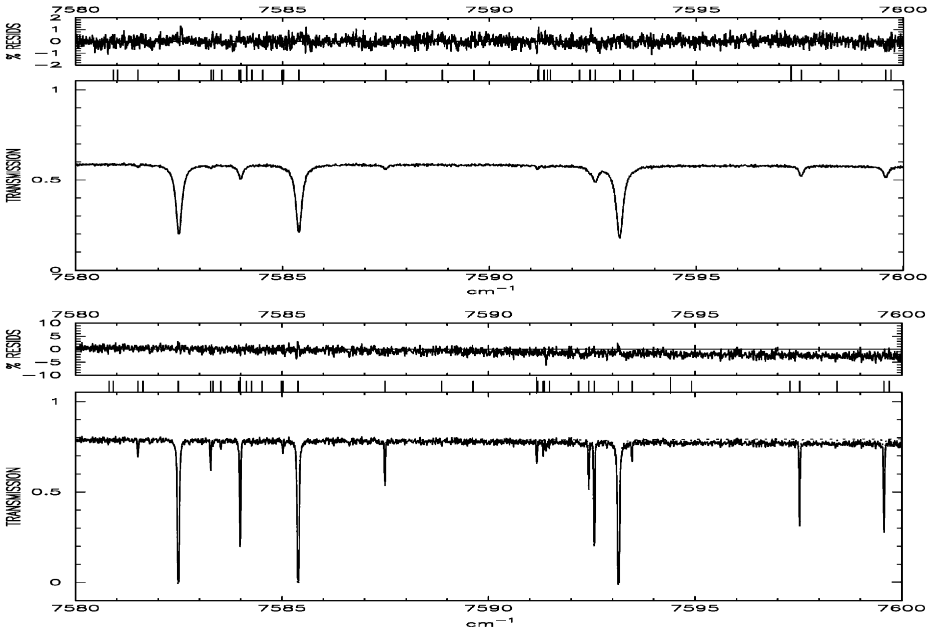

Observed upper spectrum from run J146.12 and lower one from run J119.9

Fig. 4. Observed and computed spectra of H_2O. Experimental conditions of the runs are as follows. Run J146.12: 9 Torr H_2O, 592 Torr air, and 197 m path length. Run J119.9: 5.47 Torr H_2O and a path length of 433 m. Sample temperatures for both runs were 296 K. Residual plots are located above each of the four sets of spectra and give the percent difference between the observed and computed spectra.

Table 2
Term elements used in the analysis of H_2O measured half-width coefficients

No.	Element	No.	Element
1	1	15	$(K_a'^4 + K_a''^4) \times M$
2	M	16	$K_a'^6 + K_a''^6$
3	m^2	17	$(K_a'^6 + K_a''^6) \times M$
4	M^3	18	$(K_a' + K_a'') \times m$
5	m^4	19	$(K_a'^2 + K_a''^2) \times m$
6	M^5	20	$K_a'^2 + K_a''^2) \times m^3$
7	m^6	21	$K_a'^2 - K_a''^2$
8	$K_a' + K_a''$	22	$K_a'^4 - K_a''^4$
9	$K_a'^2 + K_a''^2$	23	$(K_a'^2 - K_a''^2) \times M$
10	$K_a'^4 + K_a''^4$	24	$(K_a'^2 - K_a''^2) \times m^2$
11	$(K_a' + K_a'') \times M$	25	$(K_a'^4 - K_a''^4) \times M$
12	$(K_a' + K_a'') \times m^2$	26	$(K_a'^4 - K_a''^4) \times m^2$
13	$(K_a'^2 + K_a''^2) \times M$	27	$(K_a'^2 + K_a''^2) \times M \times (J' - J'') \times (K_a' - K_a'')$
14	$(K_a'^2 + K_a''^2) \times m^2$	28	$(K_a'^4 + K_a''^4) \times M \times (J' - J'') \times (K_a' - K_a'')$

Prime and double prime denote upper and lower states, respectively. $M = |m|$, $m = -J''$ (P-branch), $m'' = J'$ (R-branch), and $m = J$ (Q-branch).

The remaining elements (8–28) given in Table 2 were determined from trial and error using several combinations of various elements, some of which were not included in the final analysis. The terms that were selected gave the best fits to the measured data.

The air-broadened data involved in the various least-squares fits include the present measurements plus those given by Toth [1] covering the 604–2271 cm^{-1} region and those given in Refs. [2,3] for self-broadening. The statistical results from the fits are listed in Table 3 which shows that the A-type transitions of all the bands involved, required nine sets whereas the B-type transitions required 10 sets for air-broadening and the same for self-broadening. The table includes what each data set contains in terms of bands: bands with ν_2' either zero or greater than zero and in some cases all bands regardless of the vibrational states. Other entries include the rotational transition type, γ, number of elements defined in Eq. (4) and expressions in Table 2, number of measurements and number fitted and the standard deviation between computed and measured values as well as that for the measured uncertainties. The number of elements refers to the number from 1 to that value given in Table 2. The standard deviations in percent, $\sigma\%$, refer to the number fitted, N_f, and used in the expressions

$$\sigma\% = (\Sigma\{[b^o(\text{obs.}) - b^o(\text{calc.})]/b^o(\text{obs.})\}^2/N_f)^{1/2} \times 100,$$
$$\sigma\% = (\Sigma\{\Delta b^o/b^o(\text{obs.})\}^2/N_f)^{1/2} \times 100, \tag{6}$$

where b^o(obs.) is the measured width coefficient and b^o(calc.) is the computed value derived from either the fitted or smoothed parameters. The second equation is the standard deviation for the experimental estimated uncertainties, Δb^{o}. For a given measured line, b^{o}(obs.) was determined from the average of measurements from various runs using Eq. (1) and Δb^{o} was the error or uncertainty resulting from the average. The lower portion of the table summarizes the various fit statistics. The results indicate that the most accurate computed values were derived from the

Table 3
Analysis of measured linewidth coefficients of H_2O for air- and self-broadening at 296 K

$v'_2 = 0$ or >0	Band type	Rotational type		γ^* 0 or 1	No. elements	No. measured		Standard deviation in %		
		Branch	Trans.			Total	Fitted	Fitted	Smoothed	Exp.
air = 0	A	P&R	allowed	0	20	241	215	4.8	3.5	3.8
air = 0	A	P&R	allowed	1	20	208	190	4.1	3.7	4.8
air > 0	A	P&R	allowed	0	20	225	206	4.5	3.3	3.8
air > 0	A	P&R	allowed	1	20	184	170	3.3	2.7	4.2
air = 0	A	Q	allowed	0 and 1	17	124	106	2.7	3.0	3.9
air > 0	A	Q	allowed	0 and 1	17	125	113	2.8	3.2	3.5
air, all	A	Q	forbidden	0 and 1	20	150	131	3.7	2.3	4.0
air, all	A	P&R	forbidden	0	20	227	201	2.1	1.6	3.1
air, all	A	P&R	forbidden	1	20	149	135	2.6	2.3	3.2
air = 0	B	P&R	allowed	0	28	221	206	4.0	2.7	3.8
air > 0	B	P&R	allowed	0	28	558	517	4.5	3.4	4.7
air = 0	B	P&R	allowed	1	28	251	218	4.0	3.7	3.9
air > 0	B	P&R	allowed	1	28	555	508	4.3	3.4	4.1
air, all	B	P&R	forbidden	0	26	211	185	2.9	2.3	5.3
air, all	B	P&R	forbidden	1	26	115	100	3.5	5.0	6.2
air = 0	B	Q	all trans.	0	26	118	111	2.7	1.8	3.7
air > 0	B	Q	all trans.	0	26	328	282	3.5	2.4	3.8
air = 0	B	Q	all trans.	1	26	91	85	2.0	2.2	4.6
air > 0	B	Q	all trans.	1	26	220	194	3.2	2.5	5.0
self = 0	A	P&R	allowed	0	20	143	125	9.1	10.3	7.4
self = 0	A	P&R	allowed	1	20	125	108	5.2	7.9	8.1
self > 0	A	P&R	allowed	0	20	354	322	7.9	7.8	8.7
self > 0	A	P&R	allowed	1	20	286	258	7.5	8.8	9.0
self = 0	A	Q	allowed	0 and 1	17	121	108	8.0	9.9	7.8
self > 0	A	Q	allowed	0 and 1	17	245	223	7.6	7.9	9.0
self, all	A	Q	forbidden	0 and 1	20	304	279	7.7	7.6	9.1
self, all	A	P&R	forbidden	0	20	354	329	6.1	5.8	8.3
self, all	A	P&R	forbidden	1	20	229	209	8.8	9.3	8.7
self = 0	B	P&R	allowed	0	28	277	250	5.9	5.4	7.9
self > 0	B	P&R	allowed	0	28	669	611	5.6	5.2	6.6
self = 0	B	P&R	allowed	1	28	280	257	6.6	6.4	7.0
self > 0	B	P&R	allowed	1	28	674	621	5.4	5.2	6.4
self, all	B	P&R	forbidden	0	26	241	221	5.9	5.3	6.7
self, all	B	P&R	forbidden	1	26	159	146	7.0	6.0	6.0
self = 0	B	Q	all trans.	0	26	198	188	7.0	7.2	7.4
self > 0	B	Q	all trans.	0	26	450	407	4.8	4.4	6.5
self = 0	B	Q	all trans.	1	26	136	128	7.8	8.5	8.7
self > 0	B	Q	all trans.	1	26	308	278	5.9	6.2	6.2

Table 3 (*continued*)

Summary						
Broadener band type	Total number	Number fitted	Standard deviation in percent			
			All trans.	Fitted	Smoothed	Exp.
air A-type	1633	1467	7.2	3.6	2.9	3.9
air B-type	2668	2405	7.0	3.8	3.2	4.5
air A + B	4301	3872	7.1	3.8	3.1	4.3
self A-type	2157	1957	14.6	7.6	8.0	8.6
self B-type	3387	3095	11.2	5.9	5.7	6.8
selfA + B	5544	5052	12.6	6.6	6.7	7.5

Allowed means $|K'_a - K''_a| = 0$ or 1, forbidden means $|K'_a - K''_a| > 1$, prime and double prime denote upper and lower states, respectively.

* $\gamma = K_a + K_c - J$. For B-type, P and R transitions, the value of γ refers to the lower state for R-branch transitions and upper state for the P-branch.

Standard deviation is between the computed and measured values.

smoothed parameters although the width coefficients calculated from the fitted parameters were also in good agreement with the measured b^o.

An accurate determination of b^o(self) was more difficult to obtain than for b^o(air) which is mainly due to the condition that room temperature measurements of self-broadening were made for H_2O sample pressure at about 14 Torr or less which translates to observed, narrow lines of which the broadening contribution may be close to or smaller than the Doppler width. For the majority of air-broadened measurements, the broadened width is greater by a sizable amount over the Doppler width because the air sample partial pressures were from 306 to 592 Torr. Also, for air-broadening, the majority of the measured observed widths were larger than the instrument spectral resolution which was not the case for the self-broadening measurements. No attempt was made to determine the uncertainties of the element values ($a(i)$ in Eq. (4)). Also the element values are not given here since it would require several pages of added text; however these values can be obtained from the author upon request.

Fig. 5 has plots of b^o(air) of R- and P-branch transitions for A-type bands including computed and measured width coefficients with the computed values derived from the fitted parameters. The eight plots each represent a related family of rotational transitions. The error bars for the measured values pertain to Δb^o with the extent of the bars equal to $b^o \pm \Delta b^o$. As can be observed, the widths from the bands with $v'_2 = 0$ are slightly larger, on the average, than those with $v'_2 > 0$ for the same rotational transitions. A problem encountered using the fitting function is that the fitted values diverge beyond the experimental data as shown for the $v'_2 > 0$ transitions in plot G. Therefore it is important to include as many higher J transitions in a fit so that the computed values are realistic at those levels. Fig. 6 are similar plots of b^o(air) for B-type, R- and P-branch transitions and plot H shows the divergent effect. Fig. 7 are plots of b^o(air) for A- and B-type, Q-branch transitions. Plots E and F in this figure combine $v'_2 = 0$ and $v'_2 > 0$ bands for forbidden

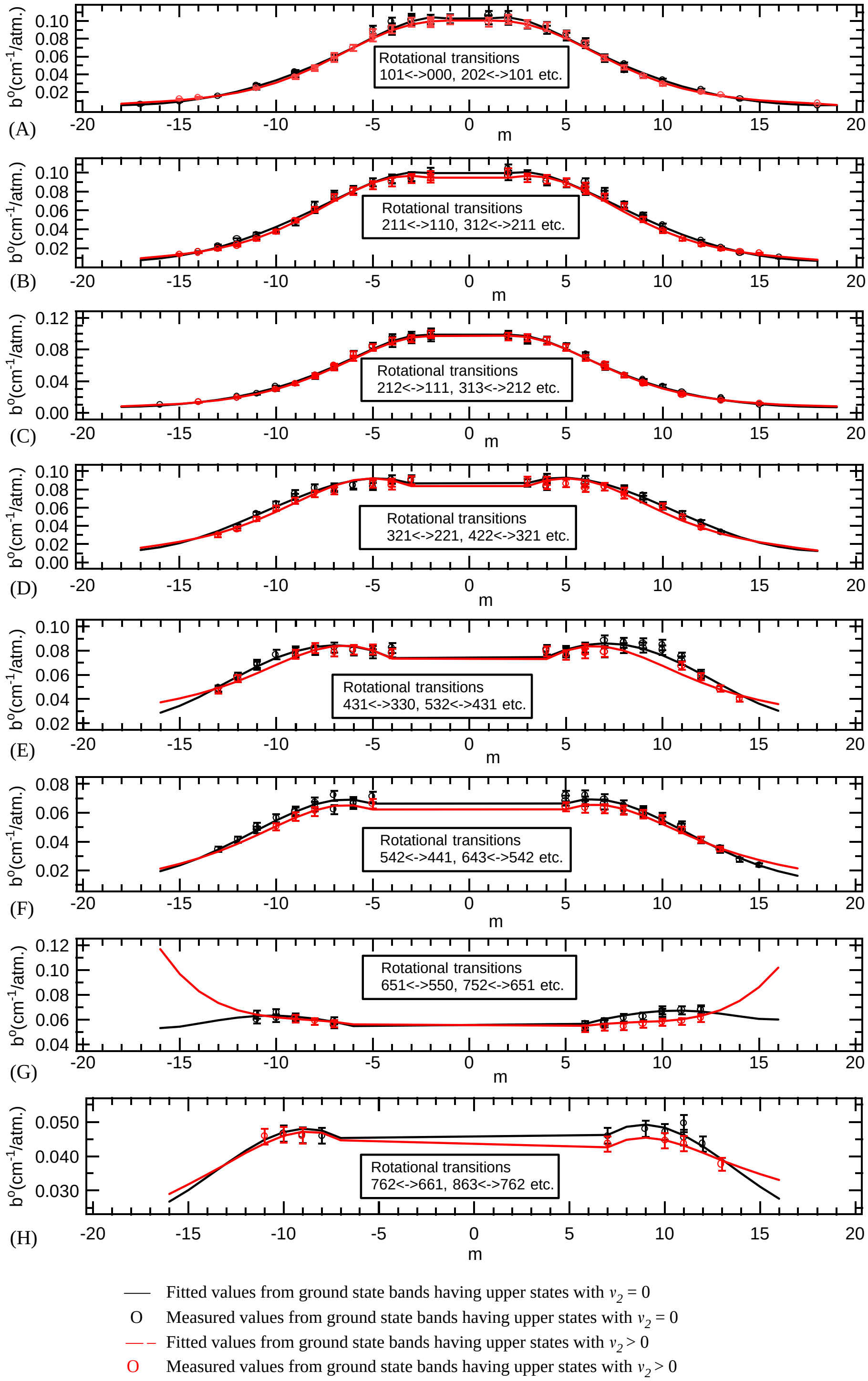

Fig. 5. Air-broadened half-width coefficients, b^{o}(air), of H_2O for A-type bands.

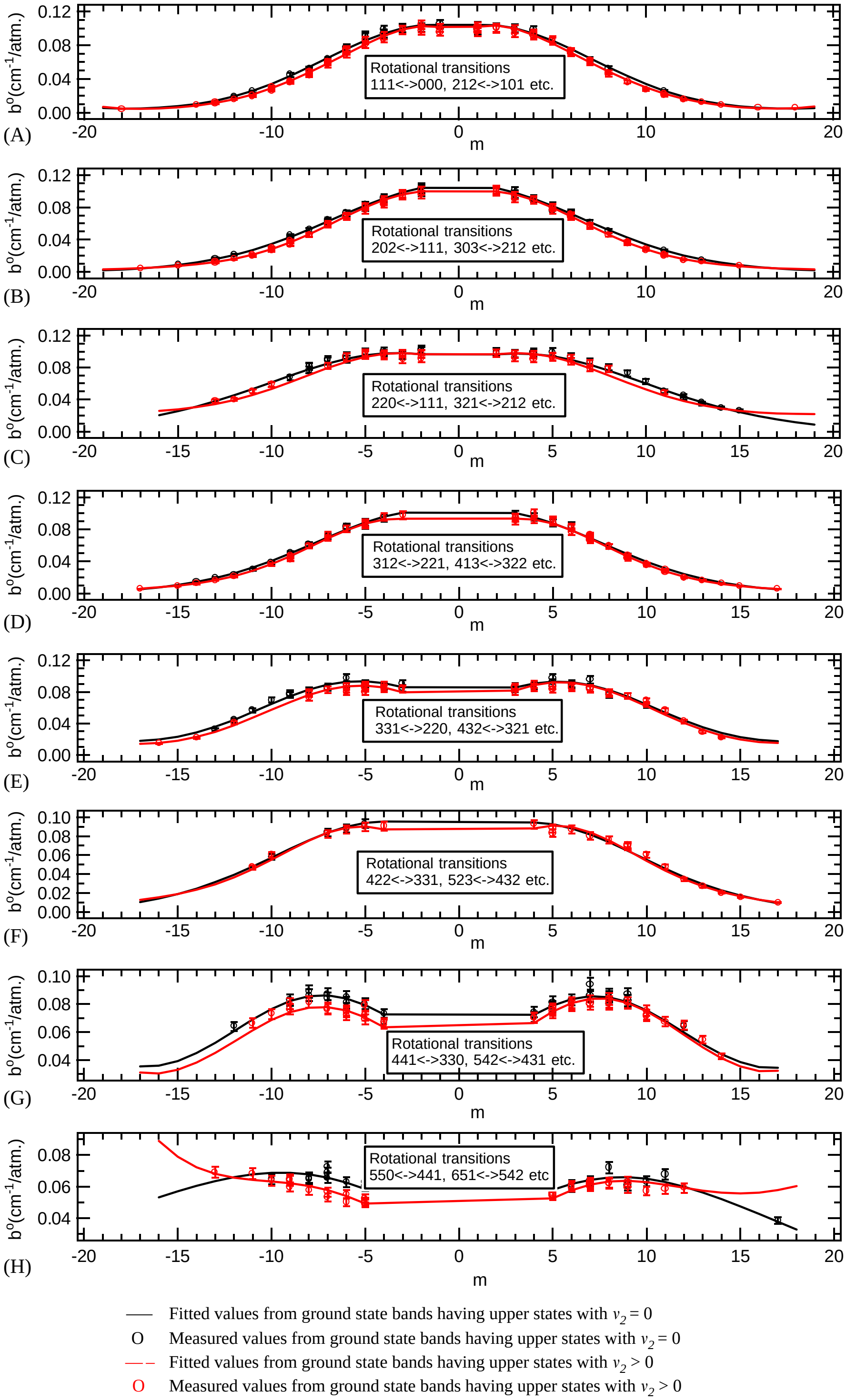

Fig. 6. Air-broadened half-width coefficients, b^{o}(air), of H_2O for B-type bands.

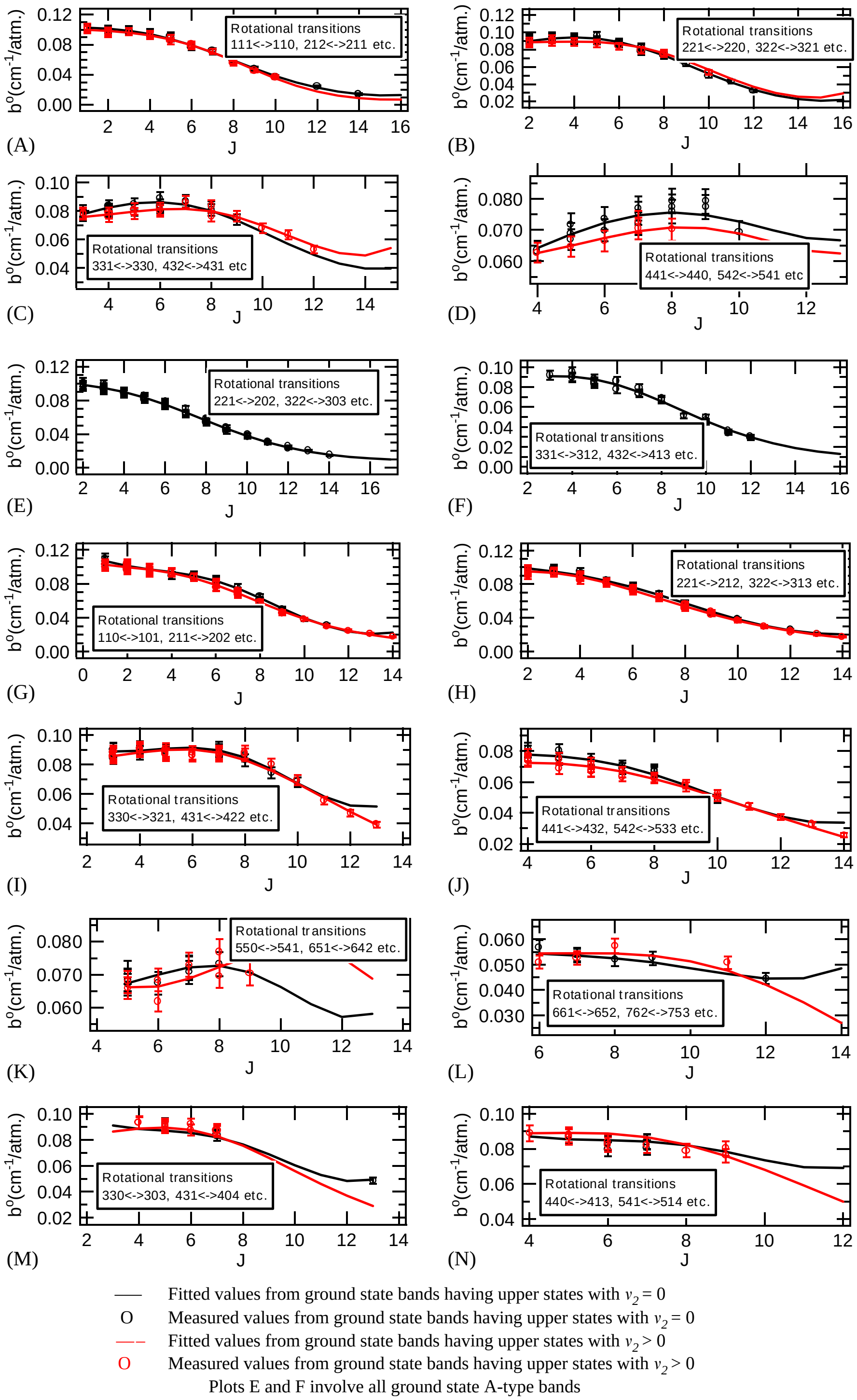

Fig. 7. Air-broadened half-width coefficients, b^o(air), of H_2O for Q-branch transitions in A- and B-type bands.

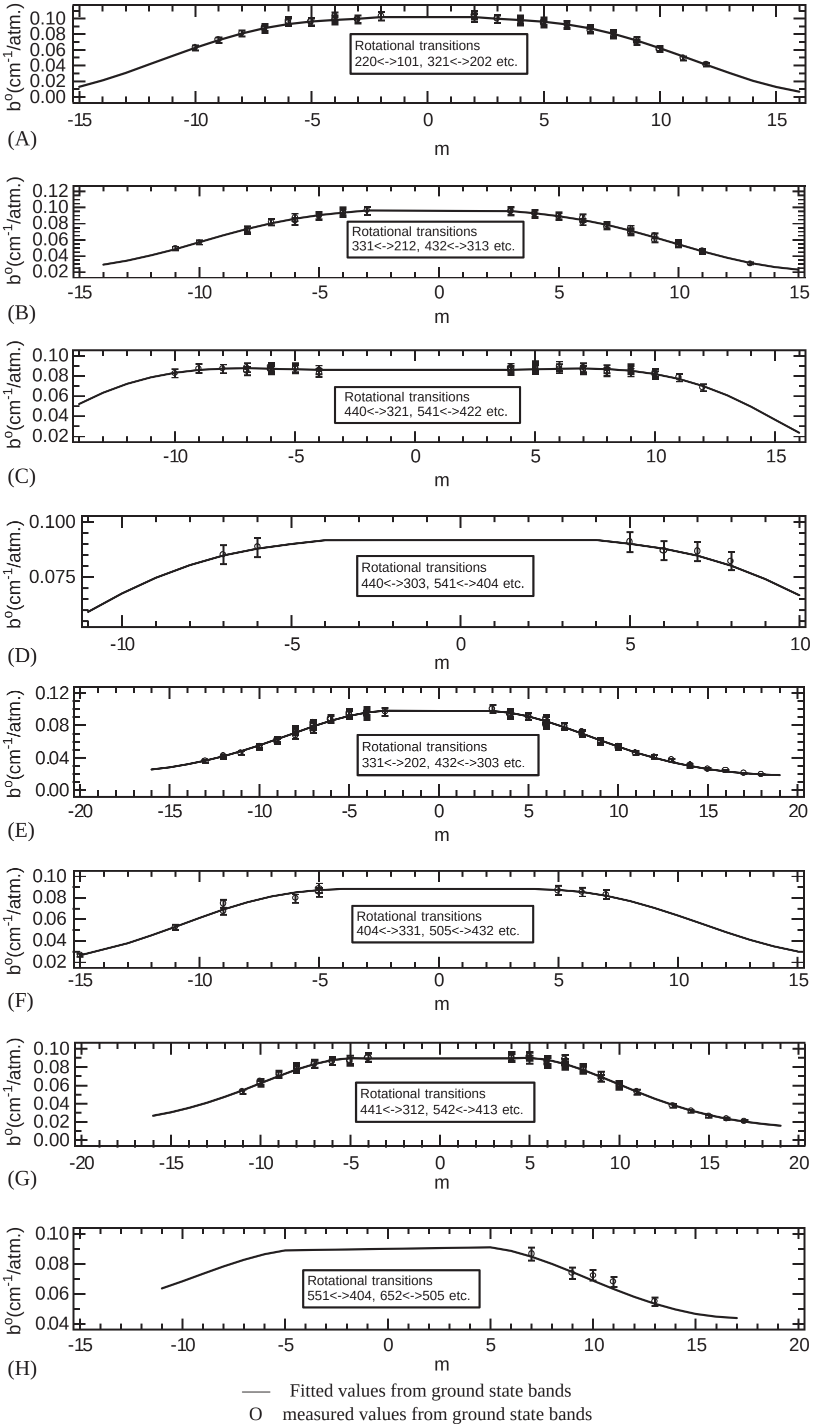

Fig. 8. Air-broadened half-width coefficients, b^{o}(air), of forbidden transitions of H_2O. Forbidden transitions denote the following: $|\Delta K_a| > 1$.

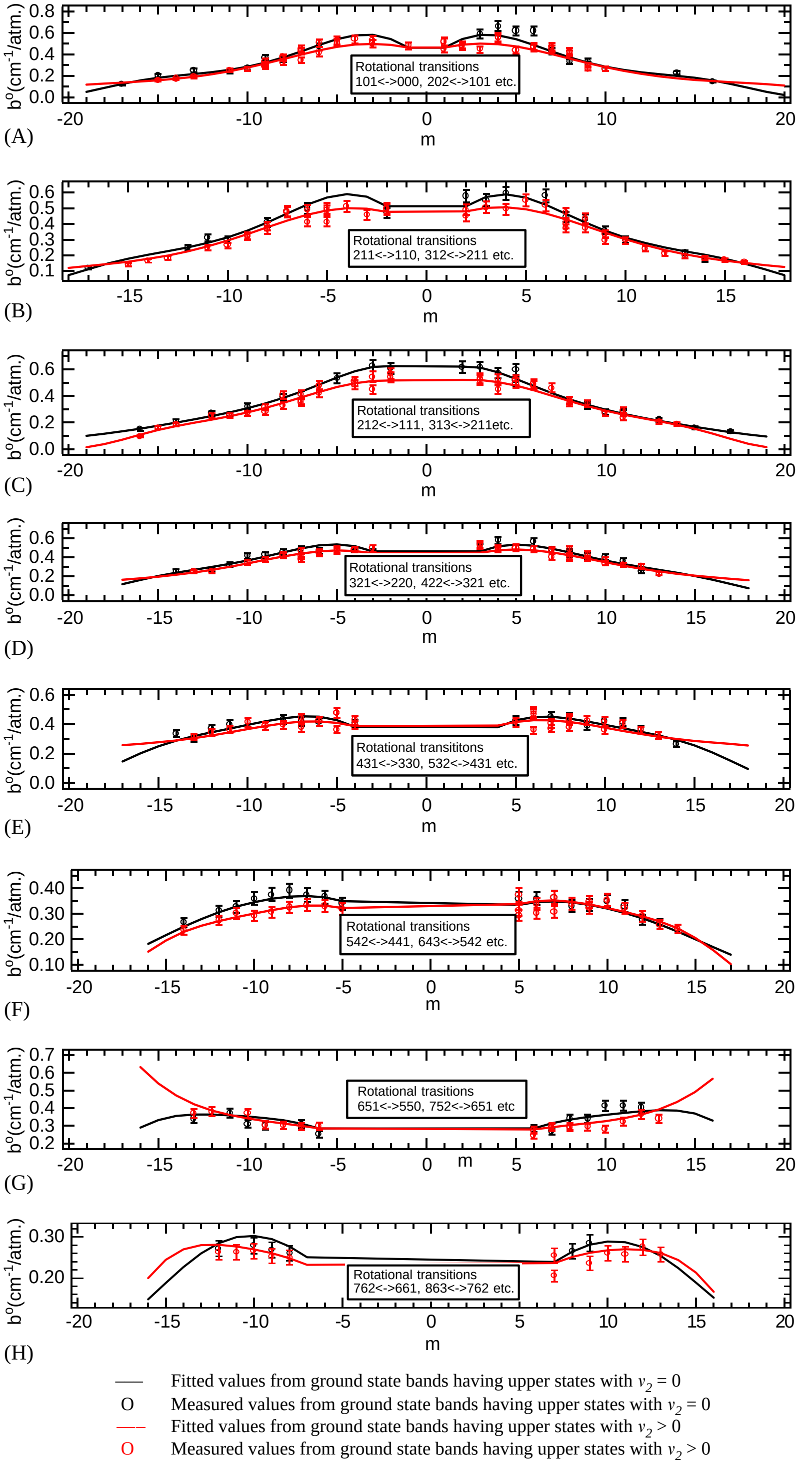

Fig. 9. Self-broadened half-width coefficients, b^{o}(self), of H_2O for A-type bands.

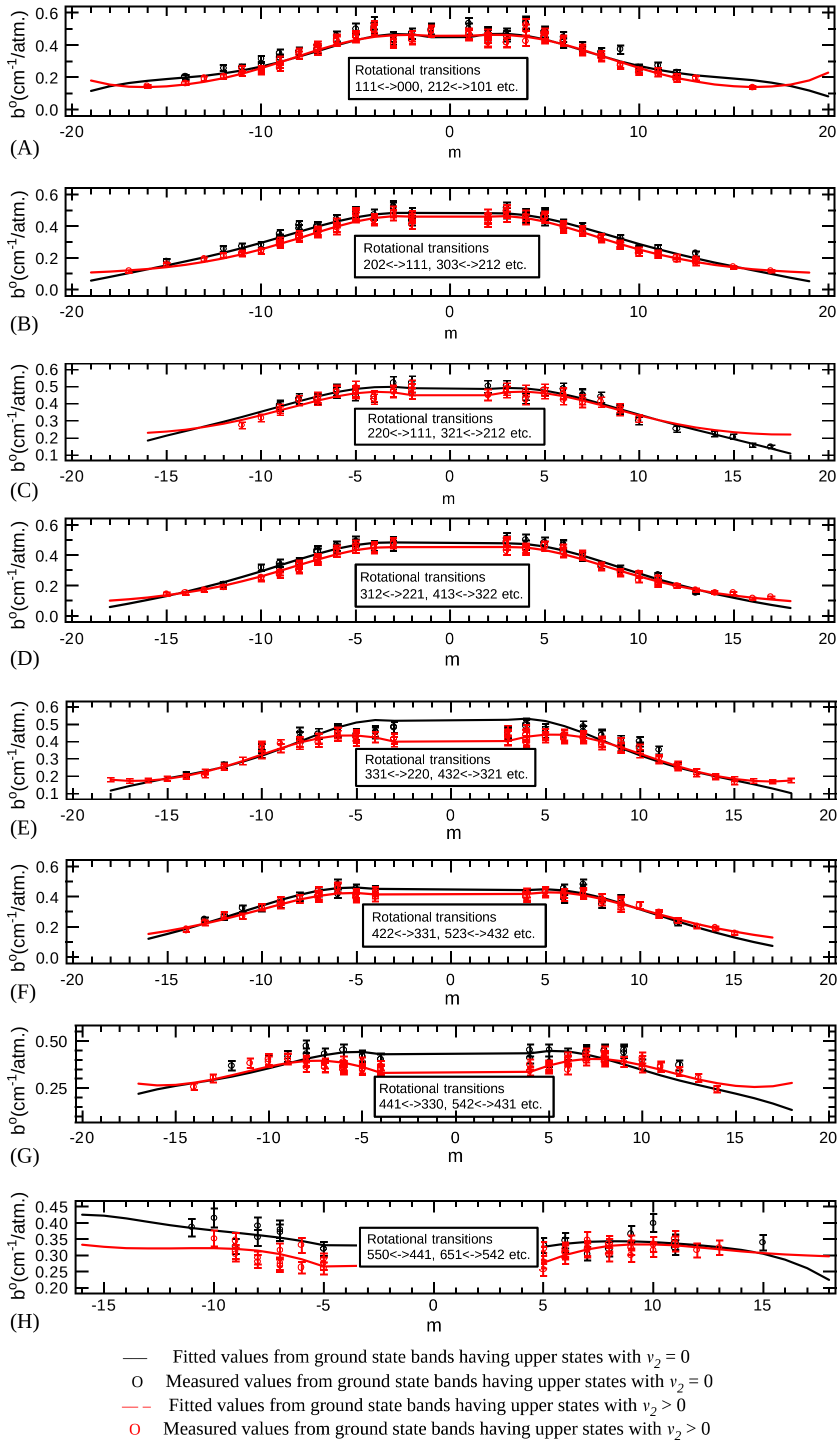

Fig. 10. Self-broadened half-width coefficients, b^{o}(self), of H_2O for B-type bands.

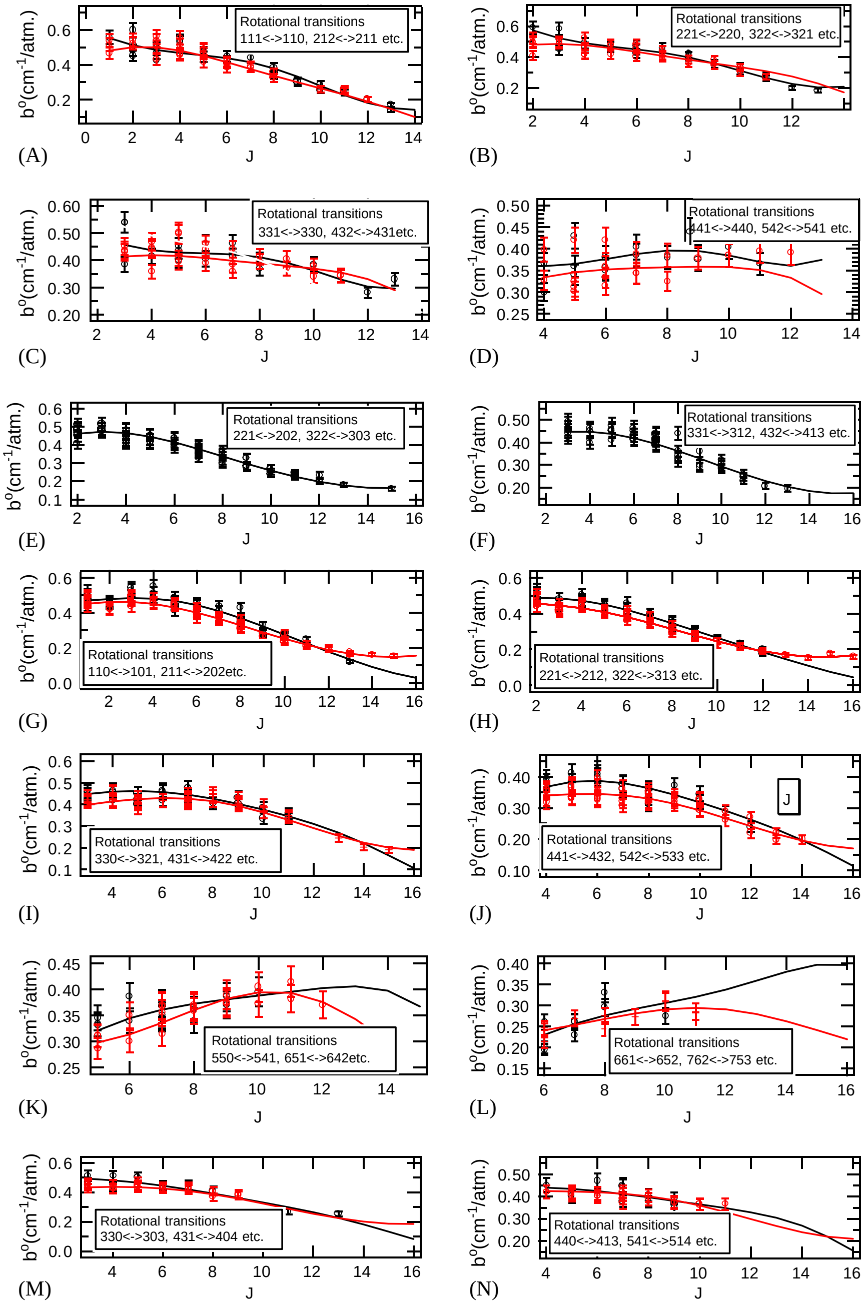

— Fitted values from ground state bands having upper states with $v_2 = 0$
O Measured values from ground state bands having upper states with $v_2 = 0$
– – Fitted values from ground state bands having upper states with $v_2 > 0$
O Measured values from ground state bands having upper states with $v_2 > 0$
Plots E and F involve all ground state A-type bands

Fig. 11. Self-broadened half-width coefficients, b^o(self), of H_2O for Q-branch transitions in A- and B-type bands.

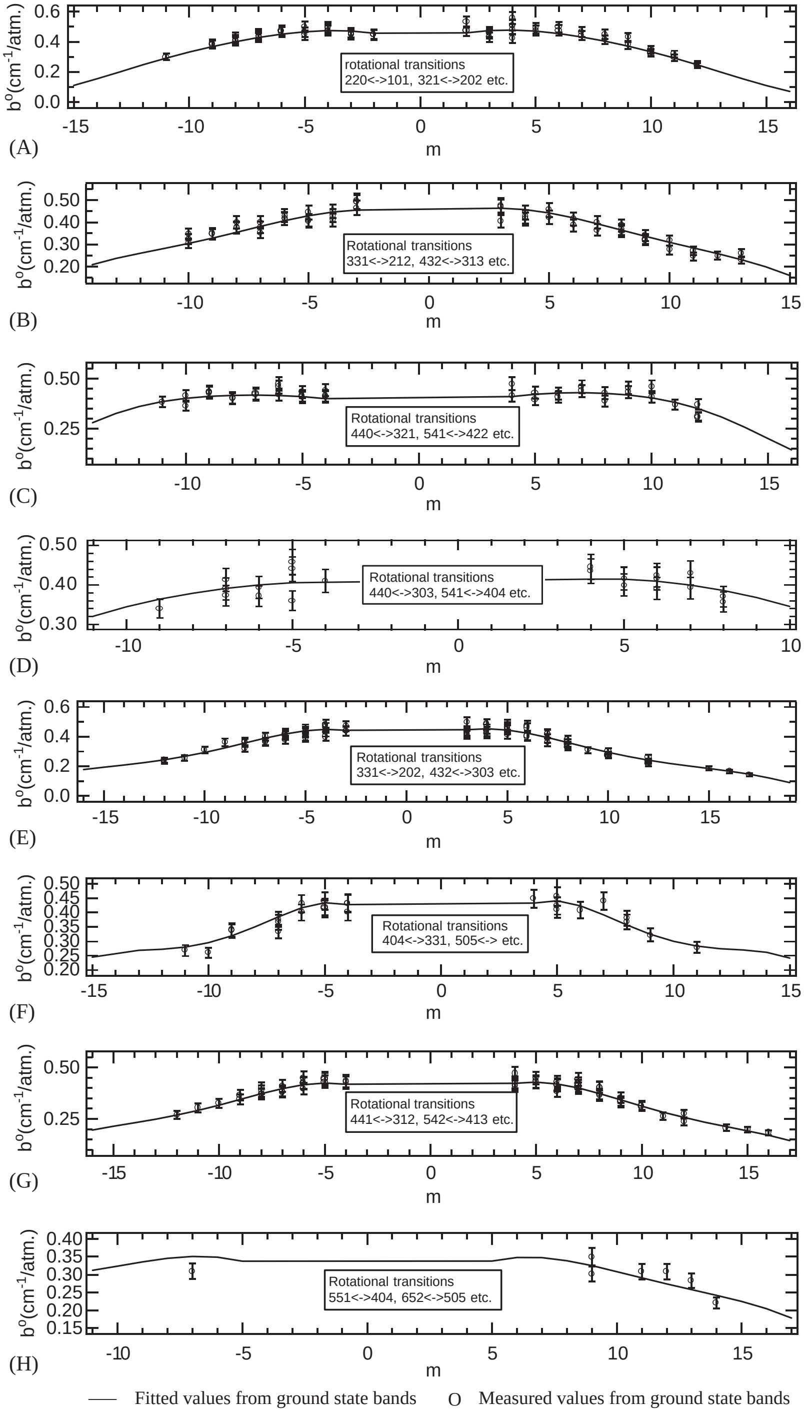

Fig. 12. Self-broadened half-width coefficients, b^o(self), of forbidden transitions of H_2O. Forbidden transitions denote the following: $|\Delta K_a| > 1$.

A-type transitions as noted in Table 3 therefore only one computed curve is given in each plot. Again divergent effects are displayed in plots K, L, M, and N. Fig. 8 shows eight plots of observed and computed $b^{\mathrm{o}}(\mathrm{air})$ for forbidden P- and R-branch transitions ($|\Delta K_{\mathrm{a}}|>1$) of A- and B-type bands which are for $v_2'=0$ and$v_2'>0$ as indicated from the fitting statistics given in Table 3. Figs. 9–12 pertain to self-broadened width coefficients and are similar plots to Figs. 5–8, respectively.

5. Pressure-induced frequency shifts

The input line list to the NLLS program included accurate, calculated line positions of H_2O and HDO which were used to derive the shifted positions of the least-squares fitted air-broadened spectra. The difference between the measured and computed position, d, is related to the shift coefficient, d^{o}, by

$$d = d^{\mathrm{o}} \times p_{\mathrm{f}}, \tag{7}$$

where p_{f} is the foreign or air partial pressure. The effect due to self-broadening was not included in this work to determine d^{o} although, if included, it could influence the value for $d^{\mathrm{o}}(\mathrm{air})$ but not by more than 10% of the value derived from Eq. (7). For a given measured line, $d^{\mathrm{o}}(\mathrm{obs.})$ was determined from the average of measurements from various runs using Eq. (7) and Δd^{o} was the error or uncertainty resulting from the average.

The averaged values of the pressure-shift coefficients, $d^{\mathrm{o}}(\mathrm{air})$, do not have nearly the smooth behavior as that of the width coefficients in terms of related families of transitions. The smoothed values of $d^{\mathrm{o}}(\mathrm{air})$ were derived from hand-drawn plots of related families of transitions. Fig. 13 show eight plots of measured and smoothed values of $d^{\mathrm{o}}(\mathrm{air})$ for two related families of R- and P-branch transitions of the A-type bands: 001-000, 011-000, 021-000, and 101-000. The error bars for the measured values pertain to Δd^{o} with the extent of the bars equal to $d^{\mathrm{o}} \pm \Delta d^{\mathrm{o}}$. Fig. 14 is a similar graph for two more related families of the same A-type bands. Fig. 15 displays two related families of Q-branch transitions for these A-type bands with d^{o} plotted against J_{K} in which $J_{\mathrm{K}} = J$ for $\gamma'' = 0$ and $J_{\mathrm{K}} = -J$ for $\gamma'' = 1$ where double prime pertains to the lower state. Fig. 16 shows $d^{\mathrm{o}}(\mathrm{obs.})$ and $d^{\mathrm{o}}(\mathrm{smoothed})$ for two related families of forbidden P- and R-branch transitions of these A-type bands. Fig. 17 plots m against d^{o} for one related family of rotational transitions of eight B-type bands including the 010-000 band of which $d^{\mathrm{o}}(\mathrm{obs.})$ and $d^{\mathrm{o}}(\mathrm{smoothed})$ were taken from Ref. [1]. Fig. 18 involves two related families of P- and R-branch transitions for four B-type bands covering the spectral region encompassed in this study.

Fig. 19 are plots of d^{o} against J_{K} for Q-branch transitions of the four B-type bands used in Fig. 18. $J_{\mathrm{K}} = J$ for $\Delta K_{\mathrm{a}} = 1$ and $J_{\mathrm{K}} = -J$ for $\Delta K_{\mathrm{a}} = -1$ with B-type transitions.

6. Results and discussion

Table 4 lists observed and computed values of $b^{\mathrm{o}}(\mathrm{air})$, $b^{\mathrm{o}}(\mathrm{self})$, and $d^{\mathrm{o}}(\mathrm{air})$ for lines with measured air-width coefficient uncertainties, of 2% or less. The fitted values of $b^{\mathrm{o}}(\mathrm{air})$ and $b^{\mathrm{o}}(\mathrm{self})$

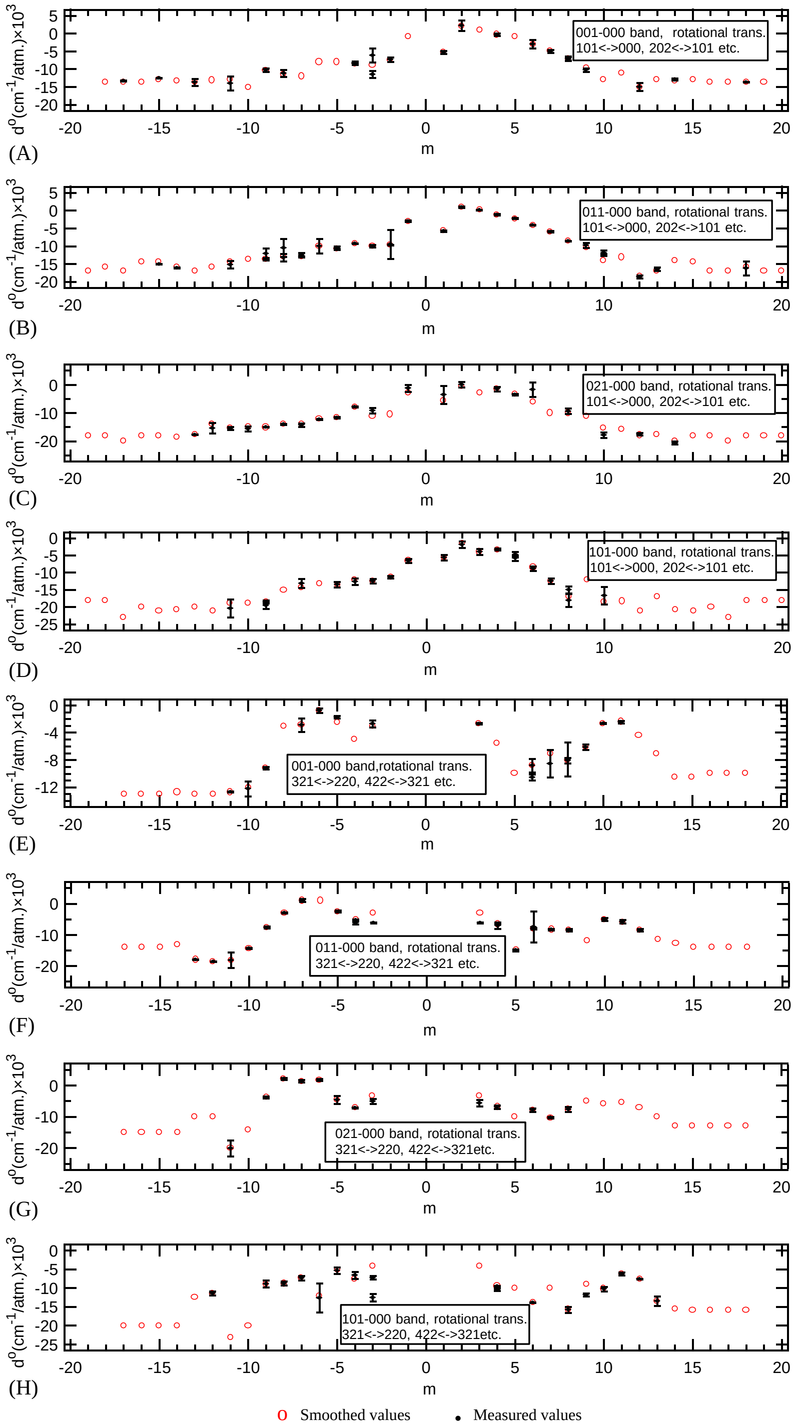

Fig. 13. Air-broadened pressure induced frequency shifts, d^{o}(air), of H_2O for A-type bands.

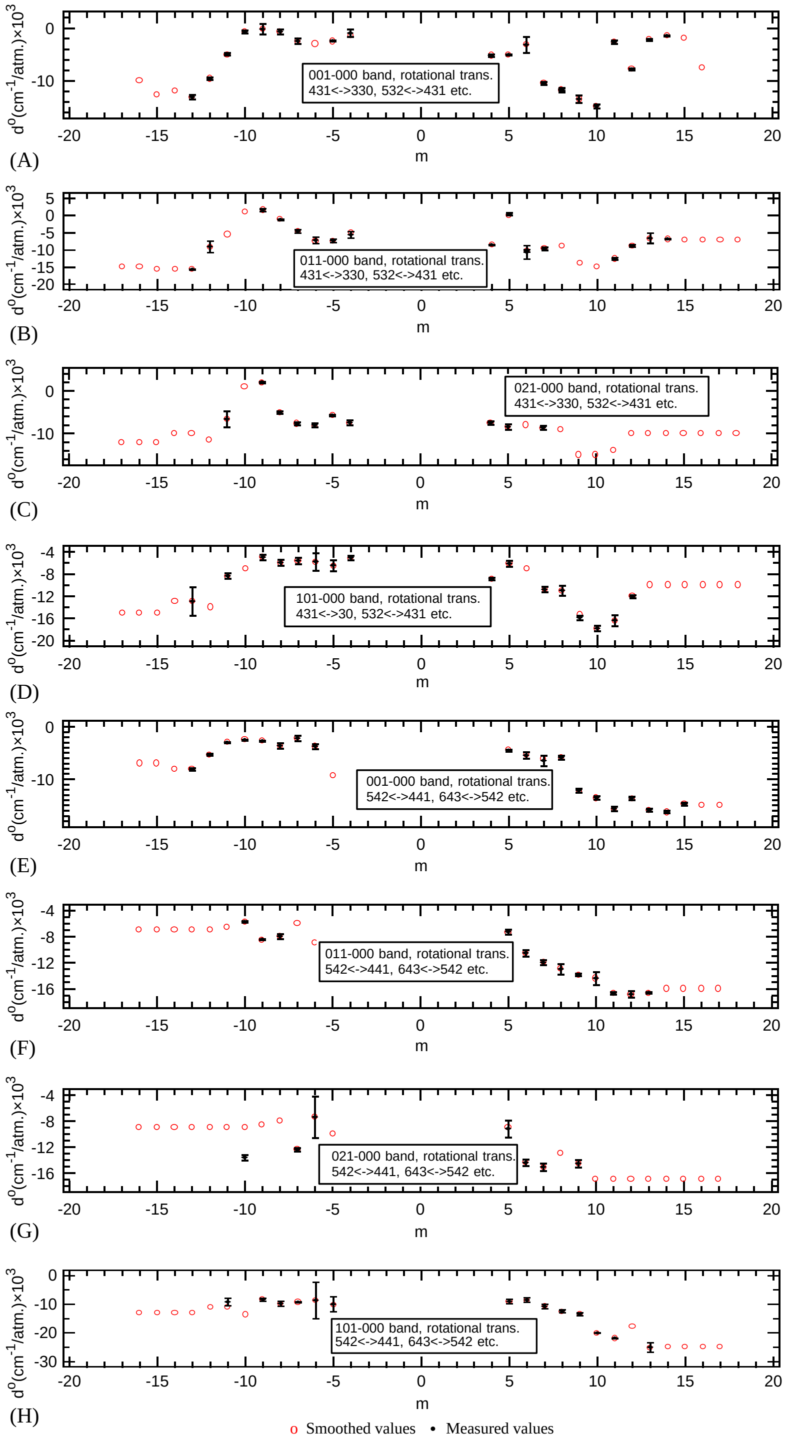

Fig. 14. Air-broadened pressure-induced frequency shifts, d^{o}(air), of H_2O for P- and R-branch transitions of A-type bands.

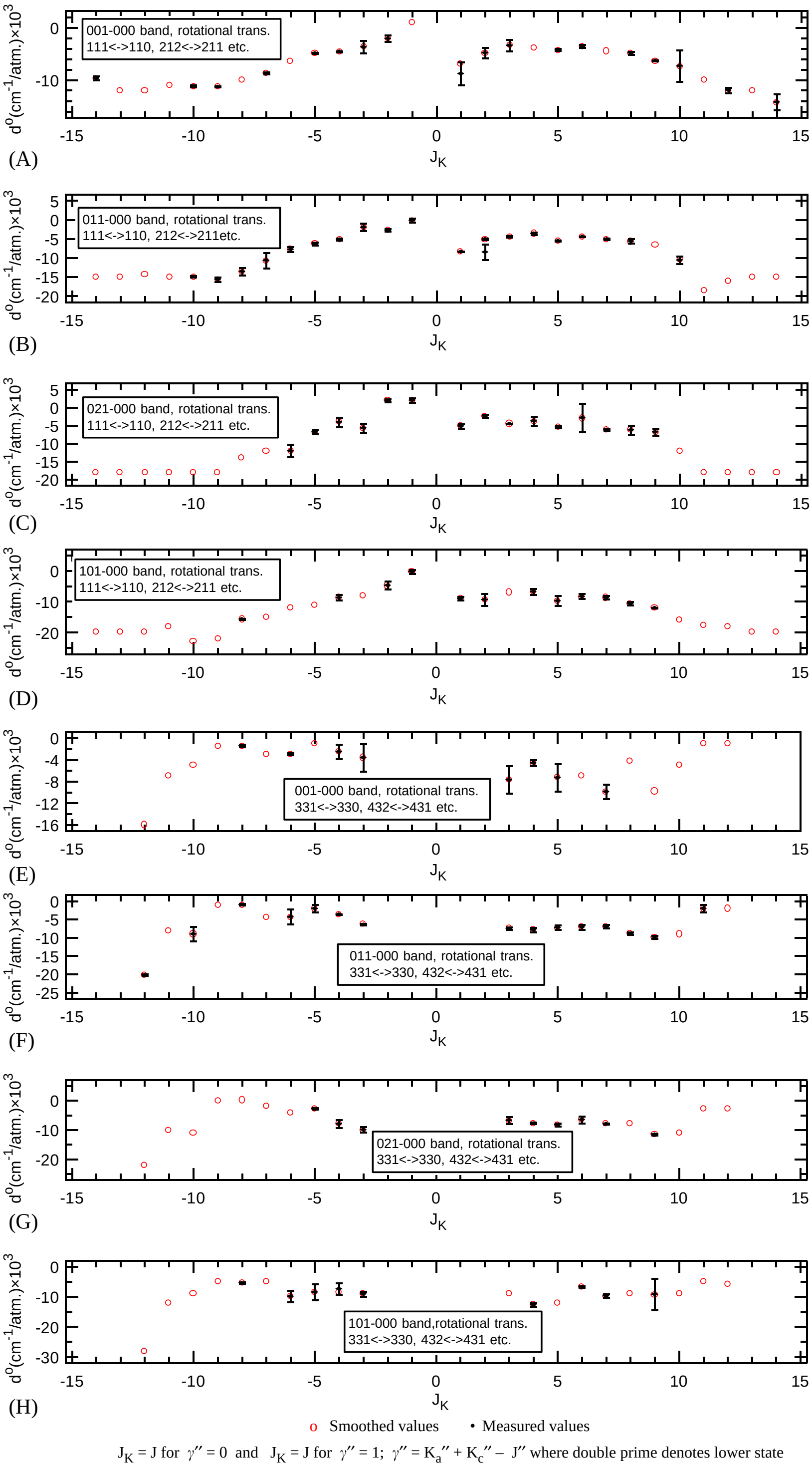

Fig. 15. Air-broadened pressure-induced frequency shifts, d^o(air), of H_2O for Q-branch transitions of A-type bands.

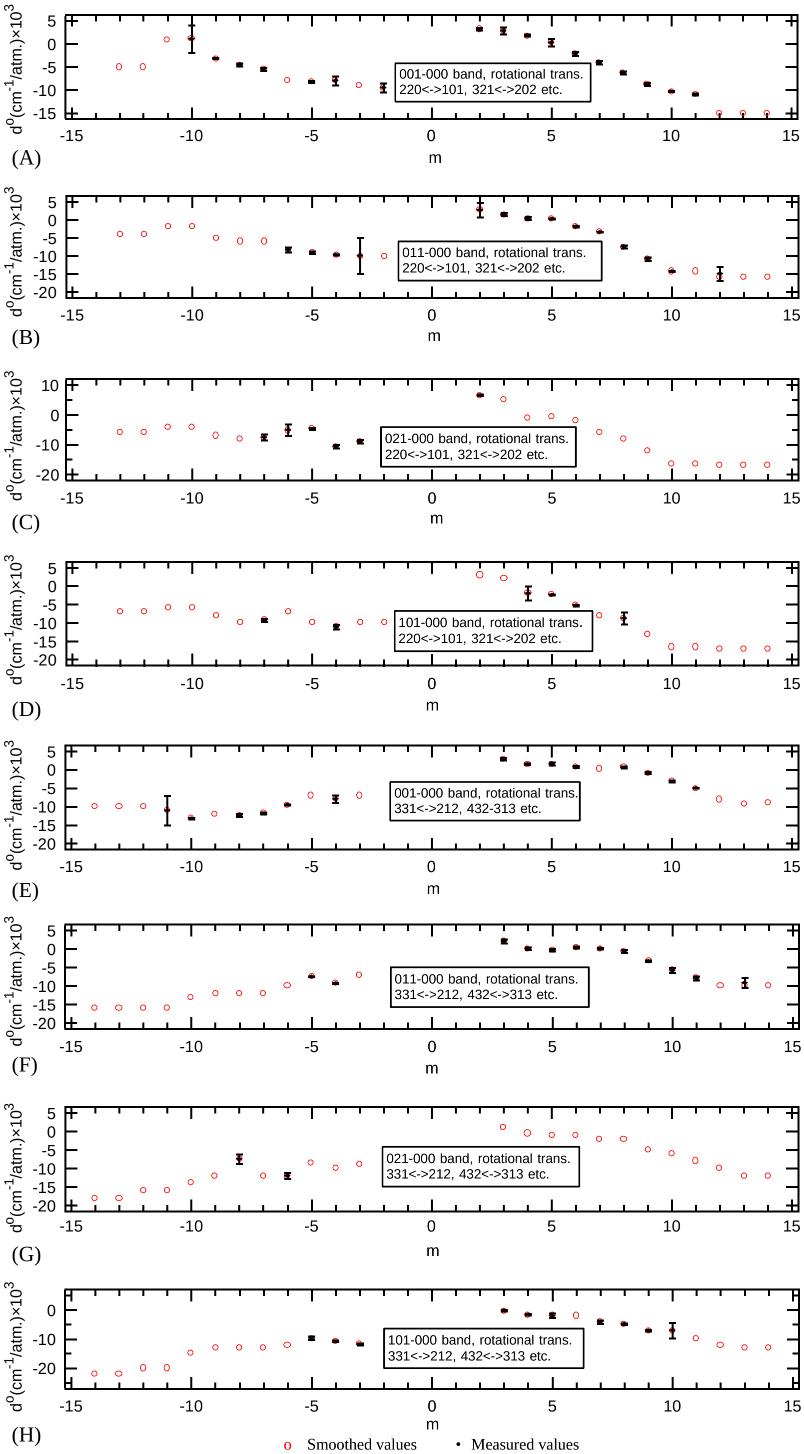

Fig. 16. Air-broadened pressure-induced frequency shifts, $d^{o}(\text{air})$, of H_2O for forbidden transitions of A-type bands. Forbidden transitions denote the following: $|\Delta K_a| > 1$.

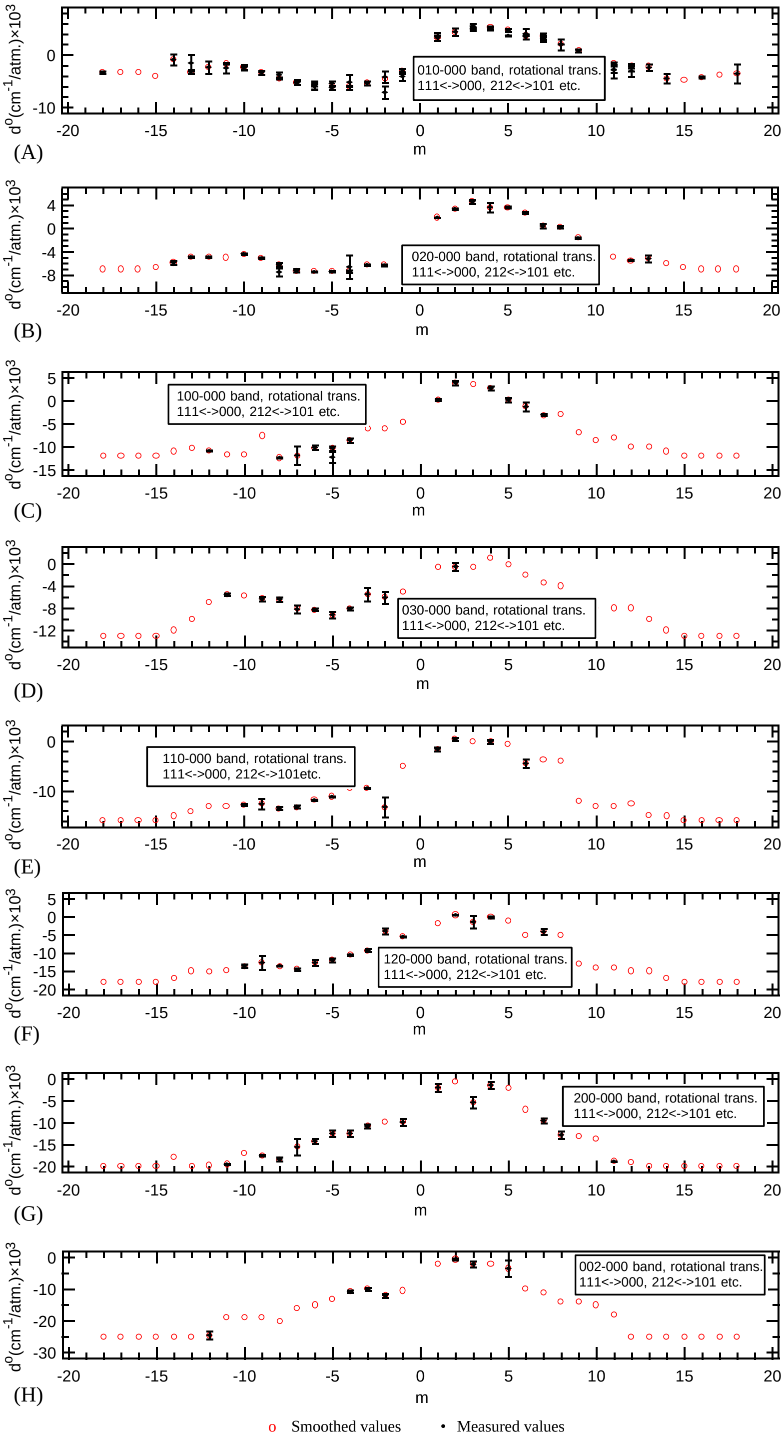

Fig. 17. Air-broadened pressure-induced frequency shifts, d^o(air), of H_2O for P- and R-branch transitions of B-type bands.

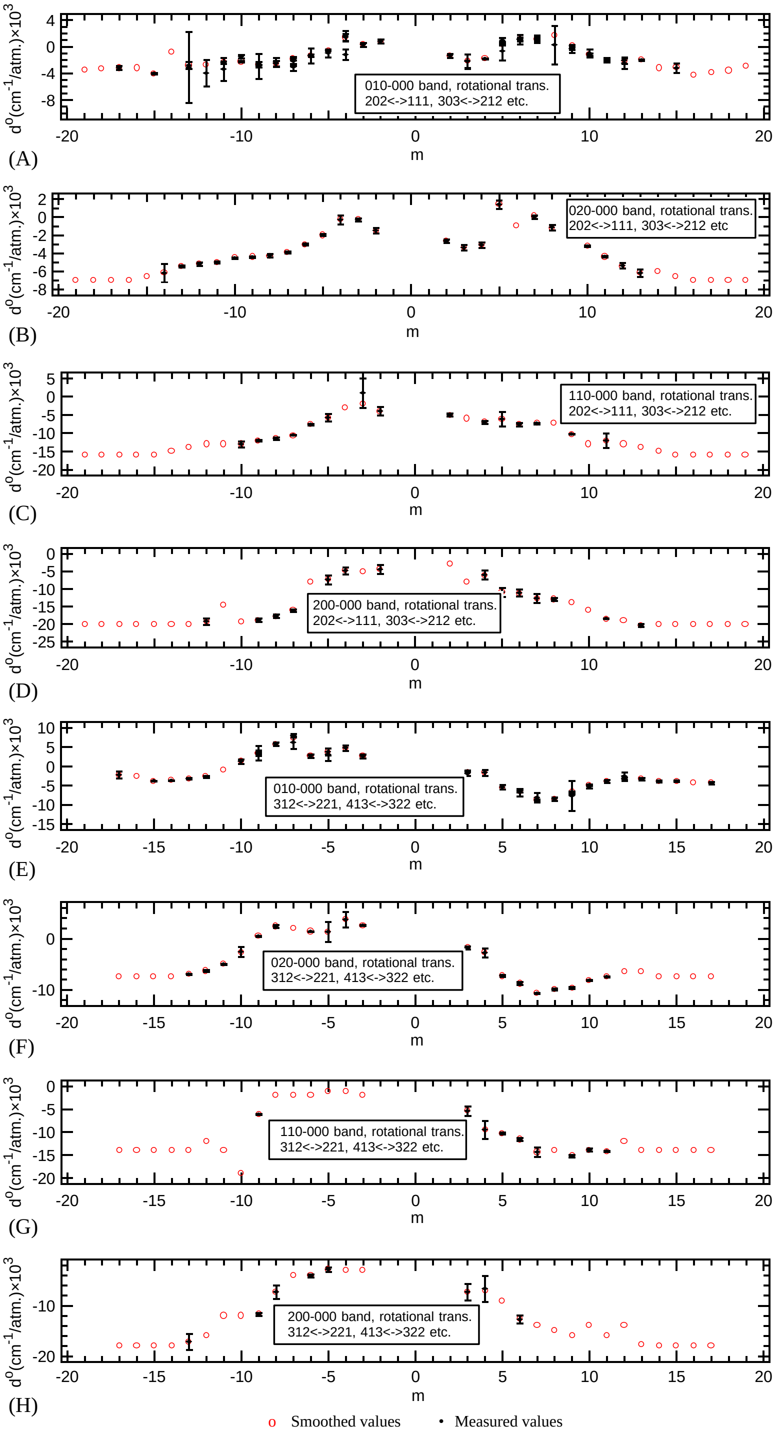

Fig. 18. Air-broadened pressure-induced frequency shifts, d^o(air), of H_2O for P- and R-branch transitions of B-type bands.

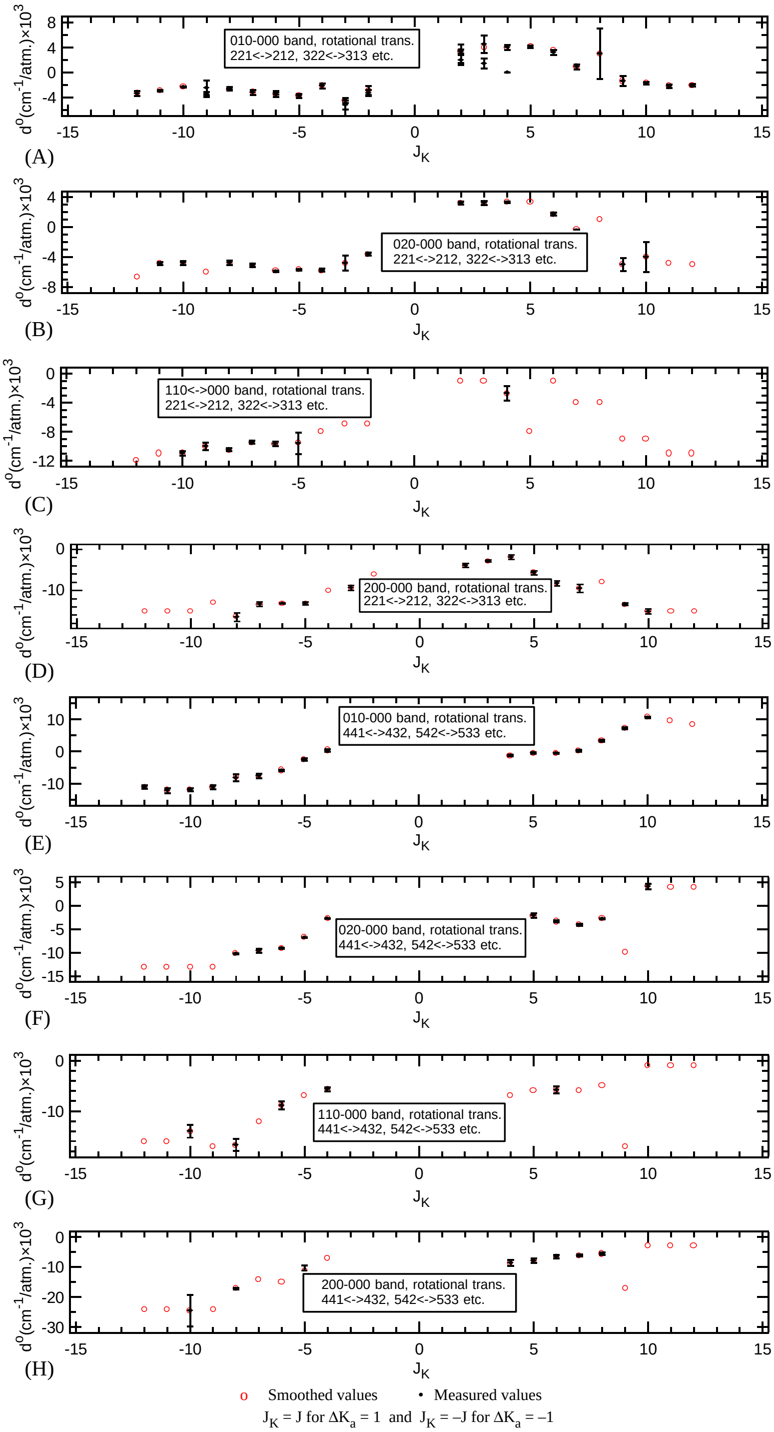

Fig. 19. Air-broadened pressure-induced frequency shifts, d^o(air), of H_2O for Q-branch transitions of B-type bands.

were computed from the coefficients derived from the various least-squares fits shown in Table 3 using the term elements given in Table 2. The air-broadened results are from measurements obtained in this study whereas the measured self-broadened width coefficients were taken from Ref. [3].

There have been numerous reports on the measurements of air- and self-broadened width coefficients [1,4–33,4,46], and it is worth a comparison of the results from several of those with the values obtained in the present work. Obviously to list these would require a very long compilation so the comparison was made by computing the widths of the measured transitions using the parameters obtained in this study and displaying the differences in a statistical mode, and this is given in Table 5. The computed values were for the conditions given in Table 3 with the term elements given in Table 2 and the expression given in Eq. (4). The table gives the frequency extent of the measurements, number of lines measured, NT, standard deviations in percent between all the observed and computed b^o, σ_T%, and the measured uncertainties, un_T%. Number of lines of which the observed b^o differs from the computed b^o by 10% or less, NA, the ratio in percent of NA/NT, the standard deviations in percent between the measured lines with $|[b^o(\text{obs.}) - b^o(\text{calc.})]/b^o(\text{obs.})|$ of 0.1 or less, σ_A%, and the associated measured uncertainties, un_A%, and the extent of the rotational quantum assignments for all the measurements. A few of the reports do not give measured uncertainties and they are denoted in the table with "NG" for un_T% and un_A%. Four of the entries, marked with an asterisk, represent N_2 broadened width coefficients of H_2O, and these data were converted to air-broadening by multiplying their values by 0.89 which is the averaged ratio of $b^o(\text{air})/b^o(N_2)$ found in Ref. [1]. Devi et al. [16] state that their measurements were of nitrogen broadening, however their values of b^o indicate that they were air-broadened and, therefore, were not modified for use in the table. Inspection of their [16] entry shows excellent agreement with the computed values. The measurements of Merienne et al. [35] and Fally et al. [36] contained several lines that were not assigned although the air-broadened width coefficients were derived. These lines were not included in the calculations for that set given in Table 5.

An indication of the overall quality of the measurements can be derived from the ratio, NA/NT%. The criterion used here for good quality measurements was for NA/NT% of about 80% or better for air-broadening and about 60% or better for self-broadening. Inspection of the table indicates that several studies other than this work fall in the good quality region: Brown et al. [30], Zou and Varanasi [33], Devi et al. [16], Rinsland et al. [14], Grossmann and Browell [13], Ponsardin and Browell [21], Claveau et al. [29], and Mandin et al. [10,12] for air-broadening and Zou and Varanasi [33], and Grossmann and Browell [11] for self-broadening. The entries from this work in Table 5 were given in terms of oxygen isotopic species with one entry for "hot" bands. This includes the measurements by Toth [1] and Toth et al. [2] for air-broadened and self-broadened widths, respectively, in the ν_2 region and other self-broadened width measurements by Toth [3]. The fitted results given in Table 3 were for ground state band measurements which included some $H_2{}^{17}O$ and $H_2{}^{18}O$ transitions. It was determined that the measured hot band values of b^o(air) and b^o(self) were smaller in value ($\approx 5\%$) than their rotational transition counterparts measured in the ground state bands and were not included in the fitting procedure.

Listings of transitions have been created which contain the computed linewidth coefficients, b^o, derived from the $a(i)$'s and Eq. (4). These listings can be obtained with other compilations from a

Table 4
Measured and fitted values of air- and self-broadened width coefficients, b^{o}, and air-broadened shift coefficients, d^{o}, for selected transitions of H_2O

m	Computed position	Upper			Lower			b^{o}(air)			b°(self)			d^{o}(air)			Band	
		J	K_a	K_c	J	K_a	K_c	Meas.	Δ%	Fitted	Meas.	Δ%	Fitted	Meas.	Δ	Smooth		
1	3055.61013	5	2	4	6	1	5	0.0820	0.7	0.0789	0.399	0.8	0.405	1.36	0.10	1.40	020	000
1	3107.33075	3	2	1	3	3	0	0.0872	0.8	0.0858	0.399	1.0	0.398	−2.15	0.11	−2.20	020	000
1	3276.96471	8	3	5	8	2	6	0.0855	0.8	0.0830	0.429	0.0	0.414	6.50	0.80	6.50	020	000
1	3458.05361	6	2	4	5	1	5	0.0907	0.7	0.0871	0.454	0.9	0.444	1.20	0.70	1.20	020	000
1	4493.95847	8	1	8	9	0	9	0.0350	1.7	0.0365	0.284	9.9	0.287	−6.50	0.40	−6.50	030	000
1	4524.09751	7	1	6	8	2	7	0.0624	4.0	0.0588	0.353	9.9	0.350	−14.50	4.00	−14.50	030	000
1	4531.50886	6	0	6	7	1	7	0.0574	1.0	0.0583	0.352	9.9	0.369	−8.20	0.70	−8.20	030	000
1	4535.19001	8	2	7	9	1	8	0.0450	1.3	0.0464	0.267	10.1	0.296	−2.00	1.00	−2.00	030	000
1	4535.35713	6	1	6	7	0	7	0.0549	0.7	0.0576	0.362	9.9	0.361	−5.40	0.40	−5.40	030	000
1	4565.11725	4	0	4	5	1	5	0.0820	1.2	0.0807	0.425	10.1	0.431	−9.20	0.60	−9.20	030	000
1	4572.25015	6	2	5	7	1	6	0.0695	1.4	0.0686	0.358	10.1	0.371	−0.60	0.30	−0.60	030	000
1	4576.78245	4	1	4	5	0	5	0.0772	1.0	0.0800	0.420	10.0	0.428	−3.33	0.15	−3.30	030	000
1	4580.07455	3	0	3	4	1	4	0.0896	1.1	0.0908	0.465	10.1	0.451	−8.10	0.30	−8.10	030	000
1	4594.92406	2	0	2	3	1	3	0.0963	1.0	0.0985	0.428	10.0	0.461	−5.50	1.20	−5.50	030	000
1	4611.08358	1	0	1	2	1	2	0.0995	2.0	0.1025	0.477	10.1	0.463	−6.10	1.10	−6.10	030	000
1	4622.26188	2	1	2	3	0	3	0.0930	1.6	0.0961	0.451	10.1	0.463	−0.98	0.20	−1.00	030	000
1	4648.20822	1	0	1	1	1	0	0.1019	1.5	0.1024	0.435	10.1	0.450	−7.10	0.90	−7.10	030	000
1	4812.92764	2	2	1	1	1	0	0.0968	1.5	0.0943	0.450	10.0	0.448	1.50	0.70	1.50	030	000
1	4918.36259	7	2	6	8	4	5	0.0714	1.1	0.0730	0.359	10.0	0.350	−16.53	0.25	−16.50	011	000
1	4938.19752	7	4	3	8	5	4	0.0628	0.8	0.0648	0.353	9.9	0.344	−1.10	0.30	−1.10	110	000
1	4942.45580	6	3	3	7	5	2	0.0798	0.9	0.0812	0.397	10.1	0.372	−5.30	0.70	−5.30	011	000
1	4948.15416	6	2	5	7	3	4	0.0865	0.7	0.0862	0.445	10.1	0.417	−7.04	0.10	−7.00	110	000
1	4966.56429	6	3	4	7	4	3	0.0745	0.8	0.0749	0.385	10.1	0.371	−11.65	0.35	−11.70	110	000
1	4992.93774	5	2	4	6	4	3	0.0785	1.0	0.0804	0.379	10.0	0.382	−10.41	0.25	−10.40	011	000
1	4994.24811	5	2	4	6	3	3	0.0860	1.7	0.0882	0.435	10.1	0.428	−6.30	2.00	−6.30	110	000
1	4996.96239	5	3	3	6	4	2	0.0731	1.4	0.0727	0.368	10.1	0.367	−9.50	0.50	−9.50	110	000
1	5008.09908	6	2	4	7	4	3	0.0846	0.6	0.0875	0.420	10.0	0.418	−6.91	0.08	−6.90	011	000
1	5010.85898	4	1	4	5	2	3	0.0978	0.8	0.0932	0.473	9.9	0.461	−5.70	0.20	−5.70	110	000
1	5013.26920	7	2	5	8	3	6	0.0792	0.6	0.0760	0.400	10.0	0.395	−10.17	0.15	−10.20	110	000
1	5020.17076	9	0	9	10	1	10	0.0305	2.0	0.0289	0.253	9.9	0.256	−12.75	0.15	−12.80	110	000
1	5024.67283	4	3	2	5	4	1	0.0714	1.8	0.0689	0.370	10.0	0.356	−5.88	0.50	−5.90	110	000
1	5025.62278	5	2	3	6	4	2	0.0874	1.1	0.08741	0.420	10.0	0.416	−8.10	1.10	−8.10	011	000
1	5029.61597	4	3	1	5	4	2	0.0788	0.9	0.0705	0.385	10.1	0.363	−6.49	0.08	−7.00	110	000
1	5032.85140	4	2	3	5	3	2	0.0878	0.8	0.0880	0.427	10.1	0.431	−8.68	0.20	−8.70	110	000
1	5042.68477	4	2	2	5	4	1	0.0868	0.8	0.0864	0.415	10.1	0.410	−7.73	0.08	−7.70	011	000

1	5043.04750	8	0	8	9	1	9	0.0377	1.3	0.0376	0.307	10.1	0.293	−12.60	1.00	−12.60	110	000
1	5043.35078	8	1	8	9	0	9	0.0380	0.8	0.0365	0.307	10.1	0.287	−12.02	0.15	−12.00	110	000
1	5043.73781	12	2	10	13	2	11	0.0293	1.7	0.0317	0.245	10.2	0.238	−17.98	0.13	−18.00	011	000
1	5046.02205	5	0	5	5	3	2	0.0918	0.9	0.0893	0.441	10.0	0.434	−12.50	2.00	−12.50	110	000
1	5049.00870	4	1	4	5	3	3	0.0902	0.7	0.0905	0.409	10.0	0.430	−7.48	0.09	−7.50	011	000
1	5049.36626	5	0	5	6	2	4	0.0951	10.1	0.0926	0.465	10.1	0.450	−8.35	0.70	−8.40	011	000
1	5049.51175	12	1	11	13	1	12	0.0187	1.6	0.0197	0.183	9.8	0.199	−16.07	0.15	−16.10	011	000
1	5051.11759	3	3	1	4	4	0	0.0688	1.0	0.0638	0.370	10.0	0.336	−5.25	0.25	−5.30	110	000
1	5051.43682	7	1	6	8	2	7	0.0683	0.7	0.0588	0.366	10.1	0.350	−15.51	0.20	−15.50	110	000
1	5054.46210	9	1	9	9	2	8	0.0468	1.1	0.0443	0.286	10.1	0.278	−10.00	0.50	−10.00	110	000
1	5060.41714	10	4	6	11	4	7	0.0723	1.4	0.0691	0.393	9.9	0.372	1.60	1.00	1.60	011	000
1	5061.00513	3	1	3	4	2	2	0.0966	1.2	0.0969	0.444	9.9	0.469	−7.18	1.50	−7.20	110	000
1	5063.01724	11	2	9	12	2	10	0.0366	1.6	0.0382	0.245	10.2	0.266	−18.60	0.10	−18.60	011	000
1	5064.14391	11	5	7	12	5	8	0.0416	1.7	0.0424	0.285	10.2	0.292	−8.65	0.25	−8.70	011	000
1	5065.45082	7	0	7	8	1	8	0.0485	0.6	0.0475	0.354	9.9	0.331	−13.45	0.30	−13.50	110	000
1	5065.91101	7	1	7	8	0	8	0.0458	1.3	0.0465	0.345	10.1	0.324	−11.51	0.27	−11.50	110	000
1	5067.18320	6	1	5	7	2	6	0.0774	0.8	0.0696	0.400	10.0	0.388	−11.15	0.15	−11.20	110	000
1	5077.91893	8	1	8	8	2	7	0.0564	0.0	0.0534	0.333	9.9	0.313	−10.46	0.23	−10.50	110	000
1	5086.97920	6	0	6	7	1	7	0.0604	1.3	0.0583	0.379	10.0	0.369	−13.15	0.30	−13.20	110	000
1	5088.06584	6	1	6	7	0	7	0.0602	1.2	0.0576	0.370	10.0	0.361	−10.56	0.12	−10.60	110	000
1	5089.02994	10	5	6	11	5	7	0.0456	1.3	0.0469	0.286	10.1	0.297	−10.00	0.30	−10.00	011	000
1	5089.64322	9	4	5	10	4	6	0.0721	0.7	0.0710	0.364	9.9	0.373	−6.65	0.15	−6.70	011	000
1	5090.62745	3	1	3	4	3	2	0.0928	0.5	0.0937	0.410	10.0	0.446	−9.31	0.07	−9.30	011	000
1	5092.36038	10	1	9	11	1	10	0.0297	2.0	0.0306	0.248	10.1	0.257	−16.80	0.30	−16.80	011	000
1	5092.79053	10	2	9	11	2	10	0.0294	1.7	0.0297	0.232	9.9	0.242	−15.05	0.20	−15.10	011	000
1	5093.32591	2	2	1	3	3	0	0.0847	1.2	0.0812	0.450	10.0	0.407	−8.00	0.60	−8.00	110	000
1	5095.09895	8	4	5	9	3	6	0.0785	1.3	0.6777	0.407	10.1	0.391	−3.90	0.20	−3.90	110	000
1	5099.12463	9	2	7	10	2	8	0.0594	1.0	0.0552	0.345	10.1	0.334	−14.37	0.18	−14.40	011	000
1	5099.47333	4	1	3	5	3	2	0.0910	1.3	0.0922	0.433	9.9	0.449	−9.65	0.10	−9.70	011	000
1	5100.36645	7	1	7	7	2	6	0.0657	1.8	0.0631	0.382	9.9	0.348	−9.45	0.15	−9.50	110	000
1	5104.16050	4	0	4	5	2	3	0.0959	1.6	0.0959	0.463	9.9	0.466	−9.10	0.30	−9.10	011	000
1	5105.39948	7	0	7	7	1	6	0.0713	0.7	0.0687	0.372	9.9	0.365	−3.40	0.10	−3.40	110	000
1	5106.19486	9	4	6	10	4	7	0.0501	1.2	0.0506	0.291	10.0	0.301	−5.75	0.07	−5.80	011	000
1	5122.46859	3	1	2	4	3	1	0.0904	1.3	0.0928	0.430	10.0	0.447	−8.05	0.25	−8.10	011	000
1	5125.70903	2	1	1	3	2	2	0.0933	0.6	0.0957	0.410	10.0	0.458	−5.45	0.40	−5.50	110	000
1	5126.48217	9	6	3	10	6	4	0.0455	1.5	0.0466	0.266	10.2	0.281	−15.00	0.60	−15.00	011	000
1	5126.84226	9	6	4	10	6	5	0.0463	0.9	0.0460	0.265	10.2	0.269	−14.51	0.30	−14.50	011	000
1	5126.94460	4	0	4	5	1	5	0.0854	0.6	0.0807	0.447	10.1	0.431	−11.14	0.10	−11.10	110	000
1	5129.67815	7	3	4	8	3	5	0.0822	1.0	0.0806	0.395	10.1	0.405	−1.20	0.20	−1.20	011	000
1	5130.28043	8	4	5	9	4	6	0.0573	1.6	0.0566	0.305	10.2	0.314	−8.47	0.11	−8.50	011	000
1	5130.55265	6	0	6	6	1	5	0.0790	1.0	0.0785	0.425	10.1	0.400	−3.56	0.28	−3.60	110	000

Table 4 (*continued*)

m	Computed position	Upper			Lower			b°(air)			b°(self)			d°(air)			Band	
		J	K_a	K_c	J	K_a	K_c	Meas.	Δ%	Fitted	Meas.	Δ%	Fitted	Meas.	Δ	Smooth		
1	5130.70234	10	1	10	10	1	9	0.0372	1.6	0.0353	0.260	10.0	0.264	−10.60	1.00	−10.60	011	000
1	5134.77712	8	2	7	9	2	8	0.0462	1.5	0.0451	0.324	9.9	0.304	−12.10	0.60	−12.10	011	000
1	5135.72233	7	2	5	8	2	6	0.0751	1.3	0.0752	0.415	10.1	0.407	−2.97	0.10	−3.00	011	000
1	5137.99388	1	1	1	2	2	0	0.0972	0.0	0.0964	0.482	10.0	0.450	−9.38	0.28	−9.40	110	000
1	5138.67156	8	5	3	9	5	4	0.0608	1.0	0.0604	0.305	10.2	0.326	−13.46	0.16	−13.50	011	000
1	5139.32144	5	2	4	5	4	1	0.0783	0.9	0.0848	0.390	10.0	0.410	−8.87	0.80	−8.90	011	000
1	5140.28324	8	5	4	9	5	5	0.0527	1.1	0.0545	0.289	10.0	0.299	−12.24	0.22	−12.20	011	000
1	5140.47578	5	1	5	5	2	4	0.0828	1.0	0.0817	0.420	10.0	0.407	−9.60	1.50	−9.60	110	000
1	5143.20334	7	4	4	8	3	5	0.0805	1.2	0.0830	0.385	10.1	0.401	−6.85	0.07	−6.90	110	000
2	5143.77284	7	1	7	8	1	8	0.0458	1.5	0.0463	0.433	6.9	0.348	−12.89	0.60	−12.00	011	000
1	5146.90628	4	3	2	4	4	1	0.0745	1.1	0.0724	0.355	10.1	0.340	−5.65	0.40	−5.70	110	000
1	5149.45788	7	4	3	8	4	4	0.0745	1.9	0.0734	0.390	10.0	0.371	−10.25	0.40	−10.30	011	000
1	5150.85455	3	0	3	4	2	2	0.0982	1.2	0.0980	0.496	10.1	0.474	−9.74	0.15	−9.70	011	000
1	5155.15438	7	4	4	8	4	5	0.0608	2.0	0.0616	0.325	10.2	0.325	−8.00	0.40	−8.00	011	000
1	5155.47095	7	2	6	8	2	7	0.0545	1.8	0.0546	0.353	9.9	0.339	−10.10	0.30	−10.10	011	000
1	5156.92642	6	2	4	7	2	5	0.0785	1.9	0.0839	0.464	9.9	0.439	1.00	0.50	1.00	011	000
1	5161.72777	2	0	2	3	1	3	0.0981	1.5	0.0985	0.423	9.9	0.461	−9.43	0.08	−9.40	110	000
1	5165.62781	7	5	2	8	5	3	0.0583	0.9	0.0594	0.303	9.9	0.313	−11.90	0.40	−11.90	011	000
1	5166.19305	7	5	3	8	5	4	0.0545	1.8	0.0563	0.285	10.2	0.296	−11.98	0.25	−12.00	011	000
1	5176.31894	8	0	8	8	2	7	0.0540	0.9	0.0559	0.337	10.1	0.337	−11.30	0.23	−11.30	011	000
1	5182.61136	6	2	4	6	4	3	0.0830	1.7	0.0834	0.403	9.9	0.407	−6.20	1.60	−7.00	011	000
1	5184.83052	6	0	6	7	0	7	0.0611	1.1	0.0586	0.430	10.0	0.397	−13.00	0.10	−13.00	011	000
1	5189.00990	5	1	4	6	1	5	0.0805	1.5	0.0803	0.486	10.1	0.458	−8.45	0.10	−8.50	011	000
1	5190.89012	7	2	5	7	4	4	0.0809	0.9	0.0799	0.413	9.9	0.398	−10.55	0.50	−7.00	011	000
1	5191.87894	6	5	1	7	5	2	0.0566	0.7	0.0581	0.295	10.2	0.300	−11.76	0.12	−11.80	011	000
1	5192.03530	6	5	2	7	5	3	0.0541	1.5	0.0559	0.285	10.2	0.287	−11.00	0.80	−11.00	011	000
1	5196.75125	5	2	4	6	2	5	0.0728	1.5	0.0738	0.485	10.1	0.410	−3.90	0.25	−3.90	011	000
1	5197.53297	5	3	3	6	3	4	0.0690	1.7	0.0728	0.434	9.9	0.378	−6.50	0.60	−6.50	011	000
1	5200.32454	2	1	1	3	1	2	0.0903	1.1	0.0918	0.410	10.0	0.472	−1.90	0.70	−1.50	021	010
1	5200.71134	6	3	3	7	2	6	0.0811	1.0	0.0838	0.373	9.9	0.409	−2.52	0.40	−2.50	110	000
1	5202.24982	7	3	4	8	2	7	0.0828	1.2	0.0809	0.385	10.1	0.397	−5.40	1.80	−5.40	110	000
1	5203.86332	6	6	0	7	6	1	0.0468	1.7	0.0471	0.270	10.0	0.244	−15.90	0.30	−15.90	011	000
1	5206.51536	4	2	2	5	2	3	0.0860	0.8	0.0922	0.480	10.0	0.471	−2.52	0.25	−2.50	011	000
1	5208.82801	4	1	3	5	1	4	0.0866	1.4	0.0891	0.500	10.0	0.486	−6.45	0.15	−6.50	011	000
3	5214.58162	4	0	4	5	0	5	0.0810	1.9	0.0804	0.507	8.9	0.469	−10.60	0.50	−10.80	011	000

1	5215.77801	5	4	2	6	3	3	0.0824	1.2	0.0836	0.398	10.1	0.383	−3.70	0.60	−3.70	110	000
1	5221.09175	3	1	2	3	3	1	0.0918	0.9	0.0909	0.462	10.0	0.446	−9.35	0.25	−10.00	011	000
1	5228.81051	6	1	6	6	1	5	0.0805	0.9	0.0795	0.410	10.0	0.414	−4.45	0.08	−4.50	011	000
1	5231.22594	4	2	2	5	1	5	0.0920	1.3	0.0919	0.502	10.0	0.454	−6.54	0.08	−6.50	110	000
1	5258.66140	7	2	6	7	2	5	0.0797	1.5	0.0827	0.413	9.9	0.409	−5.90	0.50	−5.90	011	000
1	5270.27925	9	3	7	9	3	6	0.0763	2.0	0.0758	0.370	10.0	0.379	−9.85	0.40	−9.90	011	000
1	5273.16240	1	1	1	1	1	0	0.0968	1.0	0.0949	0.421	10.0	0.458	−7.65	0.50	−8.40	021	010
1	5274.15774	1	1	1	0	0	0	0.0993	1.5	0.1017	0.470	10.0	0.457	−1.61	0.40	−1.60	110	000
1	5280.18740	1	1	0	2	1	1	0.0966	1.6	0.0946	0.500	10.0	0.477	−3.21	0.11	−3.20	011	000
1	5286.72251	5	2	3	5	1	4	0.0910	1.1	0.0927	0.477	10.1	0.452	1.20	1.40	1.20	110	000
1	5294.38095	8	3	6	8	3	5	0.0835	1.2	0.0798	0.395	10.1	0.388	−8.85	0.30	−8.90	011	000
1	5295.67650	2	1	1	2	1	2	0.0973	0.8	0.0935	0.450	10.0	0.476	−3.17	0.20	−2.80	021	010
1	5297.40319	4	2	2	4	2	3	0.0850	0.9	0.0848	0.422	10.0	0.453	1.20	0.60	−2.00	021	010
1	5299.77866	3	1	3	3	1	2	0.0974	1.8	0.0960	0.560	10.0	0.499	−4.48	0.22	−4.50	011	000
1	5311.29165	4	0	4	3	1	3	0.0889	0.9	0.0891	0.465	10.1	0.451	−7.02	0.40	−7.00	110	000
1	5316.23517	2	1	2	2	1	1	0.0980	2.0	0.0984	0.524	9.9	0.501	−5.05	0.20	−5.10	011	000
1	5330.47020	3	0	3	2	2	0	0.0957	0.0	0.0995	0.485	10.1	0.475	−6.65	0.20	−6.70	011	000
1	5346.62585	7	4	4	7	4	3	0.0705	1.7	0.0696	0.388	10.1	0.356	−10.48	0.08	−10.50	011	000
1	5347.30034	5	3	2	5	3	3	0.0782	1.5	0.0796	0.408	10.0	0.416	−2.00	1.00	−2.00	011	000
1	5354.87086	1	0	1	0	0	0	0.0988	1.4	0.1004	0.520	10.0	0.464	−5.75	0.20	−5.75	011	000
1	5360.58268	6	1	5	5	2	4	0.0816	1.7	0.0788	0.421	10.0	0.406	−11.60	0.28	−11.60	110	000
1	5370.69853	9	6	3	9	6	4	0.0447	1.8	0.0437	0.246	10.2	0.262	−13.40	0.15	−12.90	011	000
1	5372.34076	8	6	2	8	6	3	0.0420	1.7	0.0422	0.240	10.0	0.253	−13.50	1.00	−13.50	011	000
1	5388.12828	8	3	5	8	3	6	0.0764	2.0	0.0798	0.413	9.9	0.388	−0.98	0.21	−1.00	011	000
1	5402.26004	2	2	1	2	0	2	0.0981	2.0	0.0985	0.482	10.0	0.462	0.45	0.10	0.50	011	000
1	5403.90050	3	3	0	2	2	1	0.0840	1.9	0.0820	0.521	10.0	0.410	−2.75	0.10	−2.80	110	000
1	5433.42913	4	3	1	3	2	2	0.0855	0.9	0.0867	0.490	10.0	0.428	−5.01	0.07	−5.40	110	000
1	5438.33182	10	1	9	9	2	8	0.0360	1.9	0.0360	0.275	10.2	0.259	−13.88	0.25	−13.90	110	000
1	5445.09080	6	1	6	5	1	5	0.0692	1.6	0.0691	0.480	10.0	0.443	−5.71	0.07	−5.70	011	000
1	5451.29084	6	3	4	5	2	3	0.0855	1.8	0.0916	0.434	9.9	0.440	−3.85	0.50	−3.90	110	000
1	5452.28833	7	3	5	7	1	6	0.0736	1.4	0.0748	0.385	10.1	0.393	1.35	0.30	1.40	011	000
1	5454.82765	7	2	6	7	0	7	0.0630	1.6	0.0657	0.360	10.0	0.378	−6.80	0.50	−6.80	011	000
1	5460.93951	7	0	7	6	0	6	0.0585	1.7	0.0587	0.450	10.0	0.402	−5.95	0.20	−6.00	011	000
1	5469.52667	6	2	5	5	2	4	0.0747	0.9	0.0754	0.490	10.0	0.430	−7.66	0.06	−7.70	011	000
1	5471.09888	8	2	7	8	0	8	0.0527	1.1	0.0559	0.296	10.1	0.337	−9.60	0.35	−9.60	011	000
1	5475.67566	8	0	8	7	0	7	0.0476	0.8	0.0480	0.410	10.0	0.360	−8.59	0.05	−8.60	011	000
1	5478.47123	10	2	8	10	2	9	0.0539	1.9	0.0568	0.298	10.1	0.336	−18.61	0.07	−18.60	011	000
1	5481.37415	12	3	9	12	3	10	0.0529	1.9	0.0557	0.220	10.0	0.330	−20.20	0.20	−20.20	011	000
3	5481.62745	6	2	4	5	2	3	0.0800	1.3	0.0900	0.383	9.7	0.472	−10.00	0.40	−8.00	011	000
1	5486.21163	6	3	4	5	3	3	0.0719	1.4	0.0741	0.428	10.0	0.400	−10.28	0.50	−10.30	011	000
1	5487.33530	9	2	8	9	0	9	0.0425	1.9	0.0464	0.285	10.2	0.297	−10.90	0.60	−10.90	011	000

Table 4 (*continued*)

m	Computed position	Upper			Lower			b^{o}(air)			b°(self)			d^{o}(air)			Band	
		J	K_{a}	K_{c}	J	K_{a}	K_{c}	Meas.	Δ%	Fitted	Meas.	Δ%	Fitted	Meas.	Δ	Smooth		
1	5493.47865	6	3	3	5	3	2	0.0776	0.6	0.0835	0.470	10.0	0.427	−10.25	0.40	−10.30	011	000
1	5494.87600	5	4	1	4	3	2	0.0734	1.9	0.0713	0.368	10.1	0.364	−8.43	0.15	−8.40	110	000
1	5495.45316	7	4	4	7	2	5	0.0804	0.7	0.0799	0.403	9.9	0.398	−2.62	0.15	−2.60	011	000
1	5498.19974	6	4	3	5	4	2	0.0629	1.3	0.0654	0.338	10.1	0.350	−10.54	0.50	−10.50	011	000
1	5503.54126	10	0	10	9	0	9	0.0286	1.7	0.0305	0.266	10.2	0.280	−12.47	0.30	−14.00	011	000
1	5509.63806	6	5	1	5	5	0	0.0526	1.3	0.0549	0.275	10.2	0.278	−7.10	0.50	−7.10	011	000
1	5513.73385	6	4	3	5	3	2	0.0810	1.5	0.0807	0.410	10.0	0.393	−7.21	0.15	−7.20	110	000
2	5514.65520	8	2	6	7	2	5	0.0739	1.4	0.0751	0.402	9.5	0.420	−8.37	0.15	−8.60	011	000
1	5518.99679	11	2	10	11	0	11	0.0288	1.4	0.0301	0.225	10.2	0.225	−13.24	0.15	−13.20	011	000
1	5521.13817	7	4	4	6	4	3	0.0626	1.1	0.0653	0.364	9.9	0.352	−12.00	0.40	−12.00	011	000
1	5523.13236	9	1	8	8	1	7	0.0504	2.0	0.0478	0.335	10.1	0.344	−6.75	0.35	−6.80	011	000
1	5524.64294	5	3	2	5	1	5	0.0880	0.9	0.0878	0.420	10.0	0.437	−1.00	0.30	−1.00	011	000
1	5535.66148	8	4	5	7	3	4	0.0799	1.1	0.0839	0.441	10.0	0.404	−3.93	0.05	−3.90	110	000
1	5538.12878	10	1	9	9	1	8	0.0380	1.8	0.0385	0.293	9.9	0.303	−9.40	0.50	−9.40	011	000
1	5541.66565	4	4	0	4	2	3	0.0825	1.0	0.0842	0.395	10.1	0.409	−1.05	0.30	−1.10	011	000
1	5543.42138	8	4	5	7	4	4	0.0617	1.9	0.0625	0.339	10.0	0.347	−13.00	0.80	−13.00	011	000
1	5544.38558	7	4	3	6	3	4	0.0721	1.4	0.0770	0.398	10.1	0.381	−4.53	0.14	−4.50	110	000
1	5544.61699	9	4	6	8	3	5	0.0808	0.9	0.0808	0.480	10.0	0.392	−8.50	0.12	−8.50	110	000
1	5549.58003	10	4	7	9	3	6	0.0716	1.4	0.0749	0.409	10.0	0.372	−7.43	0.08	−7.40	110	000
1	5550.44669	3	3	1	2	1	2	0.0948	0.0	0.0956	0.477	10.1	0.464	2.00	0.50	2.00	011	000
1	5555.61737	8	5	4	7	5	3	0.0526	1.9	0.0558	0.299	10.0	0.309	−13.07	0.18	−13.10	011	000
1	5556.42476	6	4	2	6	2	5	0.0745	2.0	0.0834	0.360	10.0	0.407	−1.30	0.70	−1.30	011	000
1	5561.35032	5	2	3	4	0	4	0.0953	1.6	0.0957	0.475	10.1	0.470	0.25	0.20	0.30	011	000
1	5565.17473	10	3	8	9	3	7	0.0519	1.9	0.0465	0.315	10.2	0.309	−13.80	0.19	−13.80	011	000
1	5567.75750	8	6	2	7	6	1	0.0455	1.3	0.0435	0.220	10.0	0.232	−13.30	2.00	−13.30	011	000
1	5571.62532	7	4	3	7	2	6	0.0759	1.3	0.0799	0.403	9.9	0.398	−0.18	0.07	−0.20	011	000
1	5572.45354	6	3	4	5	0	5	0.0829	0.8	0.0851	0.402	10.0	0.424	−1.52	0.20	−1.50	110	000
1	5575.77140	5	3	2	4	1	3	0.0900	1.3	0.0920	0.448	10.0	0.457	−1.70	0.60	−1.70	011	000
1	5579.00322	7	5	3	7	3	4	0.0820	1.0	0.0717	0.394	9.9	0.375	−6.43	0.48	−6.40	011	000
1	5579.47736	9	5	4	8	5	3	0.0561	1.4	0.0580	0.292	9.9	0.314	−10.80	0.20	−10.80	011	000
1	5583.61285	7	5	2	6	4	3	0.0625	1.6	0.0612	0.348	10.1	0.318	−12.60	0.30	−12.60	110	000
1	5583.97641	4	3	2	3	1	3	0.0916	1.1	0.0929	0.425	10.1	0.457	0.10	0.25	0.10	011	000
1	5594.29208	8	4	4	8	2	7	0.0795	1.9	0.0744	0.370	10.0	0.383	−1.10	0.50	−1.10	011	000
1	5595.55732	10	3	7	9	3	6	0.0773	1.9	0.0674	0.417	10.1	0.376	−14.80	0.50	−14.80	011	000
1	5597.48469	5	5	1	5	3	2	0.0794	1.5	0.0781	0.375	10.1	0.367	−4.80	0.70	−4.80	011	000

1	5598.19263	12	3	10	11	3	9	0.0347	2.0	0.0330	0.257	10.1	0.259	−15.20	0.60	−16.00	011	000
1	5599.18988	10	4	6	9	4	5	0.0736	1.0	0.0690	0.353	9.9	0.373	−12.35	0.12	−12.40	011	000
1	5599.83410	10	5	6	9	5	5	0.0517	1.0	0.0515	0.307	10.1	0.311	−13.65	0.20	−13.60	011	000
1	5599.95836	12	2	10	11	2	9	0.0383	1.0	0.0380	0.308	10.1	0.278	−8.55	0.40	−8.60	011	000
1	5602.02313	8	5	4	7	4	3	0.0722	1.1	0.0709	0.375	10.1	0.355	−10.66	0.60	−10.70	110	000
1	5603.14591	10	5	5	9	5	4	0.0576	1.7	0.0587	0.280	10.0	0.326	−9.70	0.50	−9.70	011	000
1	5604.51692	11	4	8	10	4	7	0.0481	1.0	0.0462	0.322	9.9	0.307	−16.65	0.20	−16.70	011	000
1	5605.89890	8	5	3	7	4	4	0.0623	1.1	0.0632	0.336	10.1	0.329	−12.87	0.07	−12.90	110	000
1	5607.48266	9	4	5	8	3	6	0.0745	0.9	0.0755	0.400	10.0	0.371	3.95	0.60	4.00	110	000
1	5612.25214	10	6	5	9	6	4	0.0445	0.9	0.0447	0.260	10.0	0.267	−13.38	0.10	−13.40	011	000
1	5612.56895	10	6	4	9	6	3	0.0453	0.9	0.0431	0.253	9.9	0.251	−12.95	0.15	−13.00	011	000
1	5613.40384	13	3	11	12	3	10	0.0290	1.7	0.0277	0.210	10.0	0.234	−15.12	0.15	−15.10	011	000
1	5620.43039	11	4	7	10	4	6	0.0734	1.4	0.0667	0.360	10.0	0.372	−13.10	0.25	−13.10	011	000
1	5620.79784	11	5	7	10	5	6	0.0485	0.8	0.0478	0.318	10.1	0.307	−15.45	0.30	−15.50	011	000
1	5621.67332	5	3	3	4	1	4	0.0887	0.9	0.0893	0.455	10.1	0.442	−0.35	0.25	−0.40	011	000
1	5622.75817	12	4	9	11	4	8	0.0414	1.0	0.0405	0.290	10.0	0.290	−16.85	0.50	−16.90	011	000
1	5624.66838	10	7	3	9	7	2	0.0383	1.0	0.0309	0.210	10.0	0.181	−15.00	0.25	−13.50	011	000
1	5627.22534	11	5	6	10	5	5	0.0583	0.7	0.6011	0.322	9.9	0.342	−10.66	0.10	−10.60	011	000
1	5629.87161	4	4	0	3	2	1	0.0853	1.4	0.0861	0.415	10.1	0.411	−1.80	0.35	−1.80	011	000
1	5630.65795	12	3	9	11	3	8	0.0585	0.9	0.0537	0.356	10.1	0.333	−8.82	0.40	−8.80	011	000
1	5631.33214	10	5	6	9	4	5	0.0772	0.6	0.0723	0.385	10.1	0.368	−11.26	0.30	−11.30	110	000
1	5632.12080	12	5	8	11	4	7	0.0706	1.7	0.0647	0.393	9.9	0.356	−14.10	0.30	−14.10	110	000
1	5633.77740	11	6	6	10	6	5	0.0437	0.9	0.0431	0.258	10.1	0.270	−13.52	0.15	−13.50	011	000
1	5635.70064	4	4	1	3	2	2	0.0848	0.7	0.0843	0.375	10.1	0.414	−2.61	0.20	−2.60	011	000
1	5636.93007	7	3	4	6	1	5	0.0875	0.9	0.0884	0.421	10.0	0.441	−0.74	0.20	−0.70	011	000
1	5637.08704	10	8	2	9	8	1	0.0327	1.2	0.0276	0.194	9.8	0.142	−12.85	0.40	−9.20	011	000
1	5639.92528	13	4	10	12	4	9	0.0348	1.4	0.0353	0.257	10.1	0.269	−16.60	0.10	−16.60	011	000
1	5640.76320	12	5	8	11	5	7	0.0441	1.4	0.0439	0.286	10.1	0.299	−16.95	0.20	−17.00	011	000
1	5641.63013	11	5	7	10	4	6	0.0778	1.9	0.0694	0.397	10.1	0.364	−15.90	0.20	−15.90	110	000
1	5646.16625	11	7	5	10	7	4	0.0376	1.6	0.0360	0.225	10.2	0.212	−13.70	1.00	−13.70	011	000
1	5647.40461	5	4	1	4	2	2	0.0864	0.7	0.0865	0.396	10.1	0.422	−2.60	0.30	−2.60	011	000
1	5650.45528	7	4	4	6	1	5	0.0837	0.7	0.0833	0.423	9.9	0.400	−0.77	0.25	−0.80	110	000
1	5651.35323	12	5	7	11	5	6	0.0611	1.1	0.0628	0.363	9.9	0.363	−10.57	0.20	−10.60	011	000
1	5655.29040	12	4	8	11	4	7	0.0762	1.3	0.0647	0.415	10.1	0.372	−17.60	0.10	−17.60	011	000
1	5658.73148	7	6	2	7	4	3	0.0748	0.8	0.0756	0.341	10.0	0.325	−8.30	0.60	−8.30	011	000
1	5659.48650	14	3	11	13	3	10	0.0398	1.0	0.0431	0.237	10.1	0.298	−6.85	0.20	−6.90	011	000
1	5659.65154	13	5	9	12	5	8	0.0383	1.0	0.0400	0.270	10.0	0.286	−19.33	0.40	−19.30	011	000
1	5662.60142	5	4	2	4	2	3	0.0827	0.8	0.821	0.405	10.1	0.409	−1.30	0.22	−1.30	011	000
1	5662.82554	6	4	2	5	2	3	0.0870	1.4	0.0871	0.425	10.1	0.428	−3.47	0.50	−3.50	011	000
1	5667.30549	12	7	5	11	7	4	0.0352	2.0	0.0356	0.215	10.2	0.213	−14.20	0.50	−14.20	011	000
1	5671.93752	7	2	5	6	0	6	0.0847	0.7	0.0872	0.441	10.0	0.432	−3.43	0.10	−3.40	011	000

Table 4 (*continued*)

m	Computed position	Upper			Lower			b^{o}(air)			b°(self)			d^{o}(air)			Band	
		J	K_a	K_c	J	K_a	K_c	Meas.	Δ%	Fitted	Meas.	Δ%	Fitted	Meas.	Δ	Smooth		
1	5673.80403	8	4	5	7	1	6	0.0778	0.8	0.0768	0.403	9.9	0.373	0.60	0.10	0.60	110	000
1	5678.46005	7	4	3	6	2	4	0.0858	0.7	0.0873	0.438	10.0	0.430	−4.55	0.15	−4.60	011	000
1	5690.03023	8	3	5	7	1	6	0.0840	1.4	0.0845	0.424	9.9	0.423	0.20	0.60	−0.20	011	000
1	5692.10555	6	4	3	5	2	4	0.0787	0.6	0.0793	0.396	10.1	0.398	−1.50	0.40	−1.50	011	000
1	5709.25010	7	3	5	6	1	6	0.0763	0.7	0.0786	0.366	10.1	0.393	0.10	0.20	0.10	011	000
1	5722.45738	5	5	0	4	3	1	0.0771	0.8	0.0788	0.355	10.1	0.372	−6.42	0.30	−6.40	011	000
1	5723.18461	9	4	5	8	2	6	0.0833	1.2	0.0850	0.433	9.9	0.418	1.58	0.15	1.60	011	000
1	5723.77988	5	5	1	4	3	2	0.0754	0.7	0.0766	0.328	10.1	0.364	−7.33	0.15	−7.30	011	000
1	5724.95161	7	4	4	6	2	5	0.0747	0.7	0.0756	0.371	10.0	0.381	−1.20	0.50	−1.20	011	000
1	5732.47315	8	2	6	7	0	7	0.0784	0.5	0.0804	0.413	9.9	0.404	−7.45	0.35	−7.50	011	000
1	5741.66298	9	3	6	8	1	7	0.0793	0.6	0.0790	0.435	10.1	0.400	0.40	0.30	0.40	011	000
1	5742.90242	6	5	1	5	3	2	0.0788	0.8	0.0799	0.384	9.9	0.381	−5.10	0.25	−5.10	011	000
1	5747.71396	6	5	2	5	3	3	0.0740	0.7	0.0746	0.375	10.1	0.365	−6.80	0.15	−6.80	011	000
1	5757.50370	10	4	6	9	2	7	0.0825	0.8	0.0818	0.410	10.0	0.404	1.85	0.60	1.90	011	000
1	5759.99100	7	5	2	6	3	3	0.0821	0.7	0.0813	0.403	9.9	0.388	−3.88	0.25	−3.90	011	000
1	5761.55740	8	4	5	7	2	6	0.0685	0.9	0.0709	0.360	10.0	0.361	0.77	0.20	0.80	011	000
1	5772.38110	7	5	3	6	3	4	0.0721	0.7	0.0718	0.372	9.9	0.360	−7.12	0.30	−7.10	011	000
1	5773.61235	8	5	3	7	3	4	0.0829	0.6	0.0825	0.416	10.1	0.394	−6.00	0.25	−6.00	011	000
1	5783.98825	6	4	2	5	0	5	0.0868	1.7	0.0878	0.416	10.1	0.409	−0.10	0.15	1.00	011	000
1	5785.23125	9	5	4	8	3	5	0.0816	0.9	0.0832	0.401	10.0	0.397	−7.60	0.50	−7.60	011	000
1	5793.02960	9	2	7	8	0	8	0.0700	1.1	0.0719	0.379	10.0	0.371	−10.90	0.50	−10.90	011	000
1	5797.52420	10	5	5	9	3	6	0.0763	1.0	0.0829	0.400	10.0	0.397	−5.25	0.25	−5.30	011	000
1	5798.56983	8	5	4	7	3	5	0.0667	0.9	0.0682	0.354	9.9	0.349	−7.13	0.20	−7.10	011	000
1	5799.39692	10	3	7	9	1	8	0.0683	1.0	0.0719	0.386	10.1	0.371	−4.25	0.15	−4.30	011	000
1	5801.93079	9	4	6	8	2	7	0.0630	1.0	0.0651	0.325	10.2	0.339	3.09	0.23	3.10	011	000
1	5809.03571	9	3	7	8	1	8	0.0600	1.2	0.0631	0.325	10.2	0.337	−3.29	0.20	−3.30	011	000
1	5827.08945	9	5	5	8	3	6	0.0627	1.0	0.0635	0.351	10.0	0.335	−5.40	0.27	−5.40	011	000
1	5832.19280	7	6	1	6	4	2	0.0692	0.9	0.0704	0.341	10.0	0.335	−10.75	0.50	−10.80	011	000
1	5833.24376	7	6	2	6	4	3	0.0653	0.8	0.0666	0.310	10.0	0.316	−12.87	0.20	−12.90	011	000
1	5845.70225	10	4	7	9	2	8	0.0568	1.2	0.0586	0.335	10.1	0.318	4.27	0.35	4.30	011	000
1	5851.93696	10	2	8	9	0	9	0.0603	1.0	0.0621	0.330	10.0	0.334	−14.33	0.20	−14.30	011	000
1	5852.71508	8	6	2	7	4	3	0.0727	1.0	0.0722	0.366	10.1	0.340	−10.25	0.35	−10.30	011	000
1	5861.19600	10	3	8	9	1	9	0.0535	1.9	0.0543	0.275	10.2	0.310	−5.80	0.70	−5.80	011	000
1	5879.10673	9	6	4	8	4	5	0.0629	0.0	0.0601	0.324	9.9	0.314	−13.53	0.60	−13.50	011	000
1	5883.71672	10	6	4	9	4	5	0.0766	2.0	0.0751	0.368	10.1	0.354	−9.20	0.60	−9.20	011	000

1	5913.74510	11	3	9	10	1	10	0.0448	1.1	0.0457	0.246	10.2	0.284	−8.00	0.50	−8.00	011	000
1	5915.15396	8	7	1	7	5	2	0.0585	0.9	0.0583	0.264	9.8	0.284	−17.35	0.35	−17.40	011	000
1	5927.41425	11	6	6	10	4	7	0.0548	0.0	0.0501	0.325	10.2	0.292	−10.00	2.00	−10.00	011	000
1	5938.15942	9	7	3	8	5	4	0.0607	1.6	0.0561	0.281	10.0	0.282	−17.70	1.20	−17.70	011	000
1	5963.51256	12	2	10	11	0	11	0.0410	0.0	0.0408	0.251	10.0	0.247	−15.00	2.00	−16.00	011	000
1	6530.08256	6	0	6	7	2	5	0.0860	1.2	0.0876	0.429	1.6	0.428	−7.60	1.03	−7.60	021	000
1	6549.76418	5	2	4	6	4	3	0.0766	1.6	0.0804	0.370	1.4	0.382	−11.98	1.03	−12.00	021	000
1	6553.94055	4	1	4	5	2	3	0.0973	1.5	0.0932	0.477	1.7	0.461	−9.59	1.03	−9.60	120	000
1	6577.06379	5	3	2	6	4	3	0.0698	1.9	0.0755	0.361	1.1	0.385	−2.29	0.13	−2.30	120	000
1	6582.48417	6	1	5	7	3	4	0.0887	0.9	0.0887	0.475	2.1	0.433	−9.16	0.77	−9.20	021	000
1	6583.70293	8	1	8	9	0	9	0.0366	1.1	0.0365	0.318	2.2	0.287	−12.96	0.19	−13.00	120	000
1	6595.07823	4	2	2	5	4	1	0.0803	1.9	0.0864	0.407	3.7	0.410	−6.42	0.77	−6.40	021	000
1	6598.28121	8	2	7	9	1	8	0.0466	1.5	0.0464	0.277	2.2	0.296	−8.11	1.55	−8.10	120	000
1	6604.05773	7	1	6	8	2	7	0.0672	1.2	0.0588	0.349	1.7	0.350	−16.50	0.77	−16.50	120	000
1	6609.96201	3	2	2	4	4	1	0.0812	1.8	0.0847	0.423	1.2	0.400	−7.67	0.39	−7.70	021	000
1	6621.50788	3	2	2	4	3	1	0.0820	1.8	0.0857	0.415	1.9	0.424	−7.01	0.52	−7.00	120	000
1	6627.71585	3	2	1	4	3	2	0.0822	1.8	0.0853	0.433	2.3	0.424	−3.81	0.52	−3.80	120	000
1	6630.05399	6	1	6	7	0	7	0.0588	1.7	0.0576	0.365	2.2	0.361	−11.05	0.19	−11.10	120	000
1	6640.90968	4	1	3	5	2	4	0.0888	1.7	0.0880	0.494	6.1	0.445	−7.56	0.64	−7.60	120	000
1	6643.62744	6	2	5	7	1	6	0.0708	1.1	0.0686	0.397	2.0	0.371	−3.77	0.64	−3.80	120	000
1	6645.40798	4	0	4	5	2	3	0.0956	0.7	0.0959	0.445	6.7	0.466	−4.74	0.39	−4.70	021	000
1	6647.21770	2	1	2	3	2	1	0.0965	1.6	0.0979	0.485	5.2	0.466	−8.71	0.52	−8.70	120	000
1	6648.87850	5	0	5	6	1	6	0.0748	1.1	0.0696	0.440	4.5	0.403	−12.69	0.77	−12.70	120	000
1	6649.58757	2	2	1	3	3	0	0.0810	1.9	0.0812	0.395	3.8	0.407	−7.76	0.39	−7.80	120	000
1	6650.85735	2	2	0	3	3	1	0.0792	1.3	0.0792	0.421	1.7	0.400	−4.94	0.19	−4.90	120	000
1	6652.57335	5	1	5	6	0	6	0.0700	1.1	0.0691	0.400	1.3	0.397	−8.32	0.32	−8.30	120	000
1	6654.47112	3	1	2	4	2	3	0.0895	1.3	0.0937	0.475	6.3	0.457	−6.20	0.15	−6.20	120	000
1	6667.95020	4	0	4	5	1	5	0.0844	1.2	0.0807	0.470	5.3	0.431	−11.96	0.64	−12.00	120	000
1	6673.04473	9	2	8	10	2	9	0.0357	2.0	0.0368	0.270	11.1	0.271	−15.48	0.13	−15.50	021	000
1	6675.10333	4	1	4	5	0	5	0.0811	1.8	0.0800	0.455	7.7	0.428	−7.31	0.26	−7.30	120	000
1	6677.32970	8	2	6	9	2	7	0.0641	0.9	0.0652	0.375	4.0	0.371	−3.92	0.32	−3.90	021	000
1	6685.41152	3	0	3	4	1	4	0.0932	1.7	0.0908	0.495	5.1	0.451	−10.56	0.19	−10.60	120	000
1	6688.26378	8	1	7	9	1	8	0.0492	1.0	0.0478	0.311	2.3	0.335	−19.64	0.26	−19.60	021	000
1	6689.21587	1	1	0	2	2	1	0.0945	1.6	0.0932	0.475	2.1	0.447	−4.47	0.52	−4.50	120	000
1	6693.38557	7	2	5	8	2	6	0.0765	1.6	0.0752	0.435	2.3	0.407	2.11	0.32	2.10	021	000
1	6696.67318	5	0	5	5	1	4	0.0864	1.4	0.0867	0.430	9.3	0.428	−3.57	0.64	−3.60	120	000
1	6698.24086	3	1	3	4	0	4	0.0885	1.7	0.0893	0.420	8.3	0.451	−4.57	0.52	−4.60	120	000
1	6701.95690	2	0	2	3	1	3	0.0942	0.5	0.0985	0.412	4.9	0.461	−9.27	0.39	−9.30	120	000
1	6702.38917	7	3	4	8	3	5	0.0816	1.6	0.0806	0.407	7.4	0.405	−5.04	0.26	−5.00	021	000
1	6702.96903	8	3	6	9	3	7	0.0552	1.8	0.0526	0.330	6.1	0.310	−11.68	0.32	−11.70	021	000
1	6712.75013	7	2	6	8	2	7	0.0534	1.9	0.0546	0.330	9.1	0.339	−10.23	0.64	−10.20	021	000

Table 4 (*continued*)

m	Computed position	Upper			Lower			b^{o}(air)			b°(self)			d^{o}(air)			Band	
		J	K_a	K_c	J	K_a	K_c	Meas.	Δ%	Fitted	Meas.	Δ%	Fitted	Meas.	Δ	Smooth		
1	6712.90418	6	2	4	7	2	5	0.0830	1.8	0.0839	0.430	4.7	0.439	1.41	0.39	1.40	021	000
1	6715.62940	4	2	3	4	3	2	0.0842	1.1	0.0839	0.400	5.0	0.393	−9.44	0.90	−9.40	120	000
1	6715.80060	6	3	4	6	4	3	0.0714	1.4	0.0700	0.345	2.9	0.345	−14.86	0.52	−14.90	120	000
1	6716.56335	8	0	8	8	2	7	0.0553	1.8	0.0559	0.355	5.6	0.337	−12.42	0.52	−12.40	021	000
1	6719.02261	1	0	1	2	1	2	0.1015	2.0	0.1025	0.477	8.4	0.463	−3.97	0.77	−4.00	120	000
1	6724.06925	7	3	5	8	3	6	0.0610	2.0	0.0606	0.335	7.5	0.336	−9.32	0.90	−9.30	021	000
1	6724.81420	3	2	1	3	3	0	0.0860	1.2	0.0858	0.413	4.8	0.398	−7.22	0.52	−7.20	120	000
1	6727.23202	6	1	6	7	1	7	0.0592	1.7	0.0568	0.385	6.5	0.390	−12.69	0.52	−12.70	021	000
1	6729.00652	2	0	2	3	2	1	0.0984	1.0	0.0996	0.460	5.4	0.472	−9.03	0.64	−9.00	021	000
1	6731.44496	6	3	3	7	3	4	0.0848	0.8	0.0838	0.405	4.9	0.417	−7.72	0.32	−7.70	021	000
1	6735.31032	5	1	4	5	2	3	0.0900	1.7	0.0927	0.441	3.4	0.452	−9.14	0.52	−9.10	120	000
1	6736.21450	5	2	3	6	2	4	0.0849	0.8	0.0900	0.450	3.3	0.461	1.70	0.26	1.70	021	000
1	6736.81855	5	1	4	6	1	5	0.0812	1.8	0.0803	0.420	4.8	0.458	−5.91	0.97	−6.00	021	000
1	6742.12095	8	6	3	9	7	2	0.0437	1.6	0.0424	0.259	3.9	0.246	−9.25	0.52	−9.30	200	000
1	6742.67712	3	1	2	3	2	1	0.0911	1.9	0.0938	0.450	5.6	0.455	−9.90	0.13	−9.90	120	000
1	6744.98720	7	1	7	7	1	6	0.0705	1.1	0.0699	0.395	7.6	0.375	−6.15	0.19	−6.20	021	000
1	6746.51785	6	3	4	7	3	5	0.0666	1.8	0.0677	0.340	8.8	0.360	−10.41	0.26	−10.40	021	000
1	6748.88962	5	1	5	6	1	6	0.0717	1.1	0.0681	0.405	3.7	0.430	−10.66	0.10	−9.00	021	000
1	6756.14750	1	0	1	1	1	0	0.1028	0.8	0.1024	0.470	4.3	0.450	−10.11	0.45	−10.10	120	000
1	6765.23627	4	3	2	5	2	3	0.0875	1.7	0.0901	0.437	1.8	0.424	−3.07	0.26	−3.10	120	000
1	6771.47544	6	4	2	7	4	3	0.0737	2.0	0.0725	0.390	5.1	0.364	−10.50	0.13	−10.50	021	000
1	6774.22301	6	4	3	7	4	4	0.0648	0.9	0.0647	0.330	7.6	0.332	−12.41	0.32	−12.40	021	000
1	6775.16477	4	2	3	5	2	4	0.0772	1.9	0.0812	0.410	4.9	0.438	−5.94	0.19	−5.90	021	000
1	6780.87734	5	3	2	6	2	5	0.0801	1.0	0.0855	0.440	4.5	0.414	−0.49	0.77	−0.50	120	000
1	6784.51594	7	5	3	8	5	4	0.0554	0.7	0.0563	0.308	2.3	0.296	−15.50	0.39	−15.50	021	000
1	6787.83372	3	2	1	4	2	2	0.0884	1.1	0.0900	0.432	2.3	0.465	−7.21	0.19	−7.20	021	000
1	6790.64902	4	3	1	5	3	2	0.0810	1.9	0.0803	0.425	4.7	0.408	−5.78	0.19	−5.80	021	000
1	6791.55635	4	0	4	4	2	3	0.0890	1.3	0.0898	0.425	2.4	0.466	−7.80	0.90	−7.80	021	000
1	6796.68445	5	1	5	5	1	4	0.0885	1.7	0.0869	0.449	4.5	0.451	−5.49	0.32	−5.50	021	000
1	6800.32312	1	1	0	1	0	1	0.1022	1.2	0.1024	0.459	4.4	0.450	1.42	0.39	1.40	120	000
1	6806.66963	2	1	1	2	0	2	0.1002	1.0	0.0996	0.437	4.6	0.461	−0.25	0.39	−0.30	120	000
1	6809.28192	8	3	6	9	4	5	0.0817	1.8	0.0809	0.385	5.2	0.399	−13.44	0.32	−13.40	200	000
1	6810.21336	7	2	6	8	4	5	0.0750	1.6	0.0730	0.394	1.8	0.350	−18.84	0.39	−18.80	101	000
1	6812.81040	2	1	2	3	1	3	0.0922	1.1	0.0951	0.470	3.2	0.512	−5.47	0.64	−5.50	021	000
1	6821.04875	2	2	1	3	2	2	0.0865	0.9	0.0849	0.368	4.1	0.461	−4.30	0.22	−4.30	021	000

1	6824.39560	1	1	0	2	1	1	0.0953	1.0	0.0946	0.365	5.5	0.477	−1.38	0.26	−1.40	021	000
1	6824.83215	4	4	0	5	4	1	0.0679	0.9	0.0643	0.320	10.0	0.331	−10.85	1.03	−10.00	021	000
1	6830.75374	3	0	3	2	1	2	0.0950	1.1	0.0959	0.495	4.0	0.463	−6.08	1.93	−6.10	120	000
1	6833.13130	6	5	2	7	6	1	0.0518	1.2	0.0504	0.309	6.5	0.295	−7.49	0.52	−7.50	200	000
1	6833.30211	6	5	1	7	6	2	0.0511	2.0	0.0510	0.292	5.5	0.255	−7.37	0.26	−7.40	200	000
1	6837.67642	7	4	4	8	5	3	0.0657	1.5	0.0677	0.354	2.8	0.363	−9.00	0.64	−9.00	200	000
1	6841.42738	7	4	3	8	5	4	0.0736	0.8	0.0738	0.388	5.2	0.365	−6.46	0.64	−6.50	200	000
1	6842.24738	5	2	3	5	1	4	0.0933	1.5	0.0927	0.469	1.7	0.452	1.50	0.77	1.50	120	000
1	6843.35996	3	1	3	3	1	2	0.0967	1.9	0.0960	0.500	6.0	0.499	−4.53	0.13	−4.50	021	000
1	6849.67788	6	1	6	7	2	5	0.0883	2.0	0.0850	0.430	8.1	0.443	−7.74	0.77	−7.70	200	000
1	6852.29726	4	0	4	3	1	3	0.0884	0.8	0.0891	0.420	7.1	0.451	−8.04	0.39	−8.00	120	000
1	6855.50987	2	2	1	2	1	2	0.0960	1.0	0.0952	0.485	3.1	0.455	−1.39	0.64	−1.40	120	000
1	6859.91300	2	1	2	2	1	1	0.1002	1.5	0.0984	0.470	2.1	0.501	−2.41	0.39	−2.40	021	000
1	6863.07217	3	2	2	3	1	3	0.0927	1.3	0.0933	0.437	3.4	0.445	−1.76	1.03	−1.80	120	000
1	6865.96840	5	0	5	6	3	4	0.0868	1.0	0.0858	0.410	7.3	0.419	−12.76	0.26	−12.80	200	000
1	6867.15901	6	4	3	7	5	2	0.0656	1.2	0.0656	0.380	7.9	0.355	−7.33	0.64	−7.30	200	000
1	6868.27343	6	4	2	7	5	3	0.0713	1.0	0.0704	0.355	11.3	0.356	−8.78	0.19	−8.80	200	000
1	6871.29650	1	1	1	1	1	0	0.1004	1.5	0.0999	0.450	4.4	0.482	−5.18	0.64	−5.20	021	000
1	6872.90460	7	2	5	7	1	6	0.0835	1.2	0.0809	0.422	1.9	0.411	4.01	1.03	4.00	120	000
1	6875.59416	4	2	3	4	2	2	0.0903	1.0	0.0893	0.480	6.3	0.477	−4.30	0.19	−4.30	021	000
1	6887.27826	5	3	2	5	2	3	0.0894	0.8	0.0900	0.422	3.6	0.424	−4.33	0.39	−4.30	120	000
1	6887.82845	7	3	5	7	3	4	0.0850	0.5	0.0814	0.431	2.8	0.398	−7.97	0.13	−8.00	021	000
1	6888.10919	6	0	6	5	1	5	0.0716	1.1	0.0688	0.385	3.9	0.397	−6.68	0.90	−6.70	120	000
1	6890.45241	6	3	4	7	4	3	0.0800	1.3	0.0812	0.397	1.8	0.412	−11.03	0.19	−11.00	200	000
1	6891.86560	7	3	4	8	4	5	0.0890	1.7	0.0856	0.430	7.0	0.406	−7.39	2.58	−7.40	200	000
1	6893.24164	2	1	1	2	1	2	0.0974	1.2	0.0984	0.480	4.2	0.501	1.96	0.39	2.00	021	000
1	6895.14780	1	0	1	0	0	0	0.0984	2.0	0.1004	0.443	2.3	0.464	−3.58	3.22	−5.75	021	000
1	6895.89472	5	4	1	6	5	2	0.0653	1.4	0.0651	0.385	6.5	0.342	−7.16	0.64	−7.20	200	000
1	6897.31190	3	2	1	3	2	2	0.0880	0.9	0.0890	0.465	3.2	0.486	−1.74	0.13	−1.70	021	000
1	6898.51700	6	0	6	7	2	5	0.0875	0.9	0.0876	0.454	2.2	0.428	−9.32	0.39	−9.30	101	000
1	6898.93975	2	2	0	1	1	1	0.0965	1.6	0.0965	0.470	4.3	0.450	1.50	0.39	1.50	120	000
1	6901.66377	6	3	4	6	3	3	0.0831	0.8	0.0812	0.430	3.5	0.408	−6.54	1.16	−6.50	021	000
1	6902.47869	3	3	0	3	2	1	0.0872	0.8	0.0858	0.425	2.4	0.398	−0.22	0.90	−0.20	120	000
1	6905.05730	4	2	2	4	2	3	0.0870	1.1	0.0893	0.422	3.6	0.477	−0.85	0.26	−0.90	021	000
1	6908.31021	3	3	1	3	2	2	0.0833	1.4	0.0852	0.375	4.0	0.395	−1.45	0.52	−1.50	120	000
1	6909.21243	3	1	2	3	1	3	0.0956	0.8	0.0960	0.440	9.1	0.499	−5.70	1.29	−5.70	021	000
1	6910.21930	5	3	3	5	3	2	0.0830	1.0	0.0796	0.418	2.4	0.416	−8.26	0.52	−8.30	021	000
1	6911.16721	6	3	3	7	4	4	0.0872	0.9	0.0862	0.370	8.1	0.426	−7.20	0.52	−7.20	200	000
1	6911.38465	4	3	2	4	2	3	0.0841	1.2	0.0839	0.425	3.5	0.393	−1.74	0.26	−1.70	120	000
1	6913.13985	5	1	5	6	2	4	0.0907	1.3	0.0908	0.480	4.2	0.468	−8.44	0.64	−8.40	200	000
1	6914.54904	4	3	2	4	3	1	0.0779	1.9	0.0776	0.385	5.2	0.419	−7.82	0.26	−7.80	021	000

Table 4 (*continued*)

m	Computed position	Upper			Lower			b^{o}(air)			b°(self)			d^{o}(air)			Band	
		J	K_a	K_c	J	K_a	K_c	Meas.	Δ%	Fitted	Meas.	Δ%	Fitted	Meas.	Δ	Smooth		
1	6919.03295	5	3	2	5	3	3	0.0761	1.7	0.0796	0.370	5.4	0.416	−2.82	0.26	−2.80	021	000
1	6919.47938	5	2	3	6	4	2	0.0858	0.8	0.0871	0.474	5.3	0.416	−8.66	0.64	−8.70	101	000
1	6922.45610	11	2	9	12	2	10	0.0394	1.3	0.0427	0.263	3.8	0.296	−11.38	0.52	−11.40	101	000
1	6926.45177	4	2	3	5	4	2	0.0850	1.4	0.0828	0.454	6.6	0.394	−11.46	0.90	−11.50	101	000
1	6929.63990	4	1	3	4	1	4	0.0915	1.6	0.0923	0.500	8.0	0.481	−4.10	1.29	−4.10	021	000
1	6931.59244	10	3	7	11	3	8	0.0690	0.7	0.0668	0.398	5.0	0.370	−8.38	0.52	−8.40	101	000
1	6932.64075	6	1	5	7	3	4	0.0907	1.3	0.0887	0.455	2.2	0.433	−11.48	0.64	−11.50	101	000
1	6934.60200	8	2	6	9	3	7	0.0759	1.3	0.0743	0.320	12.5	0.359	−14.40	0.77	−14.40	200	000
1	6939.19180	9	5	5	10	5	6	0.0560	1.4	0.0534	0.344	5.8	0.341	−9.94	0.26	−9.90	101	000
1	6939.76028	5	2	4	6	3	3	0.0886	0.9	0.0922	0.435	5.7	0.461	−10.73	0.64	−10.70	200	000
1	6940.52307	7	4	4	7	4	3	0.0730	1.6	0.0696	0.380	10.5	0.356	−12.11	0.52	−12.10	021	000
1	6942.02408	4	2	2	5	4	1	0.0880	1.3	0.0864	0.433	4.6	0.410	−9.63	0.45	−9.60	101	000
1	6942.40269	6	2	4	6	2	5	0.0845	1.8	0.0868	0.450	5.6	0.434	−1.70	1.03	−1.70	021	000
1	6944.18675	6	4	3	6	4	2	0.0668	1.5	0.0674	0.330	6.1	0.352	−12.87	0.52	−12.90	021	000
1	6944.85174	11	1	10	12	1	11	0.0291	1.7	0.0270	0.250	8.0	0.251	−18.47	0.13	−18.50	101	000
1	6951.55305	7	2	5	8	3	6	0.0817	0.9	0.0828	0.450	5.6	0.401	−11.73	0.39	−11.70	200	000
1	6952.30748	8	3	5	8	3	6	0.0727	1.0	0.0798	0.387	5.2	0.388	0.18	0.26	0.20	021	000
1	6956.31488	3	1	2	2	1	1	0.0948	1.2	0.0967	0.450	6.7	0.501	−4.95	1.16	−6.00	021	000
1	6958.77662	4	3	1	5	4	2	0.0788	1.4	0.0793	0.420	9.5	0.442	−7.24	0.19	−7.20	200	000
1	6961.30835	3	2	2	3	0	3	0.0920	1.6	0.0948	0.515	3.9	0.472	0.94	0.26	0.90	021	000
1	6962.26730	4	1	4	5	3	3	0.0886	1.7	0.0905	0.444	4.5	0.430	−9.71	0.64	−9.70	101	000
1	6965.58418	9	4	6	10	3	7	0.0733	1.1	0.0708	0.430	5.8	0.392	−6.54	0.26	−6.50	200	000
1	6965.80225	5	4	1	5	3	2	0.0793	1.9	0.0787	0.395	2.5	0.361	−2.52	0.52	−2.50	120	000
1	6966.68955	7	2	5	7	2	6	0.0755	1.3	0.0827	0.460	6.5	0.409	−4.53	0.45	−4.50	021	000
1	6969.32089	4	2	3	4	0	4	0.0873	1.4	0.0898	0.460	4.3	0.466	0.51	0.77	0.50	021	000
1	6975.03692	8	2	7	9	1	8	0.0500	0.8	0.0499	0.347	4.3	0.332	−11.71	0.26	−11.70	200	000
1	6975.42415	5	1	4	6	3	3	0.0910	0.8	0.0910	0.470	12.8	0.444	−12.37	0.77	−12.40	101	000
1	6977.58847	6	1	5	6	1	6	0.0822	1.8	0.0795	0.395	5.1	0.414	−12.07	1.67	−12.10	021	000
1	6979.84701	7	5	3	7	5	2	0.0555	1.1	0.0542	0.286	10.5	0.298	−15.52	0.52	−15.50	021	000
1	6980.54135	4	2	3	5	3	2	0.0890	1.7	0.0916	0.450	6.7	0.469	−11.12	0.26	−11.10	200	000
1	6994.90370	7	1	6	8	2	7	0.0722	1.0	0.0654	0.390	7.7	0.365	−15.58	0.26	−15.60	200	000
1	6995.93823	6	3	3	6	5	2	0.0800	1.5	0.0745	0.385	3.9	0.371	−9.12	1.93	−9.10	101	000
1	6997.51263	8	0	8	9	1	9	0.0446	1.1	0.0435	0.349	5.7	0.295	−17.53	0.19	−17.50	200	000
1	6998.80974	7	5	3	8	5	4	0.0580	0.7	0.0585	0.320	15.6	0.335	−10.28	0.13	−10.30	101	000
1	6999.59056	4	3	2	3	2	1	0.0868	1.7	0.0885	0.460	6.5	0.428	−4.70	0.58	−4.70	120	000

1	7001.57305	7	2	6	8	1	7	0.0606	1.7	0.0598	0.357	5.6	0.372	−7.30	1.29	−7.30	200	000
1	7003.10450	7	1	6	8	4	5	0.0782	2.0	0.0774	0.400	7.5	0.372	−15.73	0.13	−15.80	002	000
1	7003.73149	3	1	3	4	3	2	0.0940	1.6	0.0937	0.450	8.9	0.446	−10.75	0.26	−10.80	101	000
1	7004.22729	5	1	4	4	1	3	0.0881	1.7	0.0892	0.514	5.8	0.493	−3.45	0.45	−3.50	021	000
1	7004.75515	2	2	0	1	0	1	0.1008	1.0	0.1017	0.470	4.3	0.458	6.57	0.26	6.60	021	000
1	7008.40017	4	1	3	5	3	2	0.0933	1.8	0.0922	0.470	8.5	0.449	−11.04	1.03	−11.00	101	000
1	7010.54760	7	3	4	8	3	5	0.0822	1.1	0.0830	0.433	6.9	0.439	−5.97	0.64	−6.00	101	000
1	7013.17203	4	3	2	3	3	1	0.0766	2.0	0.0734	0.410	7.3	0.401	−9.01	0.32	−9.00	021	000
1*	7014.46110	6	6	0	7	6	1	0.0479	1.7	0.0458	0.300	5.0	0.269	−17.82	0.39	−17.80	101	000
1	7022.47180	3	1	3	4	2	2	0.1000	2.0	0.0975	0.440	6.8	0.497	−5.82	0.64	−5.80	200	000
1	7025.38328	6	1	5	5	1	4	0.0802	1.9	0.0804	0.460	4.3	0.466	−3.11	0.52	−3.30	021	000
1	7028.31116	6	5	2	7	5	3	0.0566	1.2	0.0581	0.300	10.0	0.319	−10.85	0.77	−10.90	101	000
1	7031.23835	7	1	7	8	2	6	0.0817	1.8	0.0778	0.430	7.0	0.415	−8.89	0.77	−8.90	002	000
1	7032.35851	8	1	8	8	2	7	0.0587	1.7	0.0572	0.360	11.1	0.345	−16.50	1.03	−16.50	200	000
1	7033.56680	7	5	3	8	3	6	0.0659	1.5	0.0695	0.300	10.0	0.343	−7.43	0.77	−7.40	021	000
1	7039.55559	6	4	3	7	4	4	0.0717	1.7	0.0686	0.374	8.0	0.369	−9.34	0.23	−9.30	101	000
1	7040.44815	9	5	4	10	4	7	0.0574	1.7	0.0583	0.360	5.6	0.318	−2.40	0.39	−2.40	200	000
1	7046.80875	8	3	6	8	4	5	0.0670	1.8	0.0648	0.333	12.0	0.364	−17.18	0.26	−17.20	200	000
1	7051.92565	6	5	2	7	3	5	0.0747	2.0	0.0723	0.371	8.1	0.348	−6.75	0.39	−6.80	021	000
1	7055.86058	5	1	5	5	3	2	0.0910	0.8	0.0878	0.490	6.1	0.437	−9.73	0.52	−9.70	101	000
1	7056.53625	7	1	7	7	2	6	0.0650	1.2	0.0671	0.400	5.0	0.384	−13.36	0.52	−13.40	200	000
1	7058.40359	5	2	4	6	1	5	0.0818	1.8	0.0797	0.458	6.6	0.441	−4.12	0.26	−4.10	200	000
1	7059.24410	6	3	4	5	3	3	0.0742	1.1	0.0741	0.400	7.5	0.400	−11.90	0.26	−11.90	021	000
1	7070.78333	6	1	5	7	1	6	0.0770	1.9	0.0708	0.480	2.1	0.467	−13.37	0.26	−13.40	101	000
1	7076.67080	5	1	4	6	4	3	0.0863	1.7	0.0877	0.450	4.4	0.416	−11.82	0.32	−11.80	002	000
1	7082.25212	8	0	8	8	2	7	0.0577	1.7	0.0559	0.370	8.1	0.337	−16.57	0.39	−16.60	101	000
1	7083.33704	7	3	4	7	4	3	0.0862	0.8	0.0858	0.460	4.3	0.420	−6.45	0.77	−6.50	200	000
1	7084.63789	6	4	3	7	3	4	0.0844	1.8	0.0858	0.462	2.2	0.429	−8.41	0.64	−8.40	200	000
1	7085.00826	8	1	8	8	1	7	0.0586	1.2	0.0591	0.384	2.6	0.379	−10.64	0.64	−10.60	101	000
1	7088.97356	4	0	4	5	1	5	0.0903	1.7	0.0854	0.500	3.0	0.430	−12.49	0.77	−12.50	200	000
1	7090.47822	7	4	3	8	3	6	0.0750	1.6	0.0751	0.370	5.4	0.377	−4.02	0.26	−4.00	200	000
1	7090.99795	7	3	4	6	3	3	0.0823	1.6	0.0833	0.442	4.5	0.426	−8.68	0.45	−8.70	021	000
1	7091.85251	6	4	3	5	4	2	0.0645	0.8	0.0654	0.324	9.3	0.350	−14.43	0.45	−14.40	021	000
1	7093.24534	7	5	2	8	4	5	0.0655	1.5	0.0623	0.290	6.9	0.302	−11.61	0.19	−12.00	200	000
1	7098.09415	7	1	6	7	2	5	0.0827	1.1	0.0834	0.430	4.7	0.432	−10.58	0.26	−10.60	200	000
1	7099.70456	5	1	5	5	2	4	0.0835	1.8	0.0839	0.446	4.5	0.449	−13.17	0.39	−13.20	200	000
1	7100.64381	1	1	1	2	2	0	0.1008	2.0	0.0967	0.525	3.8	0.490	−9.13	0.90	−9.10	200	000
1	7100.82986	3	1	3	3	3	0	0.0955	1.6	0.0909	0.465	4.3	0.446	−9.15	0.90	−9.50	101	000
1	7111.22604	6	4	2	7	3	5	0.0740	2.0	0.0758	0.370	5.4	0.396	0.04	0.52	0.01	200	000
1	7113.65611	11	2	10	10	2	9	0.0294	1.4	0.0311	0.250	6.0	0.261	−16.17	0.52	−16.20	021	000
1	7115.03517	7	4	4	6	4	3	0.0626	1.3	0.0653	0.370	5.4	0.352	−15.11	0.64	−15.10	021	000

Table 4 (*continued*)

m	Computed position	Upper			Lower			b^{o}(air)			b°(self)			d^{o}(air)			Band	
		J	K_a	K_c	J	K_a	K_c	Meas.	Δ%	Fitted	Meas.	Δ%	Fitted	Meas.	Δ	Smooth		
1	7116.19857	3	1	3	4	0	4	0.0905	1.7	0.0911	0.472	4.2	0.474	−4.83	1.03	−4.80	200	000
1	7122.48091	6	2	4	6	3	3	0.0855	1.8	0.0914	0.420	4.8	0.457	−8.12	1.55	−8.10	200	000
1	7123.83459	5	2	3	5	3	2	0.0894	2.0	0.0908	0.450	6.7	0.462	−7.70	0.39	−7.70	200	000
1	7127.03478	2	0	2	3	1	3	0.1004	1.5	0.1000	0.450	3.3	0.467	−10.84	0.52	−10.80	200	000
1	7128.01516	6	0	6	6	2	5	0.0782	1.3	0.0750	0.435	3.4	0.415	−15.74	0.52	−15.70	101	000
1	7129.30289	6	3	3	7	2	6	0.0854	0.8	0.0887	0.450	7.8	0.439	−7.12	0.77	−7.10	200	000
1	7133.00496	5	1	4	5	3	3	0.0880	1.0	0.0878	0.475	5.3	0.437	−10.79	0.64	−10.80	101	000
1	7137.52315	5	3	2	6	2	5	0.0850	1.8	0.0893	0.480	6.3	0.479	−7.79	0.39	−7.80	200	000
1	7138.30726	6	1	6	6	1	5	0.0764	1.2	0.0794	0.447	4.5	0.438	−8.35	0.77	−8.40	101	000
1	7139.61000	4	1	4	5	1	5	0.0842	1.9	0.0806	0.533	5.6	0.538	−13.38	0.13	−13.40	101	000
1	7147.73710	5	0	5	5	2	4	0.0830	1.8	0.0832	0.455	6.6	0.446	−14.20	0.77	−14.20	101	000
1	7151.08386	7	5	3	6	5	2	0.0544	1.1	0.0552	0.280	10.7	0.300	−16.82	0.13	−16.80	021	000
1	7151.99286	4	1	3	4	2	2	0.0956	1.0	0.0941	0.478	4.2	0.480	−12.19	0.13	−12.20	200	000
1	7152.68225	4	3	1	5	2	4	0.0866	1.7	0.0886	0.460	3.3	0.511	−3.93	0.26	−3.90	200	000
1*	7154.35410	8	8	0	8	8	1	0.0325	1.2	0.0323	0.215	9.3	0.220	−14.59	0.39	−14.60	101	000
1	7159.23250	9	4	6	8	4	5	0.0594	1.5	0.0578	0.340	8.8	0.336	−14.57	0.64	−14.60	021	000
1	7166.71691	1	1	1	2	0	2	0.0991	2.0	0.1042	0.435	6.9	0.483	−4.54	1.29	−4.50	200	000
1	7172.69922	3	3	0	4	2	3	0.0888	1.2	0.0869	0.420	4.8	0.532	−3.78	1.29	−3.80	200	000
1*	7173.77938	8	6	2	8	6	3	0.0483	1.2	0.0449	0.330	9.1	0.275	−12.06	0.77	−12.00	101	000
1	7174.13744	2	0	2	2	1	1	0.1035	1.5	0.1009	0.460	4.3	0.478	−10.36	1.16	−10.40	200	000
1	7175.98667	3	0	3	3	2	2	0.0958	1.6	0.0948	0.488	4.1	0.472	−9.87	0.45	−9.90	101	000
1	7178.44583	6	2	5	6	2	4	0.0881	1.8	0.0889	0.450	8.9	0.451	−7.59	0.52	−7.60	101	000
1	7186.85797	8	6	3	8	7	2	0.0420	1.2	0.0421	0.270	7.4	0.209	−9.51	0.52	−9.50	002	000
1	7188.13838	8	5	4	8	5	3	0.0587	0.7	0.0615	0.315	4.8	0.345	−12.20	0.52	−12.20	101	000
1*	7188.34970	7	6	2	6	6	1	0.0413	1.0	0.0426	0.270	5.6	0.236	−11.44	0.52	−11.40	021	000
1	7189.34437	2	2	0	3	1	3	0.1001	2.0	0.0956	0.490	4.1	0.548	−3.31	0.90	−3.30	200	000
1	7190.28878	7	3	5	7	3	4	0.0863	1.2	0.0844	0.460	6.5	0.421	−9.70	0.45	−9.70	101	000
1	7192.41612	8	4	5	8	4	4	0.0760	2.0	0.0756	0.385	6.5	0.396	−15.86	0.90	−15.90	101	000
1	7197.32624	7	5	3	7	3	4	0.0815	1.3	0.0717	0.364	5.5	0.375	−5.75	1.03	−5.80	021	000
1	7207.07095	6	5	2	6	3	3	0.0828	0.7	0.0745	0.410	4.9	0.371	−7.11	0.13	−7.10	021	000
1	7208.90950	6	3	4	6	3	3	0.0841	0.8	0.0862	0.405	4.9	0.425	−6.70	0.26	−6.70	101	000
1	7209.51930	6	4	3	6	4	2	0.0738	1.1	0.0723	0.333	12.0	0.376	−12.91	1.03	−12.90	101	000
2	7210.43669	4	3	1	4	3	2	0.0765	2.0	0.0824	0.570	2.6	0.437	−6.04	0.77	−8.50	101	000
1	7211.06742	7	4	3	7	4	4	0.0754	1.3	0.0747	0.385	6.5	0.388	−7.60	0.77	−7.60	101	000
1	7212.14382	8	4	4	8	4	5	0.0793	1.5	0.0756	0.380	7.9	0.396	−6.00	0.39	−6.00	101	000

1	7227.96787	4	3	2	4	3	1	0.0798	1.3	0.0824	0.415	2.4	0.437	−12.70	0.64	−12.70	101	000
1	7229.13300	5	2	3	6	3	4	0.0893	2.0	0.0926	0.460	6.5	0.482	−5.90	3.86	−5.90	002	000
1	7236.44704	2	2	0	2	1	1	0.0980	2.0	0.0984	0.483	2.1	0.474	−5.37	0.39	−5.40	200	000
1	7236.80770	1	1	1	0	0	0	0.1022	1.8	0.1038	0.500	2.0	0.449	−1.99	0.90	−2.00	200	000
1	7248.16670	5	0	5	4	2	2	0.0895	2.0	0.0957	0.520	5.8	0.470	−7.17	0.64	−9.30	101	000
1	7252.00307	4	2	2	4	2	3	0.0905	1.2	0.0941	0.490	6.1	0.490	−6.47	0.39	−6.50	101	000
1	7255.41486	8	3	5	8	3	6	0.0828	0.8	0.0800	0.460	6.5	0.411	−5.43	0.26	−5.40	101	000
1	7256.12913	3	2	2	3	1	3	0.0940	1.9	0.0950	0.480	5.2	0.484	−2.80	0.26	−2.80	200	000
1	7259.43232	8	1	7	7	3	4	0.0891	1.7	0.0845	0.410	9.8	0.423	−9.68	1.29	−10.00	101	000
1	7266.18528	6	1	5	5	3	2	0.0902	0.7	0.0908	0.470	6.4	0.452	−10.98	1.03	−10.00	101	000
1	7266.37117	6	4	2	6	3	3	0.0840	0.6	0.0843	0.430	7.0	0.419	−7.65	0.39	−7.70	200	000
1	7274.68363	5	2	4	5	1	5	0.0837	1.0	0.0839	0.450	4.4	0.449	−5.71	0.52	−5.70	200	000
1	7276.89395	7	4	4	7	3	5	0.0704	1.3	0.0704	0.360	8.3	0.380	−6.17	0.26	−6.20	200	000
1	7277.60587	8	4	5	8	3	6	0.0679	1.2	0.0648	0.361	5.5	0.364	−5.55	0.39	−5.60	200	000
1	7278.75247	6	1	5	6	0	6	0.0831	1.8	0.0834	0.440	8.0	0.443	−10.10	0.52	−10.10	200	000
1	7279.10870	8	1	8	8	2	7	0.0560	1.8	0.0572	0.358	2.8	0.345	−12.34	2.58	−12.30	002	000
1	7283.73110	6	2	4	6	2	5	0.0885	1.7	0.0889	0.475	4.2	0.451	−8.99	1.03	−9.00	101	000
1	7284.71679	7	5	2	7	4	3	0.0722	0.7	0.0722	0.350	5.7	0.361	−13.20	0.19	−13.20	200	000
1	7286.05084	6	2	5	6	1	6	0.0755	1.6	0.0762	0.458	5.5	0.419	−8.25	0.64	−8.30	200	000
1	7302.60207	7	6	1	7	5	2	0.0570	1.4	0.0560	0.320	12.5	0.292	−17.01	0.77	−17.00	200	000
1	7316.96347	8	2	6	8	2	7	0.0785	1.3	0.0732	0.425	3.5	0.399	−12.70	0.32	−12.70	101	000
1	7331.24350	8	0	8	7	1	7	0.0508	2.0	0.0519	0.330	6.1	0.356	−13.01	0.39	−13.00	200	000
1	7351.48427	5	3	2	4	3	1	0.0800	1.3	0.0809	0.425	4.7	0.426	−6.15	0.52	−6.20	101	000
1*	7353.61442	8	7	1	7	7	0	0.0410	1.5	0.0393	0.325	6.2	0.269	−8.39	0.26	−8.40	101	000
1	7362.44798	6	1	5	5	4	2	0.0824	1.2	0.0815	0.439	9.1	0.404	−13.50	0.32	−13.50	002	000
1	7363.23370	7	0	7	6	3	4	0.0830	1.8	0.0820	0.440	5.7	0.392	−12.34	0.39	0.00	002	000
1	7370.73250	8	1	7	7	4	4	0.0748	1.6	0.0744	0.373	5.4	0.360	−15.20	0.52	−15.20	002	000
1	7371.15133	2	0	2	3	1	3	0.0988	0.8	0.1000	0.430	5.8	0.467	−10.02	0.45	−10.00	002	000
1	7371.45956	9	2	8	9	0	9	0.0482	1.2	0.0464	0.285	8.8	0.297	−15.21	0.19	−15.20	101	000
1	7372.87000	5	3	3	4	2	2	0.0913	0.9	0.0928	0.455	4.4	0.519	−9.91	0.39	−9.90	200	000
1	7382.51203	7	3	5	6	2	4	0.0842	1.2	0.0885	0.460	6.5	0.451	−8.58	0.77	−8.60	200	000
1	7388.84529	1	0	1	2	1	2	0.1010	2.0	0.1036	0.386	7.8	0.465	−12.05	0.64	−12.10	002	000
1	7396.44765	8	4	5	7	4	4	0.0652	1.2	0.0659	0.330	6.1	0.344	−12.45	0.52	−12.50	101	000
1	7399.15636	7	3	4	6	3	3	0.0882	1.1	0.0860	0.450	3.3	0.451	−10.83	0.52	−10.80	101	000
1	7401.97675	5	4	1	4	3	2	0.0753	1.3	0.0749	0.395	5.1	0.397	−10.93	0.52	−10.90	200	000
1	7402.74360	9	5	5	8	5	4	0.0583	1.7	0.0575	0.350	8.6	0.321	−10.00	0.26	−10.00	101	000
1	7407.78234	9	1	8	8	1	7	0.0547	1.8	0.0517	0.360	5.6	0.357	−10.21	0.26	−10.20	101	000
1	7411.37659	7	1	7	6	2	4	0.0906	1.7	0.0859	0.460	4.3	0.421	−9.60	0.45	−9.60	002	000
1	7413.01923	9	4	6	8	4	5	0.0616	1.3	0.0610	0.333	6.0	0.334	−13.45	0.64	−13.50	101	000
1	7415.60360	4	2	2	3	0	3	0.0963	1.7	0.0979	0.510	3.9	0.478	−2.00	1.93	−2.00	101	000
1	7421.24080	10	2	8	9	0	9	0.0581	1.2	0.0621	0.325	9.2	0.334	−16.45	1.03	−16.50	021	000

Table 4 (*continued*)

m	Computed position	Upper			Lower			b^{o}(air)			b°(self)			d^{o}(air)			Band
		J	K_a	K_c	J	K_a	K_c	Meas.	Δ%	Fitted	Meas.	Δ%	Fitted	Meas.	Δ	Smooth	
1	7421.38390	11	6	6	10	6	5	0.0495	1.2	0.0461	0.340	5.9	0.287	−7.69	1.03	−10.00	101 000
1	7424.69389	10	5	5	9	5	4	0.0673	1.2	0.0669	0.413	4.8	0.362	−6.34	0.52	−6.30	101 000
1	7427.95407	10	4	7	9	4	6	0.0569	1.4	0.0548	0.350	5.7	0.321	−20.09	0.13	−20.10	101 000
1	7429.72010	9	2	7	8	2	6	0.0727	0.8	0.0711	0.413	3.6	0.405	−11.80	0.39	−9.00	101 000
1	7431.44292	4	3	2	3	0	3	0.0942	0.8	0.0955	0.485	4.1	0.453	−0.06	0.39	−0.10	200 000
1	7432.30923	9	3	6	8	3	5	0.0825	1.8	0.0816	0.388	5.2	0.419	−15.91	0.39	−15.40	101 000
1	7435.94031	12	1	11	11	1	10	0.0278	1.4	0.0272	0.190	10.5	0.250	−18.09	0.26	−18.10	101 000
1	7437.19203	10	2	8	9	2	7	0.0630	1.7	0.0622	0.400	7.5	0.364	−10.23	0.64	−10.20	101 000
1	7438.00215	3	3	1	2	1	2	0.0950	0.7	0.0956	0.470	5.3	0.464	−0.25	0.26	−0.30	101 000
1	7439.37734	6	5	1	5	4	2	0.0595	1.7	0.0616	0.345	5.8	0.336	−16.22	0.13	−16.00	200 000
1	7441.36517	8	4	5	7	3	4	0.0868	1.0	0.0849	0.450	6.7	0.405	−11.23	0.19	−11.20	200 000
1	7444.69530	11	2	9	10	2	8	0.0534	1.7	0.0528	0.363	4.1	0.328	−6.27	0.39	−6.30	101 000
1	7447.48290	10	4	6	9	4	5	0.0789	1.5	0.0778	0.360	8.3	0.395	−13.20	0.77	−13.20	101 000
1	7453.57615	9	4	6	8	3	5	0.0873	1.1	0.0814	0.440	6.8	0.376	−12.55	2.58	−12.40	200 000
1*	7453.72212	6	6	1	5	5	0	0.0468	1.7	0.0454	0.295	6.8	0.220	−18.18	0.39	−18.20	200 000
1	7455.20694	5	2	3	4	0	4	0.0932	1.3	0.0957	0.490	4.1	0.470	−2.39	0.13	−2.40	101 000
1	7459.82997	5	3	2	4	1	3	0.0912	1.6	0.0920	0.480	6.3	0.457	−3.01	0.26	−3.00	101 000
1	7466.59702	5	3	3	4	0	4	0.0914	0.8	0.0911	0.480	8.3	0.445	−4.83	0.13	−4.80	200 000
1	7473.71200	3	2	1	3	1	2	0.0933	0.9	0.0955	0.475	5.3	0.479	−0.74	0.39	−0.70	002 000
1	7475.17393	12	3	9	11	3	8	0.0611	0.8	0.0608	0.365	8.2	0.348	−12.08	0.26	−12.10	101 000
1	7476.66190	3	1	2	3	0	3	0.0980	2.0	0.0970	0.540	4.6	0.482	−6.02	0.26	−6.00	002 000
1	7485.07982	6	3	3	5	1	4	0.0921	1.6	0.0908	0.462	6.5	0.452	−1.55	0.39	−1.55	101 000
1*	7485.34855	7	7	0	6	6	1	0.0378	1.6	0.0371	0.250	12.0	0.262	−18.13	0.19	−18.10	200 000
1	7490.96721	2	2	1	2	1	2	0.0980	1.0	0.0987	0.486	4.1	0.487	−4.31	0.26	−4.30	002 000
1	7492.59860	7	4	3	7	3	4	0.0880	2.0	0.0858	0.422	5.9	0.420	−11.28	1.29	−11.30	002 000
1	7495.56205	4	4	0	3	2	1	0.0860	0.8	0.0861	0.475	5.3	0.411	−4.45	0.90	−4.50	101 000
1	7496.34166	6	3	4	5	0	5	0.0887	1.0	0.0851	0.460	6.5	0.424	−3.60	0.26	−3.60	200 000
1	7497.14008	2	1	2	1	0	1	0.1002	0.7	0.1035	0.477	4.2	0.467	−0.56	0.26	−0.60	002 000
1	7497.78040	3	3	0	3	2	1	0.0884	0.7	0.0888	0.445	4.5	0.448	−5.19	0.26	−5.20	002 000
1	7498.10842	3	2	2	3	1	3	0.0945	1.3	0.0950	0.445	4.5	0.484	−3.17	0.26	−3.20	002 000
1	7498.47660	3	0	3	2	1	2	0.0962	1.6	0.0981	0.500	5.0	0.480	−8.85	0.39	−8.90	002 000
1	7501.33745	4	4	1	3	2	2	0.0872	0.9	0.0843	0.422	5.9	0.414	−5.72	0.39	−7.10	101 000
1	7504.71496	5	3	3	4	1	4	0.0896	0.8	0.0893	0.422	5.9	0.442	−2.04	0.77	−2.00	101 000
1	7504.94100	4	3	2	4	2	3	0.0840	1.3	0.0858	0.440	6.8	0.437	−5.77	0.52	−5.80	002 000
1	7507.46557	4	2	3	4	1	4	0.0895	1.2	0.0902	0.500	4.0	0.471	−4.71	0.39	−4.70	002 000

1	7509.15770	5	4	1	5	3	2	0.0802	1.4	0.0815	0.410	4.9	0.411	−8.79	0.90	−8.80	002	000
1	7511.29464	6	2	4	5	0	5	0.0915	0.7	0.0923	0.496	8.1	0.455	−5.30	0.19	−5.30	101	000
1	7511.92551	3	1	3	2	0	2	0.0986	1.1	0.0999	0.470	5.3	0.470	−2.15	1.03	−2.20	002	000
1	7512.90900	6	4	3	6	3	4	0.0701	1.4	0.0743	0.420	9.5	0.387	−6.69	1.16	−6.70	002	000
1	7513.89862	6	3	4	6	2	5	0.0779	1.5	0.0773	0.425	3.5	0.416	−5.90	0.39	−5.90	002	000
1	7523.16432	6	4	2	5	2	3	0.0895	0.7	0.0871	0.410	6.1	0.428	−6.62	0.52	−6.60	101	000
1	7527.53661	6	4	3	5	1	4	0.0830	1.8	0.0879	0.430	4.7	0.420	−1.23	0.39	−1.20	200	000
1	7528.09198	2	2	1	1	1	0	0.1003	1.8	0.0962	0.475	5.3	0.526	−7.15	0.26	−7.20	002	000
1	7534.79812	2	2	0	1	1	1	0.0990	1.6	0.0963	0.500	6.0	0.487	−1.60	0.13	−1.60	002	000
1	7536.03795	7	4	3	6	2	4	0.0861	0.9	0.0873	0.460	5.4	0.430	−6.74	0.39	−6.70	101	000
1	7539.56939	7	1	6	7	0	7	0.0760	1.7	0.0745	0.345	2.9	0.409	−12.02	0.52	−12.00	002	000
1	7545.21110	3	2	2	2	1	1	0.0980	0.9	0.0977	0.494	4.0	0.534	−5.87	0.26	−5.90	002	000
1	7551.09080	6	4	3	5	2	4	0.0796	1.0	0.0793	0.460	6.5	0.398	−8.15	0.39	−8.20	101	000
1	7557.31687	8	3	5	7	1	6	0.0851	0.6	0.0845	0.485	4.1	0.423	−5.63	0.52	−5.60	101	000
1	7558.93823	4	2	3	3	1	2	0.0935	1.8	0.0960	0.460	6.5	0.524	−5.97	0.64	−6.00	002	000
1	7561.26400	7	2	5	6	0	6	0.0800	0.9	0.0872	0.465	4.3	0.432	−7.97	0.18	−8.00	101	000
1	7562.12560	5	5	0	4	3	1	0.0820	0.9	0.0788	0.362	1.9	0.372	−9.58	0.90	−9.60	101	000
1	7567.58142	3	2	1	2	1	2	0.0971	1.0	0.0974	0.500	6.0	0.493	−1.10	0.26	−1.10	002	000
1	7567.86130	9	1	8	9	0	9	0.0500	2.0	0.0511	0.290	13.8	0.322	−18.83	0.39	−18.80	002	000
1	7569.73771	5	2	4	4	1	3	0.0922	1.8	0.0914	0.457	2.2	0.498	−4.91	2.58	−4.90	002	000
1	7573.50298	3	3	1	2	2	0	0.0868	2.0	0.0855	0.450	6.7	0.526	−7.61	0.39	−7.60	002	000
1	7575.03527	3	3	0	2	2	1	0.0866	1.7	0.0847	0.502	2.0	0.454	−6.44	0.32	−6.40	002	000
1	7579.16430	6	5	1	5	3	2	0.0815	1.5	0.0799	0.340	8.8	0.381	−6.60	0.39	−6.60	101	000
1	7579.50777	8	4	5	7	1	6	0.0793	1.1	0.0768	0.405	4.9	0.373	−1.20	0.64	−1.20	200	000
1	7582.49193	7	4	4	6	2	5	0.0775	0.9	0.0756	0.455	4.4	0.381	−3.43	0.26	−3.40	101	000
1	7583.98990	6	5	2	5	3	3	0.0740	0.4	0.0746	0.393	2.5	0.365	−9.00	0.90	−9.00	101	000
1	7585.39340	7	3	5	6	1	6	0.0786	1.1	0.0786	0.400	5.0	0.393	−4.20	0.64	−4.20	101	000
1	7593.14688	4	3	2	3	2	1	0.0892	0.4	0.0905	0.490	3.1	0.532	−7.43	0.26	−7.40	002	000
1	7600.77365	4	3	1	3	2	2	0.0847	1.1	0.0882	0.435	4.6	0.460	−5.31	0.64	−5.30	002	000
1	7602.35181	8	5	3	7	3	4	0.0856	1.2	0.0825	0.430	4.7	0.394	−8.48	0.52	−8.50	101	000
1	7605.79651	10	4	6	9	2	7	0.0830	2.0	0.0818	0.460	6.5	0.404	−0.15	1.55	−0.20	101	000
1	7612.02720	4	4	1	3	3	0	0.0743	0.8	0.0724	0.450	2.2	0.435	−12.39	0.39	−12.40	002	000
1	7614.58370	8	4	5	7	2	6	0.0729	1.1	0.0709	0.425	9.4	0.361	−1.52	0.32	−1.50	101	000
1	7627.35530	8	5	4	7	3	5	0.0707	1.6	0.0682	0.354	2.8	0.349	−6.70	2.58	−7.00	101	000
1	7629.72880	8	3	6	7	1	7	0.0709	1.0	0.0713	0.385	7.8	0.365	−4.77	0.32	−4.80	101	000
1	7630.49069	5	3	2	4	2	3	0.0888	1.4	0.0902	0.490	4.1	0.457	−4.99	0.26	−5.00	002	000
1	7635.45255	5	4	1	4	3	2	0.0742	1.8	0.0749	0.362	4.1	0.397	−10.58	0.13	−10.60	002	000
1	7650.12785	9	4	6	8	2	7	0.0648	1.7	0.0651	0.350	8.6	0.339	−1.16	0.39	−1.20	101	000
1	7654.15556	8	6	2	7	4	3	0.0727	1.4	0.0722	0.374	2.7	0.340	−14.21	1.29	−14.20	101	000
1	7659.50890	6	4	2	5	3	3	0.0770	1.0	0.0778	0.406	1.2	0.399	−7.06	1.16	−7.10	002	000
1	7666.10870	6	3	3	5	2	4	0.0876	1.4	0.0905	0.470	8.5	0.446	−7.31	1.55	−7.30	002	000

Table 4 (*continued*)

m	Computed position	Upper			Lower			b^{o}(air)			b°(self)			d^{o}(air)			Band	
		J	K_a	K_c	J	K_a	K_c	Meas.	Δ%	Fitted	Meas.	Δ%	Fitted	Meas.	Δ	Smooth		
1	7667.03672	6	5	2	5	4	1	0.0641	0.9	0.0647	0.350	2.9	0.340	−15.22	0.26	−15.20	002	000
1	7667.32338	6	5	1	5	4	2	0.0610	1.3	0.0616	0.330	9.1	0.336	−17.16	1.55	−17.20	002	000
1*	7671.69792	6	6	1	5	5	0	0.0453	2.0	0.0454	0.285	8.8	0.220	−17.83	0.39	−17.80	002	000
1	7685.97658	7	4	3	6	3	4	0.0769	1.7	0.0793	0.415	6.0	0.394	−5.05	0.90	−5.10	002	000
1	7688.30900	7	5	3	6	4	2	0.0760	2.0	0.0699	0.368	1.4	0.351	−14.99	0.26	−15.00	002	000
1	7689.68610	7	5	2	6	4	3	0.0626	1.0	0.0642	0.305	6.6	0.341	−15.18	0.26	−15.20	002	000
1	7717.71170	8	6	3	7	5	2	0.0567	1.8	0.0552	0.294	5.1	0.264	−18.59	1.03	−18.60	002	000

b^{o} and d^{o} in cm^{-1}/atm at 296 K.
m represents the oxygen isotopic species: 1 $=H_2{}^{16}O$, 2 $=H_2{}^{18}O$, and 3 $=H_2{}^{17}O$. An asterisk after m denotes a doubled line with the quantum assignment given for the stronger of the two comparable transitions.
Computed positions in cm^{-1} and derived from the energy level values given in Refs. [1,39,40].
Δ % is the estimated uncertainty in percent of the measured half-width coefficient.
Δ is the estimated uncertainty in cm^{-1}/atm. of the pressure-induced frequency shift coefficient.

Table 5
Comparison of the values of the linewidth coefficients, b^{o}, computed from the coefficients derived from the fitting analysis to those obtained from measurements in this and other studies

B	Frequency range		NT	σ_T%	un$_T$%	NA	NA/NT%	σ_A%	un$_A$%	Min.		Max.		Study
	Min.	Max.								J	K_a	J	K_a	
air	604.448	7758.555	3959	7.1	4.4	3616	91.3	3.9	4.1	0	0	18	10	This work, $H_2{}^{16}O$ ground state bands
air	639.431	6372.261	340	6.0	6.3	308	90.6	4.4	6.3	0	0	15	7	This work, $H_2{}^{17}O$ and $H_2{}^{18}O$
air	676.550	7301.435	199	7.9	7.7	199	83.4	4.9	7.1	0	0	12	6	This work, $H_2{}^{16}O$ hot bands
air	10150.659	11190.047	507	6.1	4.3	456	89.9	4.4	4.2	0	0	11	6	Brown et al. [30]
air	1271.788	4019.467	699	10.9	NG	636	91.0	3.9	NG	0	0	13	6	Zou and Varanasi [33]
air	3593.198	3948.177	104	4.9	1.2	102	98.1	4.2	1.2	0	0	10	4	Devi et al. [16]
air	802.989	1149.700	63	11.1	9.9	54	85.7	4.4	9.9	5	0	18	9	Rinsland et al. [14]
air	13612.379	13948.815	120	8.9	NG	93	77.5	4.7	NG	0	0	9	7	Grossmann and Browell [13]
air	12190.744	12291.046	32	7.6	NG	27	84.4	5.7	NG	2	0	7	3	Ponsardin and Browell [21]
air	3367.643	3446.941	8	18.2	2.9	2	25.0	7.5	1.1	0	0	11	4	Bruno et al. [31]
air	1211.256	2090.103	271	14.1	1.6	171	63.1	5.3	1.2	2	0	18	9	Yamada et al. [17]
air	9251.241	22636.750	6235	44.4	24.4	2507	40.2	5.5	14.0	0	0	15	8	Merienne et al. [35] and Fally et al. [36]
air	8601.987	14476.177	4154	21.5	NG	1841	44.3	5.7	NG	0	0	16	8	Schermaul et al. [25]
air	397.322	576.117	37	22.9	4.1	6	16.2	5.1	3.5	5	2	12	10	Steyert et al. [26]
air[a]	1296.490	1433.608	30	5.4	2.3	28	93.3	4.9	2.3	2	0	13	7	[a]Claveau et al. [29]
air[a]	8592.308	11124.636	242	7.0	NG	209	86.4	4.8	NG	0	0	10	5	[a]Mandin et al. [10,12]
air	922.135	1967.442	19	16.6	9.8	10	52.6	5.5	10.1	6	0	16	7	Eng et al. [4]
air[a]	7117.249	7185.596	8	7.9	14.0	6	75.0	3.4	15.5	4	0	6	6	[a]Nagali et al. [20]
air[a]	7181.156	7185.209	7	20.2	0.9	5	71.4	4.9	10.6	1	0	6	6	[a]Moretti et al. [23]
self	600.662	7939.593	4752	12.7	8.4	3740	78.7	4.9	7.6	0	0	17	10	This work, $H_2{}^{16}O$ ground state bands
self	617.350	7474.256	784	12.3	6.2	545	69.5	5.1	5.5	0	0	13	7	This work, $H_2{}^{17}O$ and $H_2{}^{18}O$
self	609.716	7489.398	478	18.0	7.4	268	56.1	5.5	6.0	0	0	12	6	This swork, $H_2{}^{16}O$ hot bands
self	1308.179	4044.910	1122	12.9	NG	770	68.6	5.3	NG	0	0	18	10	Zou and Varanasi [33]
self	13563.322	13965.030	170	13.2	NG	97	57.1	5.7	NG	0	0	9	6	Grossmann and Browell [11]
self	1777.886	4060.610	482	19.9	18.7	149	30.9	5.6	17.2	1	0	16	8	Mandin et al. [7,9]
self	7226.024	7233.423	12	14.7	8.7	5	41.7	4.5	11.4	0	0	7	3	Langlois et al. [19]
self	3367.643	3446.941	9	16.9	1.6	2	22.2	5.4	1.4	4	0	11	4	Bruno et al. [31]
self	9251.241	25219.093	7583	45.4	32.7	2355	31.1	5.6	22.1	0	0	16	8	Coheur et al. [27] and Merienne et al. [35]
self	7117.249	7185.596	8	29.8	9.5	3	37.5	7.3	11.3	4	0	6	6	Nagali et al. [20]
self	7182.209	7185.596	3	40.7	4.9	0	0	—	—	1	0	6	6	Moretti et al. [23]

B = Broadener, frequencies in cm^{-1}, NT = total number of lines measured, σ% = standard deviation in percent between observed b^{o} and computed b^{o}, NA = number of lines in which $|[b^{o}(\text{obs.}) - b^{o}(\text{computed})]/b^{o}(\text{obs.})| \times 100 \leqslant 10$. un% = standard deviation in percent of the reported, individual experimental uncertainties. NG = not given.

$\sigma_I\% = \{\Sigma[b^{o}(\text{obs.}) - b^{o}(\text{computed})/b^{o}(\text{obs.})]^2/\text{NI}\}^{1/2} \times 100$, $\text{un}_I\% = \{[\Sigma\Delta b^{o}(\text{obs.})/b^{o}(\text{obs.})]^2/\text{NI}\}^{1/2} \times 100$, σ_T% for NI = NT and σ_A% for NI = NA. Same for un$_T$% and un$_A$%.

[a]Means that the data used from the study was N_2 broadened and to use them as air broadened here, a factor of 0.89 was applied to their values of b^{o} Δb^{o}(obs.) is the experimental uncertainty in b^{o}(obs.).

web site, http://mark4sun.jpl.nasa.gov. The names of these numeric files are labeled: widv20.tra, widv20trb, widv21.tra, and widv21.trb. The middle part of the file name relates to the upper state v_2 value with "v20" for $v_2' = 0$ and "v21" for $v_2' > 0$. The part of the file after the decimal pertains to the type of rotational transitions. Also included on the web site are spectral plots from which Figs. 1–4 were taken.

7. Conclusion

High-resolution laboratory spectra of water plus air mixtures covered the region between 2800 and 8000 cm^{-1}. Over 4000 linewidth and pressure-induced frequency shift coefficients were derived from the spectral data with sample temperatures near or at room temperature (296 K). The measurements include transitions of $H_2{}^{16}O$, $H_2{}^{17}O$, and $H_2{}^{18}O$ with the rare oxygen species observed in normal H_2O gas samples. The measurements were analyzed with consideration of collision-narrowing effects. The analysis requires a knowledge of the self-broadened linewidth coefficients, and the data measured and reported in the previous study [3] were used along with earlier results [2] for this purpose. The self-broadened and air-broadened measured linewidth coefficients obtained here as well as those reported in earlier studies [1–3], covering the 600–2400 cm^{-1}, were fitted to an empirical expression which contains up to 28 terms. Two fitting procedures were used: one considered the fit of families of transitions and the other was more global in scope. The computed linewidth coefficients derived from the fitted parameters are compared statistically to measurements in this work as well as other studies.

The averaged values of the pressure-shift coefficients, d^o(air), do not have nearly the smooth behavior as that of the width coefficients in terms of related families of transitions. Smoothed values of d^o(air) were derived from hand-drawn plots of related families of transitions. The effect due to self-broadening was not included in this work to determine d^o although, if included, it could influence the value for d^o(air) but not by more than 10%.

Acknowledgements

The author thanks the National Solar Observatory at Kitt Peak for the use of the FTS and C. Plymate and L. Brown for assistance in obtaining the H_2O spectra. This research was performed at the Jet Propulsion Laboratory, California Institute of Technology, under contract with the National Aeronautics and Space Administration.

References

[1] Toth RA. J Mol Spectrosc 2000;201:218–43.
[2] Toth RA, Brown LR, Plymate C. JQSRT 1998;59:529–62.
[3] Toth RA. JQSRT, doi:10.1016/j.jqsrt.2004.08.042.
[4] Eng RS, Kelley PL, Mooradin A, Calawa AR, Harman TC. Chem Phys Lett 1973;19:524–8.

[5] Chang YS, Shaw JH. JQSRT 1977;18:491–9.
[6] Eng RS, Mantz AW. J Mol Spectrosc 1979;74:388–99.
[7] Mandin J-Y, Camy-Peyret C, Flaud J-M, Guelachvili G. JQSRT 1980;23:351–70.
[8] Mucha JA. Appl Spectrosc 1982;36:141–7.
[9] Mandin J-Y, Camy-Peyret C, Flaud J-M, Guelachvili G. Can J Phys 1982;60:94–101.
[10] Mandin J-Y, Chevillard J-P, Camy-Peyret C, Flaud J-M. J Mol Spectrosc 1988;132:352–60.
[11] Grossmann BE, Browell EV. J Mol Spectrosc 1989;136:264–94.
[12] Mandin J-Y, Chevillard J-P, Camy-Peyret C, Flaud J-M. J Mol Spectrosc 1989;138:272–81.
[13] Grossmann BE, Browell EV. J Mol Spectrosc 1989;138:562–95.
[14] Rinsland CP, Goldman A, Smith MA, Devi VM. Appl Opt 1991;30:1427–38.
[15] Giesen T, Schieder R, Winnewisser G, Yamada KMT. J Mol Spectrosc 1992;153:406–18.
[16] Devi VM, Benner DC, Smith MAH, Rinsland CP. J Mol Spectrosc 1992;155:333–42.
[17] Yamada KMT, Harter M, Giesen T. J Mol Spectrosc 1993;157:84–94;
Yamada KMT, Harter M, Giesen T. JQSRT 1993;50:463–75.
[18] Avetisov VG, Nadezhdinskii AI, Khusnutdinov AN, Amarova PM, Zyrianov MV. J Mol Spectrosc 1993;160: 326–34.
[19] Langlois S, Birbeck TP, Hanson RK. J Mol Spectrosc 1994;163:27–42.
[20] Nagali V, Chou SL, Baer DS, Hanson K. JQSRT 1997;57:795–809.
[21] Ponsardin PL, Browell EV. J Mol Spectrosc 1997;185:58–70.
[22] Upschulte BL, Allen MG. JQSRT 1998;59:653–70.
[23] Moretti L, Sasso A, Gianfrani L, Ciurylo R. J Mol Spectrosc 2001;205:20–7.
[24] Lepere M, Henry A, Valentin A, Camy-Peyret C. J Mol Spectrosc 2001;208:25–31.
[25] Schermaul R, Learner RCM, Newnham DA, Williams RG, Ballard J, Zobov NF, Belmiloud D, Tennyson J. J Mol Spectrosc 2001;208:32–42.
[26] Steyert DW, Wang WF, Sirota JM, Donahue NM, Reuter DC. JQSRT 2002;72:775–82.
[27] Coheur P-F, Fally S, Carleer M, Clerbaux C, Colin R, Jenouvrier A, Merienne M-F, Hermans C, Vandaele AC. JQSRT 2002;74:493–510.
[28] Schermaul R, Learner RCM, Canas AAD, Brault JW, Polyansky OL, Belmiloud D, Zobov NF, Tennyson J. J Mol Spectrosc 2002;211:169–78.
[29] Claveau C, Henry A, Lepere M, Valentin A, Hartmans D. J Mol Spectrosc 2002;212:171–85.
[30] Brown LR, Toth TA, Dulick M. J Mol Spectrosc 2002;212:57–82.
[31] Bruno A, Pesce G, Rusciano G, Sasso A. J Mol Spectrosc 2002;215:244–50.
[32] Tolchenov RN, Tennyson J, Brault JW, Canas AAD, Schermaul R. J Mol Spectrosc 2002;215:269–74.
[33] Zou Q, Varanasi P. JQSRT 2003;82:45–98.
[34] Gamache RR, Fischer J. JQSRT 2003;78:289–304.
[35] Merienne M-F, Jenouvrier A, Hermans C, Vandaele AC, Carleer M, Clerbaux C, Coheur P-F, Colin R, Fally S, Bach M. JQSRT 2003;82:99–117.
[36] Fally S, Coheur P-F, Carleer M, Clerbaux C, Colin R, Jenouvrier A, Merienne M-F, Hermans C, Vandaele C. JQSRT 2003;82:119–31.
[37] Toth RA, Brown LR. J Mol Spectrosc 2003;218:135–50.
[38] Gamache RR, Hartmann J-M. JQSRT 2004;83:119–47.
[39] Toth RA. J Mol Spectrosc 1998;190:379–96.
[40] Toth RA. J Mol Spectrosc 1999;194:28–42.
[41] Pollock CR, Petersen FR, Jennings DA, Wells JS, Maki AG. J Mol Spectrosc 1983;99:357–68.
[42] Toth RA. J Mol Spectrosc 1999;195:73–97.
[43] Toth RA, Gupta VD, Brault W. Appl Opt 1982;21:3337–47.
[44] Toth RA, Brault W. Appl Opt 1983;22:908–26.
[45] Toth RA. J Mol Spectrosc 1997;186:66–89.
[46] Toth RA. J Mol Spectrosc 1998;190:379–96.
[47] Toth RA. Appl Opt 1994;33:4868–79.

[48] Rothman LS, Barbe A, Benner DC, Brown LR, Camy-Peyret C, Carleer MR, Chance K, Clerbaux C, Dana V, Devi VM, Fayt A, Flaud J-M, Gamache RR, Goldman A, Jacquemart D, Jucks KW, Lafferty WJ, Mandin J-Y, Massie ST, Nemtchinov V, Newnham DA, Perrin A, Rinsland CP, Schroeder J, Smith KM, Smith MAH, Tang K, Toth RA, Vander Auwera J, Varanasi P, Yoshino K. The HITRAN molecular spectroscopic database: edition of 2000 including updates of 2001. JQSRT 2003;82:5–44.
[49] Galatry L. Phys Rev 1961;122:1218.
[50] Varghese PL, Hanson RK. Appl Opt 1984;23:2376–85.